ABSTRACT

Title of Dissertation: DEVELOPMENT OF A MOUSE MODEL FOR THE t(10;11) (p13; q14) CHROMSOMAL TRANSLOCATION ASSOCIATED WITH ACUTE LEUKEMIA IN HUMANS

David L. Caudell, DVM, PhD, 2008

Directed By: Professor Siba K, Samal, Department of Veterinary Medical Science and,
Peter D. Aplan, MD, Genetics Branch, Center for Caner Research, National Cancer Institute, National Institutes of Health

Acute leukemia is associated with a wide spectrum of gross chromosomal rearrangements. These acquired mutations include balanced and unbalanced chromosomal translocations. The analysis of chromosomal translocations has provided much insight into understanding the biology of hematologic malignancies, leading to improved diagnosis and classification, as well as identification of novel therapeutic targets. The rare but recurring chromosomal translocation [t(10;11)(p13;q21)] results in a *CALM-AF10* fusion that occurs in patients with both acute lymphoblastic leukemia (ALL) and acute myeloid leukemia (AML). *CALM-AF10* transgenic mice developed AML with lymphoid features and had *Hoxa* gene cluster upregulation. In this model, mice developed leukemia after a long latency period with incomplete penetrance. These findings suggest that additional genetic

events are needed to complement *CALM-AF10* mediated leukemic transformation. Retroviral insertional mutagenesis was used to identify complementary genetic events that might collaborate with *CALM-AF10* during leukemic transformation. A cohort of *CALM-AF10* mice was infected with the Mol4070LTR retrovirus; by 5.5 months of age, 50% of the transgenic mice developed AML, a clear acceleration of disease onset compared to either wild type littermates injected with the retrovirus or *CALM-AF10* mice not injected with the retrovirus. The tumors assayed by Southern blotting for viral integration showed clonal to oligoclonal expansion. Ligation-mediated PCR and sequence analysis of DNA derived from leukemic cells was used to identify potential collaborating genes at the retroviral insertion sites including *Evi1, Nf1, kRas, Zeb2,* and *Mnl*. Identification of these genes as a potential collaborating gene with *CALM-AF10* supports the emerging paradigm in leukemia biology that predicts that most, if not all leukemic cells must undergo at least two collaborative events to produce a fully transformed cell. One of these events typically leads to impaired differentiation and enhanced renewal of stem cells, whereas the second event leads to increased proliferation and/or decreased apoptosis. It has been shown here that retroviral infection accelerates the onset of acute leukemia, and identified genes that potentially collaborate with the *CALM-AF10* fusion gene in the leukemic transformation process. This transgenic murine model serves as a model system for studying leukemogenesis similar to that observed in humans with leukemia.

DEVELOPMENT OF A MOUSE MODEL FOR THE t(10;11) (p13; q14) CHROMSOMAL TRANSLOCATION ASSOCIATED WITH ACUTE LEUKEMIA IN HUMANS

By

David L. Caudell, DVM

Dissertation submitted to the Faculty of the Graduate School of the
University of Maryland, College Park, in partial fulfillment
of the requirements for the degree of
Doctor of Philosophy
2008

Advisory Committee:
Professor Siba K. Samal, Chair
Peter D. Aplan, MD, Co-Chair
R. Mark Simpson, DVM, PhD
Associate Professor Nathaniel Tablante
Assistant Professor Iqbal Hamza
Associate Professor Nickolas Zimmerman (Dean's Representative)

Preface

Saint Augustine once wrote “Men go forth to wonder at the heights of mountains, the huge waves of the sea, the broad flow of the rivers, the vast compass of the ocean, the courses of the stars; and they pass by themselves without wondering”. As I reflect upon my medical education, I am deeply honored and humbled by the opportunity to observe the intricacies of the human body each day. These observations occurred on many levels and presented their own challenges. Yet, through it all, each challenge brought reward. Many times it was difficult to appreciate the benefit, and the path to discovery was often clouded by fear and unrealistic expectations. However, there was a constant source of inner strength that continuously fueled the call of purpose, perseverance, and service. These elements take their roots beginning with values instilled into me as a child. They were further enforced through my formal education at Virginia Tech that echoed the motto “*Ut prosium*”. Finally, they were called into practice by the Benedictine brothers at Conception Monastery who challenged my imagination, independent will, purpose, and daily contemplation. I am forever indebted to those individuals who remained behind the walls of Conception. They faithfully watched as I chose secular over monastic life; sought purpose in a different direction; and continued to serve humanity. I am forever committed to public service and discerning my purpose in this life. The pages that follow reflect the work of human hands with the intent of serving those who suffer—the cancer patient.

Foreword

Invictus

by William Ernest Henley; 1849-1903

Out of the night that covers me,
Black as the Pit from pole to pole,
I thank whatever gods may be
For my unconquerable soul.

In the fell clutch of circumstance
I have not winced nor cried aloud.
Under the bludgeonings of chance
My head is bloody, but unbowed.

Beyond this place of wrath and tears
Looms but the horror of the shade,
And yet the menace of the years
Finds, and shall find me, unafraid.

It matters not how strait the gate,
How charged with punishments the scroll,
I am the master of my fate;
I am the captain of my soul.

Dedication

To my Mother and Father, who in this world, gave me life.

Acknowledgements

There are numerous people whose contribution to this scholarly work must be recognized.

First I wish to thank my advisor Peter D. Aplan who supported me as a mentor in developing and encouraging my pursuit of science. I also wish to thank Dr. Samal for serving as the chair of my committee; Dr. R. Mark Simpson for his support as director of the Comparative Molecular Pathology Fellowship at the NIH; Dr. Nathaniel Tablante for his role both on my committee and as the Department's Graduate School Coordinator; Dr. Iqbal Hamza for serving on my committee and his excellent insight throughout this process; and Dr. Nickolas Zimmerman for serving as the Dean's Representative.

The success of the work was made possible through many talented colleagues who worked in Dr. Aplan's lab. These people include Zhenhua Zhang, Chris Slape, Helge Hartung, David Harper, Rachel Pierce, Rachel Novak, Yang Jo Chung, Chul Won Choi, Tony Gill, Yue Cheng, Sheryl Gough, and Sarah Beachy. I would also like to thank Shelley Hoover and the Fellows in my training program and who offered overwhelming support as colleagues and friends. Each individual made a significant contribution to this work through thoughtful and insightful discussions, performing experiments, or offering editorial assistance and critiques.

I also wish to extend a heart-felt thanks to my family who was there every step of the way, and whose childhood discipline and devotion kept me focused in the most difficult of times. Finally, I thank my closest friends, who heard about every failed experiment and celebrated every success.

Research funding support was provided through the Intramural Research Program, Center for Cancer Research, National Cancer Institute, Bethesda, MD. I received a Cancer Research Training Award and was a Molecular Pathology Graduate Fellow in the NCI Molecular Pathology Graduate Partnership Program with the University of Maryland, College Park.

Table of Contents

List of Tables

List of Figures

Chapter 1: Introduction

Introduction

Cancer is a disease of the genome that results, in large part, from mutations in proto-oncogenes or tumor suppressor genes that yield a dominant gain or recessive loss of function respectively (Hanahan and Weinberg 2000). Although the incidence of cancer appears to be decreasing in the US population, it still accounted for 26% of all deaths compared to 18% of deaths related to cardiovascular disease in patients less than 65 years of age in 2005 (Ries, Melbert D et al. 2008). The most frequent tumors that occur in men involve the prostate, lung, colon/rectum; in woman, the most common tumors include breast, lung and colon/rectum. Cancers involving these body systems make up about 50% of all cancer diagnoses compared to 3% of leukemic diagnoses. However, leukemias make up a much larger percentage of cancers in children, and as a group, are the most common malignancy resulting in dramatic loss of productive life years (Ries, Melbert D et al. 2008). Leukemias are seen in both pediatric and adult patients; of the childhood cancers, acute leukemias are the most common malignancies with a median age at diagnosis being 13 for ALL and the median age at diagnosis being 67 for AML (Ries, Melbert D et al. 2008). According to the NCI Surveillance Epidemiology and End Results (SEER), the age-adjusted death rate for leukemia in 2004 was 7.2 per 100,000 per year for men and women. In 2004 there were 21, 472 deaths associated with leukemia in the United States; this is in contrast to 553,800 total deaths due to cancer; 40,954 in women with breast

cancer; 29,002 case in men with cancer that involved prostate; and 158,000 cases of lung cancer (Ries, Melbert D et al. 2008).

Clinical and molecular basis of leukemia

The hematopoietic system is the source of erythrocytes, leukocytes, and platelets that function in oxygen exchange, immune surveillance, and coagulation respectively. This system is reviewed in Figure 1.1. Leukemia refers to a disease characterized by a predominance of immature hematopoietic or lymphoid precursor cells (acute leukemia) or an expansion of mature marrow elements (chronic leukemia) (Niemeyer and Sallen 1998). Historically, leukemia and lymphoma have been classified using the French-American-British system which defined tumors based on their morphology (Harris, Jaffe et al. 2001; Gilliland and Tallman 2002). This included the following four categories: acute lymphocytic leukemia (ALL), chronic lymphocytic leukemia (CLL), acute myelogenous leukemia (AML), or chronic myelogenous leukemia (CML). The more recent WHO classification scheme stratifies hematopoietic neoplasms according to lineage, but also extends the classification to incorporate immunophenotype, genetic features, and clinical syndromes (Harris, Jaffe et al. 2001). Signs and symptoms associated with acute leukemia are attributed to leukemic infiltration into either bone marrow or parenchymal organs (Lowenberg, Downing et al. 1999). Symptoms related to bone marrow infiltration lead to bone marrow failure and are reflected by lethargy and listlessness due to anemia, bleeding disorders due to thrombocytopenia, and secondary infections because of leukopenias (Figure 1.2). The clinical presentation seen with organ infiltration varies with the

type of organ involved and the degree of infiltration. If left untreated, acute leukemia is uniformly fatal.

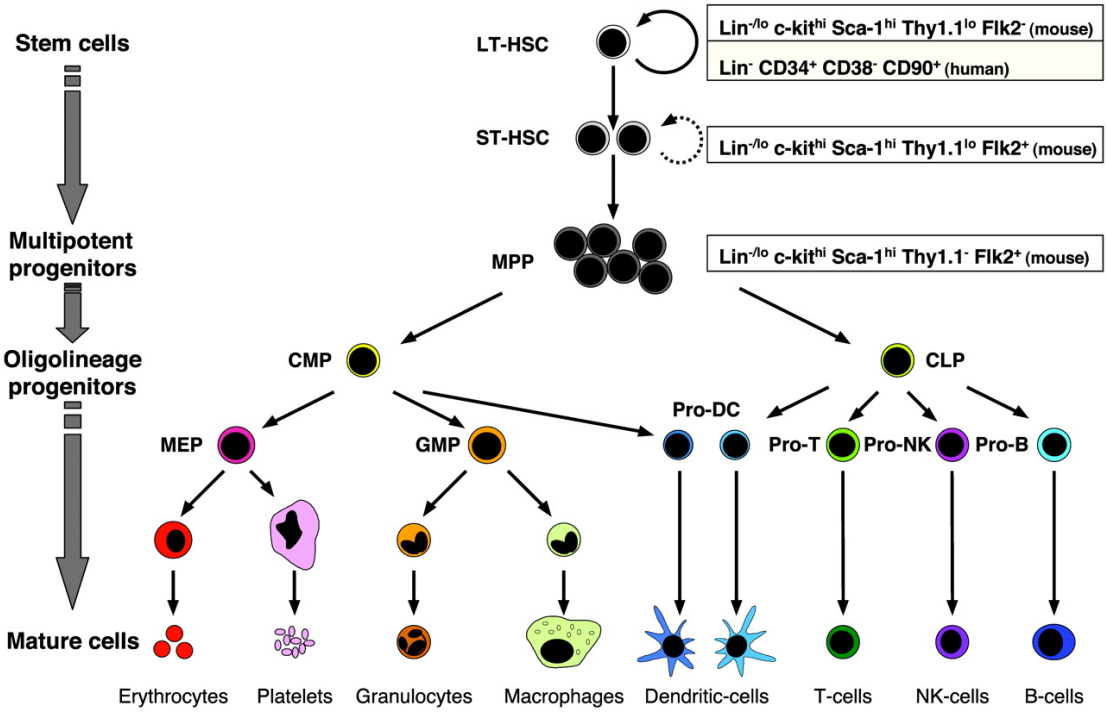

Figure 1.1. **Hematopoietic and progenitor cell lineages.** HSCs can be divided into LT-HSCs, highly self-renewing cells that reconstitute an animal for its entire life span, or ST-HSCs, which reconstitute the animal for a limited period. ST-HSCs differentiate into MPPs, which do not or briefly self-renew, and have the ability to differentiate into oligolineage-restricted progenitors that ultimately give rise to differentiated progeny through functionally irreversible maturation steps. The CLPs give rise to T lymphocytes, B lymphocytes, and natural killer (NK) cells. The CMPs give rise to GMPs, which then differentiate into monocytes/macrophages and granulocytes, and to megakaryotic/erythroid progenitors (MEP), which produce megakaryocytes/platelets and erythrocytes. Both CMPs and CLPs can give rise to dendritic cells. All of these stem and progenitor populations are separable as pure populations by using cell surface markers. ((Passegue, Jamieson et al. 2003) Used with permission, copyright, 2003)

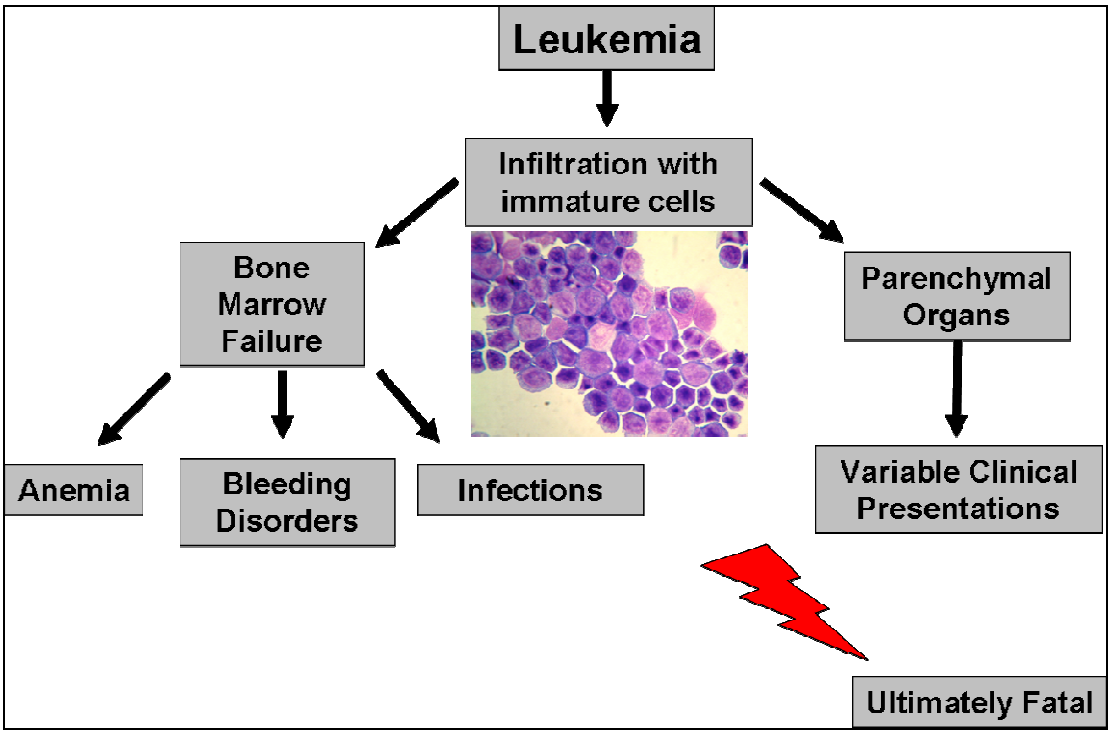

Figure 1.2. Outcome of leukemia

Acute leukemia results as a consequence of multiple acquired mutations that accumulate in hematopoietic precursor cells. These mutations can be grouped into three general categories: point mutations, gross chromosomal rearrangements, and epigenetic changes (Lin and Aplan 2004). The analysis of theses altered genetic events has proven to be especially useful in understanding the biology of hematopoietic malignancies, leading to improved diagnosis and classification, as well as identification of novel targets for therapy (Rowley 1999).

Acquired point mutations in genes that encode hematopoietic transcription factors play a significant role in leukemogenesis. First, gain of function point mutations have been identified in several genes that resulted in acute leukemia. For example, internal tandem duplications or missense point mutations have been observed in patients in the FMS-like tyrosine kinase (*FLT3*) gene (Renneville, 2008). Mutations in *FLT3* confer a proliferative advantage to myeloid blasts cells through constitutive phosphorylation of FLT3-ligand and downstream activation of PI3/AKT, Ras/MAPK, and JAK/STAT pathways (Rannevile, 2008). Secondly, point mutations that involve the proto-oncogene *KIT* have been observed in less than two per cent of AML patients (Bacher, Kern et al. 2005), KIT, a tyrosine kinase, binds to Stem Cell Factor (SCF) and results in the activation of several downstream pathways including proliferation. Mutations in either exon 8 that involves the extracellular receptor domain or codon 816 of the catalytic domain activation loop are seen in AML patients with t(8;21) or inv(16)/t(16;16) (Frohling, Scholl et al. 2005). Detection of *KIT* mutations offer a prognostic indicator in patients and help guide therapy. Third,

in contrast to patients with either *FLT3* or *cKIT* mutations that lead to activation of a transcription factor, point mutations that involve base substitutions, deletions, or insertions in *GATA1* result in gene inactivation (Wechsler, Greene et al. 2002). GATA1 plays a critical role as a transcription factor in erythroid and megakaryocytic cell differentiation (Shimizu, Engel et al. 2008). Point mutation in *GATA1* can result in an amino-terminus truncated protein that has been observed in Down's syndrome patients with acute megakaryoblastic leukemia (Wechsler, Greene et al. 2002) and transient myeloproliferative disorder (TMD) (Greene, Mundschau et al. 2003).

Numerous gross chromosomal rearrangements (GCR) have been observed in leukemia biology. These mutations include balanced and unbalanced chromosomal translocations, as well as chromosomal inversions, deletions, and amplifications(Rabbitts 1991; Cline 1994; Rabbitts 1994; Thandla and Aplan 1997). Of these GCRs, chromosomal translocations (CTs) have been observed in many cases of acute and/or chronic leukemia (Solomon, Borrow et al. 1991; Raimondi 1993). Research into the molecular pathogenesis has revealed at least four important concepts about these mutations (Lin and Aplan 2004). First, specific CTs are typically associated with a particular leukemic phenotype. For example, the t(15:17) is associated only with promyelocytic leukemia that gives rise to a PML-RARα fusion seen in patients with M3 AML. Secondly, at least two outcomes are associated with CTs: either they produce a novel chimeric protein as in the case of BCR-ABL; or they lead to unscheduled expression of proto-oncogenes such as *MYC-IGH*. Third, CTs often are involved in genes that encode for either transcription factors or proteins

associated with signal transduction pathways (Aplan 2006). Finally, genes affected by CTs can also be associated with point mutations. For example, the t(8;21) which produces an *AML1-ETO* fusion has been associated with point mutations (Rhoades, Hetherington et al. 1996).

The pathogenesis of AML is a multistep process. The current paradigm in leukemic biology proposes collaboration between two categories of mutations. Class I mutations lead to enhanced cell proliferation as well as impaired apoptosis. The mutations affect signal transduction or tyrosine kinase pathways and involve genes including *RAS*, *cKIT*, *FLT3*, or *BCR/ABL*. Class II mutations result in mutant DNA binding transcription factors, these include *PML/RARα*, *AML/ETO*, and *MLL* fusions. These novel fusions lead to impaired hematological precursor cell differentiation (Kelly and Gilliland 2002).

Techniques for studying collaborative pathways

Earlier it was discussed that AML results from mutations that affect at least two different yet collaborative cellular pathways. Until recently, potential cancer-causing genes and their associated pathways have been difficult to study. The use of carefully designed genetically engineered mice (GEMs) for has provided much insight into the molecular biology of hematopoietic malignancy. One of the major limitations of these model systems has been compartmentalization or limited expression of altered genetic events. The observation that certain inbred strains of mice develop spontaneous leukemia as a result of retroviral integration, and the cloning of these specific retroviral integrations has led to the discovery of important cancer genes.

Numerous high throughput techniques have been used to identify these genes in mice. For example, the combined strategy of generating subgenomic lamda libraries and Southern blotting with retroviral specific probes identified proviral DNA junctions in tumors from mice. Another system relied upon cloning of proviral insertion sites near CpG islands using PCR to identify proviral insertion sites (Largaespada 2000). More recent advances have been developed using a combination of high-throughput PCR-based cloning techniques coupled with the use of an annotated mouse genome to identify cancer genes (Li, Shen et al. 1999; Mikkers, Allen et al. 2002). High throughput application of this technology applied to the "sensitized" GEMs has lead to a better understanding of concepts in clonal expansion and multiple gene interactions in mouse model systems (Largaespada 2000; Touw and Erkeland 2007)

In terms of clinical relevance, cloning of CTs has led to much insight with regards to prognosis and treatment of leukemia. For example, cloning of the *BCR-ABL* fusion gene highlighted the role of tyrosine kinases in leukemic transformation and led to the subsequent development of imatinib, a tyrosine kinase inhibitor (Rowley 2001). Furthermore, chromosomal abnormalities are now routinely used to help classify leukemia patients for risk-directed therapy (Rubnitz, Behm et al. 1996).

<u>The t(10; 11) translocation</u>

The t(10; 11) translocation was first observed in a patient with diffuse histiocytic lymphoma (Sundstrom and Nilsson 1976); the U937 cell line was established from this patient and has been used extensively as an *in vitro* model of monocyte differentiation (Harris and Ralph 1985). The presence of a reciprocal translocation

between chromosomes 10 and 11, a t(10; 11)(p13-14; q14-21) in the U937 cell line was confirmed and subsequently refined by cytogenetic analysis (Kobayashi, Thirman et al. 1995; Shipley, Williams et al. 1995). Using positional cloning techniques to narrow the chromosome 10 breakpoint to a 3 cM region, *AF10* was identified as a candidate gene on chromosome 10 potentially involved in this translocation. Subsequent studies showed that the *AF10* gene was indeed disrupted by the t(10;11) translocation, and identified *CALM* as the *AF10* fusion partner in this recurrent translocation (Dreyling, Martinez-Climent et al. 1996).

Structure and function of CALM

*CALM (*for *C*lathrin *A*ssembly *L*ymphoid *M*yeloid; also known as *PICALM)* is located on chromosome 11q23, ubiquitously expressed, and encodes a 652 aa protein with multiple domains involved in endocytosis (Figure 1.3)(Dreyling, Martinez-Climent et al. 1996). These domains include the epsin N-terminal homology (ENTH) domain (Asp-Pro-Phe), a DPF (ASP-Pro-Phe) motif, an NPF (Asn-Pro-Phe) motif, and type I and type II clathrin-binding sequences (CBS I and II) (Tebar, Bohlander et al. 1999; Klebig, Wall et al. 2003; Meyerholz, Hinrichsen et al. 2005). The predicted CALM protein is similar to the neuronal specific monomeric clathrin assembly protein AP180, which was first identified in coated vesicles of bovine brain (Ahle and Ungewickell 1986; Takei, Mundigl et al. 1996). CALM homologues have been identified in rat, mouse and cow.

Endocytosis is the active cellular process of removing proteins from the plasma membrane (Mukherjee, Ghosh et al. 1997). The active formation of transport vesicles

that shuttle cytosolic cargo, such as transmembrane and luminal proteins from the plasma membrane and the trans-Golgi network (TGN) to endosomes requires participation of clathrin coated pits (Schmid 1997). Clathrin is composed of three major proteins; a 192 kDa heavy chain bound to two ~30 kDa light chains that forms a structure known as a triskelion (Schmid 1997). In order for coat proteins to function properly in vesicle transport, they link to adaptor proteins (APs) (Robinson and Bonifacino 2001). The role of APs is complex. First, studies suggest that AP-3 likely functions as a clathrin adaptor protein and aids in signal mediated protein sorting events (Dell'Angelica, Klumperman et al. 1998). Secondly, AP1 and AP2 function to attach clathrin to the plasma membrane and help form complexes in the TGN (Robinson and Bonifacino 2001). AP180 homologues have been observed in yeast (Wendland and Emr 1998) and *Drosophila* (Zhang, Koh et al. 1998) where they were identified as participants in clathrin binding and endocytosis respectively. Likewise, *AP180/CALM* homologues identified in *C. elegans* presumably regulate endocyte vesicle size (Zhang, Koh et al. 1998). Finally, point mutations in the *CALM* gene led to ineffective hematopoiesis, functional iron deficiency, and altered growth in mice, suggesting that CALM may play a role in endocytosis-mediated iron transport (Klebig, Wall et al. 2003).

In addition to an established role in endocytosis, a recent study suggested that CALM may interact with nuclear proteins (Archangelo, Glasner et al. 2006). In this study, the novel protein CATS (CALM interacting protein, expressed in thymus and spleen) was shown to interact with a region of the CALM protein that is retained in the

CALM-AF10 fusion protein and increased the nuclear localization of both CALM and a CALM-AF10 fusion protein. This study further suggested that CATS may be important for malignant transformation mediated by CALM-AF10, through either mis-localization of the CALM-AF10 protein, or via transcriptional regulatory properties of the CATS protein (Archangelo, Glasner et al. 2006).

A single case report described an *MLL-CALM* fusion in a 12-week-old Caucasian female who presented with rapidly progressive AML (Wechsler, Engstrom et al. 2003). In this study, the authors used panhandle PCR to determine that *MLL* was fused to *CALM* at 11q14-q21. By assaying RNA from the patient's leukemic cells, fusion transcripts were identified. The breakpoints for this particular translocation were within *MLL* intron 7 (in the known *MLL* breakpoint cluster region) and *CALM* intron 7. This finding is intriguing since, in this case, *CALM* sequences are present at the 3' portion of the fusion gene, in contrast to *CALM-AF10* fusions, where *CALM* sequences form the 5' portion of the fusion gene. In addition the breakpoint lay within *CALM* intron 7, whereas the breakpoints for *CALM-AF10* fusions typically occur within *CALM* introns 17-19.

Structure and function of AF10

The *AF10* (also known as *MLLT10*) gene is located on chromosome 10p12 and encodes a 109-kDa protein containing 1,027 aa residues, and was initially cloned as an *MLL* partner gene in the recurrent t(10;11)(p13;q23) translocation (Chaplin, Bernard et al. 1995). It is important to note that the reference sequence for human *AF10* (NM_004641 or U13948) is missing 124 nucleotides between exons 22 and

23; these 124 nucleotides are present in most human expressed sequence tags (ESTs) and a homologous 124 nucleotide sequence is present in the mouse reference sequence (NM_010804). Insertion of these 124 nucleotides leads to a frameshift of the COOH terminal portion of the AF10 protein. Studies in both humans and mice have demonstrated that *AF10* expression is highest in the testis, and is also expressed in the thymus, ovary, colon, peripheral blood, brain, and kidney (Chaplin, Ayton et al. 1995; Linder, Jones et al. 1998). AF10 is a member of a small highly conserved protein family that includes the AF17, BR140, and CEZF proteins (Chaplin, Ayton et al. 1995; Linder, Newman et al. 2000). Although the precise function of AF10 is not known, both structural and functional data suggest that it functions as a transcription factor (Figure 1.3). The AF10 protein contains PHD (Plant Homeo Domains) fingers, which are structurally conserved domains present in a number of known transcription factors that are involved in chromatin-mediated gene regulation, including the CBP, MLL, TRX, and Drosophila Polycomb group (PCL) proteins (Aasland, Gibson et al. 1995). In addition to the N-terminal PHD domain, AF10 contains an extended PHD domain also known as a leukemia-associated protein domain (LAP) that functions in homo-oligomerization and is conserved in several other proteins including MLL, AF17, and BR140 (Linder, Newman et al. 2000). AF10 also contains an AT-hook motif, a motif that was initially described in the high-mobility group of non-histone chromosomal proteins and other DNA-binding proteins, and is thought to mediate protein binding to cruciform DNA (Aravind and Landsman 1998). In addition to these domains, AF10 contains a bipartite nuclear localization signal (NLS) and a C-

terminus glutamine-rich region. However, due to alternative splicing the latter is not present in all isoforms (Linder, Newman et al. 2000; Debernardi, Bassini et al. 2002).

A role for *AF10* in leukemic transformation was proposed as the gene was initially cloned as an *MLL* chromosomal translocation partner in 3 patients with AML-M5 and an *MLL-AF10* fusion (Chaplin, Ayton et al. 1995). An additional report presented two cases of pediatric AML-M5 in which there was paracentric inversion of the 11q region with chromosome 10p12 (Morerio, Rapella et al. 2005). Although pediatric acute megakaryoblastic leukemia (AML-M7) is considered rare, two independent case reports demonstrated fusions between *MLL* and *AF10* in pediatric patients (Borkhardt, Haas et al. 1995; Morerio, Rapella et al. 2005). Deletion analysis of the *MLL-AF10* fusion protein has demonstrated that the leucine zipper (LZ) motif in the carboxy terminus of AF10 is essential for leukemogenesis (DiMartino, Ayton et al. 2002), and the H3K79 methyltransferase hDOT1L has been shown to be involved in *MLL-AF10* mediated leukemogenesis through interaction of hDOT1L and AF10 (Okada, Feng et al. 2005).

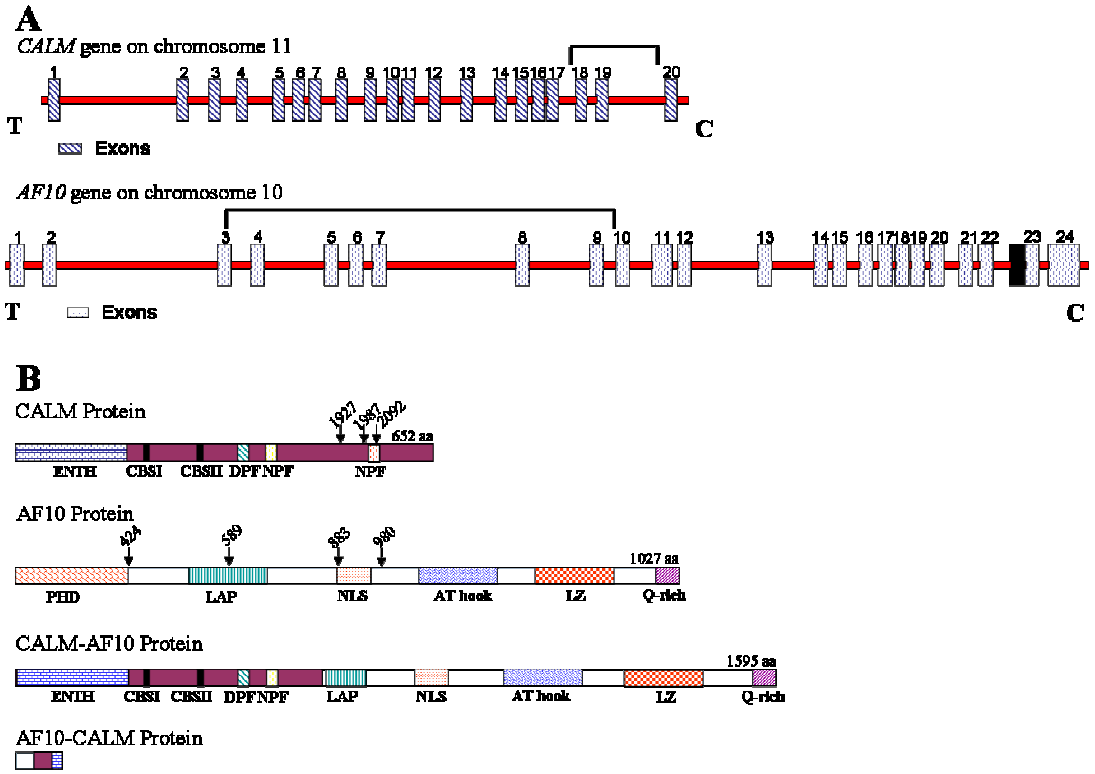

Figure 1.3. Structure of *CALM*, *AF10* and *CALM-AF10* fusions. (A) Schematic representation of the human *CALM* and *AF10* genes based on the reference sequences NM_007166 and U13948 respectively. *CALM* exons 1-20 are indicated by striped rectangles. The bracket spanning introns 18-19 indicate the genomic region where translocations are known to occur within *CALM*. *AF10* exons 1-24 are indicated by stippled rectangles. The bracket spanning introns 3-9 indicate the genomic region where translocations are known to occur within *AF10*. The black box immediately adjacent to exon 23 represents 124 bp of exon sequence this is present in most ESTs but missing from the reference sequence (U13948). Centromere (C) and telomere (T) orientation is as indicated. (B) Schematic representation of the predicted protein structure for CALM, AF10 and the two chimeric proteins CALM-AF10 and AF10-CALM. Protein domains are indicated in each structure: ENTH (espin N-terminal homology; Asp-Pro-Phe), DPF (ASP-Pro-Phe) motif, NPF (Asn-Pro-Phe) motif, CBS I & II (clathrin binding sequence I & II), PHD (plant homology domain), LAP (leukemia-associated protein), NLS (nuclear localization signal), LZ (leucine zipper), and Q (glutamine)-rich region. Vertical arrows indicate known nucleotide breakpoint regions.

Clinical features of leukemia with CALM-AF10 fusions

Although the t(10;11)(p13:q14-21) translocation was initially observed in a patient with histiocytic lymphoma, Groupe Français de Cytogénétique Hématologique (GFCH) subsequently identified the t(10;11) translocation as a recurrent reciprocal translocation in patients with T-cell acute lymphoblastic leukemia (GFCH 1991). *CALM-AF10* translocations appear to be most frequently associated with T-cell ALL, specifically T-cell ALL of either γ/δ or immature phenotypes. In the largest series of its kind, 20 cases of *CALM-AF10* fusion leukemias were identified in a study of 144 patients with T-ALL (Asnafi, Radford-Weiss et al. 2003). Patients with a *CALM-AF10* fusion ranged from 3-43 years of age (mean 20.7), and were more frequently male (M:F=2.8). WBC at presentation ranged from 3.3-556 x 109/L, and 8 of 20 patients had a mediastinal mass. Although the numbers were small, patients with a *CALM-AF10* fusion and an immature phenotype had a poor prognosis, as 10/12 patients either did not respond to therapy or relapsed. In contrast, 8/8 patients with a *CALM-AF10* fusion and a TCR γ/δ phenotype were in complete remission at the time of the report. In this series, *CALM-AF10* fusions were present in 12/29 cases with an immature TCR γ/δ phenotype and 8/32 cases with a TCR γ/δ phenotype, but in 0/78 α/β or IM β T-ALLs, demonstrating a marked bias toward T-cell ALL of the γ/δ lineage. This study also suggested that the *AF10* content of the *CALM-AF10* fusion might correlate with the stage of maturation arrest. All but the final four amino acid residues of the protein encoded by the *CALM* gene are retained in most *CALM-AF10* fusion transcripts (Figure 1.3) (Dreyling, Martinez-Climent et al. 1996; Asnafi, Radford-Weiss et al. 2003), although due to alternate splicing, 20, 35, or 55 amino

acid residues are excluded in some *CALM-AF10* fusions. At least four common *AF10* fusion sites have been described (Asnafi, Radford-Weiss et al. 2003). The resultant *CALM-AF10* fusion transcripts can be classified as either 5' or 3', depending on how much *AF10* sequence is included in the fusion transcript. 5' fusion transcripts, which retain almost all of the *AF10* coding sequence, are associated with TCRγδ T-cells, whereas 3' fusion transcripts, which contain less *AF10* sequence, are associated with more immature T-cells that do not express a TCR on the cell surface (Asnafi, Radford-Weiss et al. 2003).

CALM-AF10 fusions have also been observed in a variety of myeloid leukemias including AML-M0 ,M1, M2, M4, M5, and M7, as well as eosinophilic leukemia and granulocytic sarcoma (Table 1.1) (Kobayashi, Hosoda et al. 1997; Narita, Shimizu et al. 1999; Bohlander, Muschinsky et al. 2000; Salmon-Nguyen, Busson et al. 2000; Jones, Chaplin et al. 2001; Abdou, Jadayel et al. 2002; Nakamura, Maki et al. 2003; La Starza, Crescenzi et al. 2006; Abdelhaleem, Beimnet et al. 2007). Interestingly, most of the AML M0, M1, and M2 cases that have been analyzed show clonal *IGH*, *TCRG*, and/or *TCRD* gene rearrangements, suggesting that the target for malignant transformation may have been a multipotential hematopoietic precursor cell (Asnafi, Radford-Weiss et al. 2003; Deshpande, Cusan et al. 2006). *CALM-AF10* translocations have been identified in both children and adults with AML; specific lesions include splenomegaly, hepatomegaly, mediastinal masses, and CNS leukemia (Kumon, Kobayashi et al. 1999). Cytochemical and immunophenotypic data varies with the diagnosis but includes markers for lymphoid as well as myeloid antigens

(Kobayashi, Hosoda et al. 1997; Kumon, Kobayashi et al. 1999; Narita, Shimizu et al. 1999; Bohlander, Muschinsky et al. 2000).

Table 1.1 Characteristics of patients with the t(10:11) *CALM-AF10* translocation

Patient	Diagnosis	CALM-AF10 Breakpoint(s)	References
M/22	T-ALL	CALM 2091; AF10 589	Bohlander 2000
F/16	pre T-ALL	CALM 1926; AF10 883	Bohlander 2000
M/5	pre T-ALL	CALM 2091; AF10 979	Bohlander 2000
1	ALL	CALM 1926; AF10 980	Kumon 1999
2	ALL	CALM 2091; AF10 883	Kumon 1999
3	ALL	CALM 1926; AF10 589	Kumon 1999
F/10	ALL	NR	Kobayashi 1997
M/25	LBL	NR	Kobayashi 1997
F/17	T-ALL	NR	Salmon-Nguyen 2000
M/26	T-ALL	CALM 2091; AF10 979	Carlson 2000
M/12	T-ALL	CALM 1926; AF10 589	Carlson 2000
F/23	NHL Tcell LBL AML	NR	Carlson 2000
M/33	T-ALL TCRγδ	AF10 424	Asnafi 2003
M/29	T-ALL TCRγδ	AF10 589	Asnafi 2003
M/20	T-ALL TCRγδ	AF10 883/979	Asnafi 2003
M/15	T-ALL TCRγδ	AF10 589	Asnafi 2003
F/11	T-ALL TCRγδ	AF10 589	Asnafi 2003
M/7	T-ALL TCRγδ	NR	Asnafi 2003
M/6	T-ALL TCRγδ	AF10 589	Asnafi 2003
M/3	T-ALL TCRγδ	AF10 424	Asnafi 2003
M/43	T-ALL IMγ	AF10 589	Asnafi 2003
M/37	T-ALL IMγ	AF10 883/979	Asnafi 2003
M/28	T-ALL IMγ	AF10 883/979	Asnafi 2003
M/26	T-ALL IMγ	AF10 424	Asnafi 2003
M/25	T-ALL IMγ	AF10 883/979	Asnafi 2003
F/25	T-ALL IMδ	AF10 883/979	Asnafi 2003
M/24	T-ALL IMγ	AF10 883/979	Asnafi 2003
M/23	T-ALL IMγ	AF10 424	Asnafi 2003
F/20	T-ALL IMγ	AF10 883/979	Asnafi 2003
M/14	T-ALL IMδ	AF10 883/979	Asnafi 2003
F/12	T-ALL IMδ	AF10 883/979	Asnafi 2003
F/12	T-ALL IMγ	AF10 883/979	Asnafi 2003
F/78	B-ALL	AF10 883/979	Asnafi 2003
M/18	AUL	AF10 883/979	Asnafi 2003
M/18	AUL	AF10 883/979	Asnafi 2003
F/29	AUL	AF10 589	Asnafi 2003
M/39	AUL	CALM 2091; AF10 424	Asnafi 2003
M/13	T-ALL	CALM 2091; AF10 424	La Starza 2003
F/38	T-ALL	CALM 2091; AF10 589	La Starza 2003

Table 1.1 Characteristics of patients with the t(10:11) *CALM-AF10* translocation (Cont.)

Patient	Diagnosis	CALM-AF10 Breakpoint(s)	References
U937	Histiocytic Lymphoma	CALM 2091; AF10 423	Dreyling 1996
M/19	AML-M1	CALM 1926; AF10 883, CALM 2091; AF10 883	Bohlander 2000
M/47	AML-M0	CALM 1926; AF10 883	Bohlander 2000
F/21	AML-M1	CALM 1926; AF10 589, CALM 2091; AF10 589	Bohlander 2000
4	AML-M0	CALM 2091; AF10 589	Kumon 1999
M/12	AMoL	NR	Kobayashi 1997
F/30	Granulocytic sarcoma	NR	Kobayashi 1997
M/6	AML-M7	CALM 1926; AF10 424	Jones 2001
F/10	Acute eosinophilic leukemia	NR	Salmon-Nguyen 2000
M/16	AML-M4	CALM 1926; AF10 424	Nakamura 2003
M/20	AML-M4	NR	Abdou 2002
F/44	AML-M0	CALM 2091; AF10 424	Carlson 2000
F/28	AML-M1	CALM 2091; AF10 883	Carlson 2000
M/41	AML-M5	CALM 2091; AF10 979	Carlson 2000
F/4	AML-M7	CALM 2091; AF10 423	Abdelhaleem 2007
M/2	AML-M7	CALM 2091; AF10 796	Abdelhaleem 2007
M/25	AML-M1	AF10 883/979	Asnafi 2003
F/16	AML-M1	AF10 424	Asnafi 2003
M/22	AML-M0	CALM 2091; AF10 883	Asnafi 2003
F/33	AML-M2	CALM 1926; AF10 883	Asnafi 2003
F/36	AML-M1	CALM 2091; AF10 978	Asnafi 2003
M/19	AML-M1	CALM 2091; AF10 424	Deshpande 2006
M/47	AML-M1	CALM 2091; AF10 424	Deshpande 2006
F/12	AML-M1	CALM 2091; AF10 424	Deshpande 2006
F/19	AML	CALM 2091; AF10 1048	Deshpande 2006
F/4	AML-M5a	NR	Deshpande 2006
F/12	AML-M1	CALM 2091; AF10 424	La Starza 2003
M/36	AML-M2	NR	La Starza 2003
M/27	AML-M0	CALM 2091; AF10 424	La Starza 2003
M/47	AML-M1	CALM 2091; AF10 424	La Starza 2003
M/19	AML-M1	NR	La Starza 2003

Abbreviations: AML, acute myeloid leukemia; Amol, acute monocytic leukemia; AUL, acute undifferentiated leukemia; LBL lymphoblastic lymphoma; NHL, non-Hodgkin's lymphoma; NR, not reported; T-cell ALL, T-cell acute lymphoblastic leukemia.

Mouse Models of *CALM-AF10* Leukemia

Animal models have provided tractable systems with which to study a wide range of human diseases, including the recurrent chromosomal translocations involved in hematologic malignancies (Rabbitts 2001). Given the shared physiology between mice and humans, the mouse has become a standard animal model used to study pathophysiology and explore novel therapeutic approaches. Chromosomal translocations have been studied in mouse models using a variety of techniques including retroviral transduction and bone marrow transplantation as well as gene-targeting and transgenic approaches (Rabbitts 2001; Bernardi, Grisendi et al. 2002; Forster, Pannell et al. 2005). Recently, two groups have published reports that used mice to study *CALM-AF10* leukemia; findings from each of these reports are summarized in Table 1.2.

The first study used a vector based RNA interference system to "knock down" *CALM-AF10* expression in the U937 cell line, which expresses a CALM-AF10 fusion protein. The "knock-down" clones proliferated less rapidly *in vitro*, and showed a modest survival benefit following xeno-transplantation into NOD/SCID mice (median survival 27 vs. 19.5 days post transplant) (Okada, Jiang et al. 2006).

A second study used retroviral transduction and bone marrow transplantation to generate acute leukemia in mice (Deshpande, Cusan et al. 2006). Recipient mice transplanted with bone marrow cells that expressed a *CALM-AF10* fusion gene developed disease a median of 110 days following transplantation. Mice with

leukemia were anemic and had circulating blasts. Parenchymal infiltration by leukemic myeloid cells was noted in a variety of organs and these cells were positive for the myeloid markers myeloperoxidase and chloracetate esterase. Further analysis of leukemic cells from these mice demonstrated that myeloid cells positive for Mac1 and Gr1 were also positive for the lymphoid marker B220 and had clonal immunoglobulin DH-JH rearrangements, consistent with the observation of clonal *IGH* gene rearrangements in patients with *CALM-AF10* fusions, and suggesting that the target cell for malignant transformation was multi-potential. Interestingly, these authors went on to show that AML could be propagated from a leukemic cell with lymphoid features, as Mac1+ myeloid leukemia could be established by serial transplantation of Mac1+/B220+ or Mac1-/B220+ leukemia cells (Deshpande, Cusan et al. 2006).

Table 1.2 Summary of *CALM-AF10* Mouse Models

Model	Mouse Strain	Disease	Survival Median (range)	Immunophenotype Markers	Tissue/Organ Involvement	Antigen Receptor Gene Rearrangement	Serial Transplantation	Reference
Xenograft of siRNA clones	NOD/SCID	AML	19.5 d (16-23d) control 27d (22-33d) siRNA clones	CD45	Spleen, Kidney, Pancreas	not applicable	nd	Okada, 2006
Retroviral infection and bone marrow transplantation	C57Bl/6xC3H	AML	110 d (46-366d)	Mac1++, Gr1++, B220+/-, MPO++	Bone Marrow, Spleen, Liver, Lung, Kidney, Brain, Intestine	*Igh*	yes	Deshpande, 2006

Abbreviations: AML, acute myeloid leukemia; d, day; FVB, Friend virus B-type; nd, not done; NOD/SCID, non-obese diabetic/severe combined immunodeficiency.

Putative targets of the *CALM-AF10* fusion gene

Understanding the flow of genetic information that occurs between the chromosomal translocation and the protein product that results as a consequence of these mutations is critical to the identification of therapeutic targets and development of effective therapies (Rabbitts and Stocks 2003). In many events these fusion proteins are either transcription factors that regulate hematopoietic cell differentiation or tyrosine kinases that control cellular proliferation (Aplan 2006). Gene expression profiling of patients with AML has identified several putative targets including members of the Polycomb group (PcG), HOX, and MEIS1 genes (Grubach, Juhl-Christensen et al. 2008). Furthermore, additional experiments have shown that *HOXA* cluster genes, including *HOXA5*, *HOXA9*, and *HOXA10* are upregulated in the leukemic cells of patients with *CALM-AF10* fusions (Dik, Brahim et al. 2005). In this same study *BMI1*, a PcG member that is located in close proximity to AF10 on chromosome 10 was also aberrantly expressed (Dik, Brahim et al. 2005). This finding suggests that genes that are juxtaposed to fusion genes and differentially expressed may contribute to a growth advantage of malignant clones. In addition, U937 cells (which express a *CALM-AF10* fusion) transduced with an siRNA directed to the *CALM-AF10* fusion showed a modest decrease in *HOXA5*, *HOXA7*, *HOXA9*, and *HOXA10* expression (Okada, Jiang et al. 2006). This same study suggested that *CALM-AF10* upregulates *HOXA* genes, particularly *HOXA5*. In this study, it was shown that hDOT1L contributes to *CALM-AF10* leukemia by preventing the nuclear export of CALM-AF10 and upregulating the Hoxa5 gene through H3K79 methylation (Okada, Jiang et al. 2006).

Mammalian *HOX* genes are members of the evolutionarily conserved homeodomain family of genes that are structurally organized into four discreet clusters (A, B, C, and D), located on four different chromosomes in mammals, that encode for transcription factors (Garcia-Fernandez 2005; Pearson, Lemons et al. 2005). In addition to their well-studied role as executive regulators of anterior-posterior body pattern organization during early embryonic development, *HOX* genes play a fundamental regulatory role in hematopoietic system organization and development (van Oostveen, Bijl et al. 1999). Of the distinct clusters, A, B, and C, but not D are thought to be important for normal hematopoiesis (Abramovich and Humphries 2005). Gene ablation studies have shown specifically that *Hoxa9*, *Hoxc8*, and *Hoxb6* are necessary for hematopoietic cells to progress though development (Abramovich and Humphries 2005). In addition to their role in normal development, *HOX* genes also play roles in cell cycle control, cell adhesion, and cell death. Given the central role of *HOX* genes in normal development, it is not surprising that *HOX* genes have been implicated in a number of neoplastic and non-neoplastic disease processes (Grier, Thompson et al. 2005).

Several lines of evidence, based on clinical observations as well as data from experimental animal models, suggest that *HOX* genes are involved in leukemic transformation. First, global gene expression profiling has identified *HOX* genes as being consistently overexpressed in AML (Armstrong, Golub et al. 2003; Mullighan, Kennedy et al. 2007). Chromosomal translocations lead to fusions of *NUP98* with *HOXA9*, *HOXA11*, *HOXA13*, *HOXC11*, *HOXC13*, *HOXD11*, and *HOXD13* in

patients with myelodysplastic syndrome (MDS) or AML (Lam and Aplan 2001). Chromosomal translocations also lead to ectopic expression of *HOXA* cluster genes by juxtaposition of *TCRA* regulatory elements with *HOXA* coding sequences in some patients with T-cell ALL (Soulier, Clappier et al. 2005; Speleman, Cauwelier et al. 2005). In addition to these translocations which directly lead to overexpression of *HOX* genes, a number of recent studies have demonstrated that chromosome translocations which result in *MLL* fusions lead to unscheduled expression of *HOX* genes in both AML and T-cell ALL patients (Hess 2004).

Direct experimental evidence supporting a role for *Hox* gene dysregulation in myeloid leukemia comes from several mouse models. Transplantation of bone marrow cells that overexpressed *Hoxa5*, *Hoxa9*, or *Hoxa10* consistently led to myeloid expansion, and, in collaboration with the *Hox* cofactor *Meis1*, AML (Abramovich and Humphries 2005; Grier, Thompson et al. 2005). Transplantation of bone marrow cells that overexpressed *Nup98-Hox* fusions led to abnormal myeloid differentiation and AML, again in collaboration with *Meis1* (Kroon, Thorsteinsdottir et al. 2001; Pineault, Buske et al. 2003; Pineault, Abramovich et al. 2004). Lastly, transgenic mice that expressed a *NUP98-HOXD13* fusion showed upregulation of *Hoxa7*, *Hoxa9*, and *Hoxa10*, and developed a myelodysplastic syndrome (MDS) that progressed to acute leukemia in about half of the mice (Lin, Slape et al. 2005). Finally, a number of *Hox* genes and *Hox* co-factors, including *Hoxa7*, *Hoxa9*, *Meis1* and *Pbx1* are among the most common upregulated genes in murine leukemias that

result from retroviral insertional mutagenesis (Nakamura T, Largaespada DA et al. 1996).

In summary, *HOXA* cluster genes are associated with normal hematopoietic development and are upregulated in patients with leukemia. The *CALM-AF10* gene is associated with increased expression of *HOXA* genes and inhibition of *CALM-AF10* results in a modest decrease in *HOXA* expression in vitro. These findings suggest that the *CALM-AF10* fusion gene may be involved in the aberrant upregulation of *HOXA* genes that result in impaired hematopoietic cell differentiation. Therefore, the *HOXA* genes in particular may be important therapeutic targets in patients with *CALM-AF10* leukemias.

Thesis goals and outline

CALM-AF10 fusions result from a rare but recurring t(10;11) chromosomal translocation seen in both adult and pediatric patients with AML or ALL, and are often associated with a poor prognosis. In the context of a current working model for AML, in which complementary mutations that lead to either impaired differentiation or increased proliferation collaborate to produce a fully leukemic clone, (Gilliland and Tallman 2002) it seems likely that the *CALM-AF10* fusion functions to impair differentiation based on its influence on *HOXA* cluster gene expression. The corollary of this hypothesis is that *CALM-AF10* leukemias should acquire spontaneous mutations leading to increased proliferation. In this study, it is the hypothesized that mice which express an aberrant fusion protein associated with acute

leukemia will develop acute leukemia, demonstrating that the fusion protein is indeed leukemogenic. To accomplish this, the following three specific aims are proposed:

- Characterize leukemia in a transgenic mouse that expresses *CALM-AF10*
- Identify (through insertional mutagenesis) genes which collaborate with *CALM-AF10* to induce leukemia
- Identify differentially expressed genes in *CALM-AF10* hematopoietic precursor cells

A discussion will be provided in chapter 2 that focuses on the development of a transgenic mouse model that expresses a fusion *CALM-AF10* cDNA. These transgenic mice develop a myeloid leukemia with lymphoid features after a long latency period and incomplete penetrance. In addition to these findings, the *CALM-AF10* transgenic mice have impaired T-cell differentiation.

Chapter 3, will focus on acceleration of leukemia in *CALM-AF10* transgenic mice infected with MOL4070LTR virus. The identification of potential collaborating genes using retroviral insertional mutagenesis, anchored PCR, and sequence analysis will also be reported. A description of the clinical and pathological findings identified in both *CALM-AF10* transgenic mice and FVB wild-type mice infected with the MOL4070LTR virus will be provided. Two potential collaborating genes and/or pathways that were identified through Southern blot analysis and RQ-RTPCR that were initially identified by PCR will also be described.

Chapter 4 will demonstrate that *Hoxa* cluster genes are upregulated, as determined by RQ-RTPCR analysis in *CALM-AF10* transgenic mice as well as in tumors from these mice. There will also be a report on differentially expressed genes using microarray analysis that are upregulated in the bone marrow from clinically healthy *CALM-AF10* transgenic mice. Here it was confirmed that *Hoxa9* and *Meis1* are important genes in *CALM-AF10* mice. In addition to these genes, an additional gene was also identified as being was up-regulated, desmoplakin. Not only was there an up-regulation in *abd b Hox* genes, but there was also a concomitant down regulation of immunoglobulin genes as well.

In chapter 5, an overall discussion and conclusion will be presented that will offer insight regarding the utility of this mouse model and the direction of future experiments.

Chapter 2: Characterization of the transgenic mouse for t(10;11) (p13; q14) chromosomal translocation

Introduction

Because cancer develops in the context of an intact organism, with the influence of nearby cells and tissues, genetically engineered animal models have become a standard model for demonstrating that a lesion associated with any form of malignancy causes the malignancy (Bernardi, Grisendi et al. 2002). Moreover, generation of genetically engineered mouse models allows one to study the process of malignant transformation over time *in vivo*.

Until now, mouse models for the t(10;11) chromosomal translocation have only included xenograft and retroviral transduction systems. This chapter will describe the characterization of a transgenic model for *CALM-AF10*. It will also be shown that the fusion gene leads to impaired hematopoietic differentiation in clinically healthy mice. Finally, the phenotypic features of mice that developed acute leukemia will be discussed.

Materials and Methods

Generation of Transgenic Mice

A *CALM-AF10* fusion cDNA fragment was amplified from the U937 cell line using RT-PCR, and fragments of *CALM* and *AF10* derived from EST clones were ligated to the 5' and 3' portion of the fusion cDNA. Although several different *CALM-AF10* fusion cDNAs have been described (Asnafi, Radford-Weiss et al. 2003), the predominant fusion cDNA that was detected in the U937 cell line joined *CALM* nucleotide 2230 (Genbank reference NM_007166.2) to *AF10* nucleotide 241 (Genbank reference NM_001009569.1). Next, the fusion cDNA 5' and 3' was extended by ligating portions of *CALM* and *AF10* cDNAs to the *CALM-AF10* PCR product, and introduced a human beta-globin 5' untranslated region to aid in the translation of the *CALM-AF10* fusion mRNA. The entire coding sequence of the *CALM-AF10* cDNA was 4881 nucleotides encoding a 1627 aa protein (see Appendix I for nucleotide sequence). The resultant cDNA was cloned into the *Sfi*I and *Not*I sites of the HS21/45-*vav* vector to orchestrate expression specifically in the hematopoietic tissue compartment (Adams, Harris et al. 1999). In order to delete all plasmid backbone sequences, the *CALM-AF10* insert was then shuttled into the pSV40zeo (Invitrogen, Carlsbad, CA) vector by using a partial *Hin*dIII digest. The resultant plasmid, pSVZvavCA was digested with *Pme*I to remove all plasmid sequences. The *CALM-AF10* expression cassette was purified over a sucrose gradient, and FVB/N zygotes were microinjected with the construct at the NCI transgenic animal facility (NCI-Frederick, Frederick MD). Transgenic mice that had incorporated the construct were identified by Southern blot analysis of tail DNA.

Genotyping

The transgenic lines were maintained by breeding to wild-type FVB/N mice. Offspring of the founders were genotyped using polymerase chain reaction (PCR) amplification of the *CALM-AF10* fusion gene from tail biopsy at weaning (2 months of life). Briefly, approximately 6 mm of the distal tail was removed by sharp dissection and placed into an Eppendorf tube labeled with the mouse identification that corresponded to mouse ear tag, snap frozen in dry ice and stored at -80°C until the time of genotyping. To extract genomic DNA used for genotyping, 2 mm of frozen tail was sterilely cut and placed into an Eppendorf tube containing 300 µl of 250 µM NaOH and heated to 95°C for 60 min. Following heating, 25µl of 1M Tris Buffer, pH 7.5 (Quality Biologicals, Gaithersburg, MD) was added to each sample, vortexed and centrifuged in a table-top centrifuge at full speed for 6 minutes and stored at 4°C until time for PCR analysis. The genotype of each sample was determined by PCR assay using 1 µl of supernatant from each boiled DNA sample in a mixture of 17 µl of PCR Supermix High Fidelity (A 22 U/ml DNA polymerase mixture in 66 mM Tris-SO4 (pH 9.1 at 25°C), 19.8 mM (NH4)2SO4, 2.2 mM MgSO4, 220 µM dGTP, 220 µM dATP, 220 µM dTTP, 220 µM dCTP and stabilizers) (Invitrogen), and 10 µM of each of the following primers: 5'TGTTCCTGTAATGACGCAACCAACC3' and 5'CTCTGGAATATACAGGGCACAAACA3'. Samples were then processed in a PTC-200 Peltier Thermal Cycler (MJ Research, Watertown, MA) at a thermal cycling profile of 94°C for 3 min; 34 cycles of 94°C for 30 seconds, 62°C for 30 seconds, 72°C for one min; followed by a terminal extension of 72°C for 10 min. Quality

control of the DNA samples was determined by PCR analysis for *SCID* gene using the following primers 5'GGAAGAGTTTTGAGCAGACAATG3' and 5'CATCACAAGTTATAACAGCTGGG3'. Samples were processed in a PTC-200 Peltier Thermal Cycler (MJ Research, Watertown, MA) at a thermal cycling profile of 94°C for 3 min; 29 cycles of 94°C for 60 seconds, 54°C for 60 seconds, 72°C for one minute; followed by a terminal extension of 72°C for 5 min. See Appendix II for an example of genotype results.

Expression of the CALM-AF10 transgene

RNA extraction from tissue

Expression of the *CALM-AF10* transgene was determined by Northern blot analysis and RT-PCR. Total RNA was isolated from thymus, spleen, bone marrow, liver and kidney of mice using Trizol (Invitrogen) reagents and protocols. To extract the RNA, frozen tissue was cut using a razor blade and placed into a 1.5 ml Eppendorf tube that contained 200 µl of Trizol. The tissue was ground using an electric tissue grinder, and 800 µl of additional Trizol was added to the tube. After a five minute incubation at room temperature, 200 µl of chloroform (Mallinkrockdt Baker, Paris KY) was added to each sample and vortexed vigorously for 15 seconds, followed by a 2-3 min incubation at room temperature. Samples were placed into a table top centrifuge and spun at 12000 x g for 15 min at 4ºC. The organic supernatant layer was removed and transferred to a clean Eppendorf tube and 500 µl of isopropanol (Mallinkrockdt Baker) was added, gently mixed and incubated on ice for 10 min. Next, samples were spun at 12000 x g for 10 min at 4ºC. The supernatant was decanted and 1 ml of 75 per cent ethanol (Warner-Graham Company, Cockeysville, MD) was added and

samples were then spun at 7500 x g for 5 min at 4ºC. The supernatant was decanted and samples were air-dried for 5-10 min and resuspended in 60 µl of deionized water and stored at -80ºC until future use.

Northern blot analysis

Total RNA (10µg) was size-fractionated on an agarose/formaldehyde gel, transferred to a nitrocellulose membrane (Schliecher & Schuell, Dassel, Germany) over night (O/N) using 20X Salt Sodium Citrate (3.0 M NaCl, 0.3 M Sodium Citrate, pH 7.0; SSC) buffer (Roche Diagnostics, Indianappolis IN). The next day the membrane was removed, crosslinked with 1200 µ joules x100 UV light in a UV Stratalinker 1800 (Stratagene, La Jolla, CA) and hybridized with a ^{32}P-labeled-human *CALM* fragment (0.5 kb HindIII-EcoRI fragment; nucleotides 1588-2121 of NM_007166.2) as described below.

The nitrocellulose membrane was prehybridized with 20 ml of NC Hybridization Solution (100 ml 20X SCC (Roche), 1.75 ml of 1M Tris HCl, ph 7.5, 10 mg Herring sperm DNA (Invitrogen), 200 ml Formamide (Sigma), 8 ml-50X Denhardt's solultion (a solution of ficoll, bovine serum albumin, polyvinylpyrrolidone, and a high concentration of non-specific DNA to prevent non-specific binding of DNA) and 84.5 ml deionized H_20 added to 100 ml of 50% Dextran Sulfate (Ichemicon International, Temecula, CA) in a glass hybridization bottle for two to four hours at 42ºC in a rotating hybridization oven. To generate the radiolabled probe, 50 ng of DNA fragment was resuspended in a total volume of 45 µl deionized H_20 (diH_20), boiled for 3 min in a water bath, followed by 3 min on wet ice. Next, the DNA fragment

was mixed with Ready-To-Go™ DNA Labeled Beads (dCTP) (Amersham, Bioscience, Little Chalfont Buckinghamshire, England) and labeled with 5 µl of ^{32}P-dCTP (10µCi/mL) at 37°C for 30 min. The labeled probe (total volume 50 µl) was purified over a Performa DTR Gel Filtration Cartridge (EdgeBio, Gaithersburg, MD) and diluted in 500 µl of diH20. Two hundred and fifty µl of the diluted probe was added to 1.0 mg of Herring Sperm (Invitrogen). Next, the probe was denatured by adding 50 µl of 10 mM NaOH for 1 min, and neutralized by adding, 140 µl of 1 M Tris pH 7.5, 1 min and 500 µl of 1M HCl for 1 min. The total mixture was transferred to 20 ml of hybridization solution. The total mixture was added to the prehybridized membrane for overnight incubation at 42°C.

On the following day, the nitrocellulose membrane underwent stringency washes for 20 min x 3 in 200 ml of 0.1x SSC/0.1% SDS (Sodium Dodecyl Sulfate, Quality Biological, Inc.) at 52°C. After the last wash, the membrane was removed, wrapped in clear plastic wrap and placed in an intensifying screen-containing film cassette with BioMax XAR film (Kodak, Rochester, NY) and stored overnight at -80°C. The film was removed from the cassette and exposed using an RP-X-OMAT Processor, Model M6B (Kodak) auto processor.

RT-PCR

RT-PCR amplification of the *CALM-AF10* mRNA was performed by first DNA-ase treating 10 µg of RNA with 2U/µl rDNase, and 0.1 vol 10X DNase I buffer (Ambion, Austin, TX) in a total volume of 50 µl. The samples were incubated for 20-30 min at 37ºC. To inactivate the DNase, 0.1 vol DNase Inactivation Reagent was added to

each sample, vortexed and incubated at room temperature for 2 min. Each sample was centrifuged at 10,000 x g for 1. 5 min at room temperature and the supernatant was transferred to a new new tube. One microgram of total *DNase*-treated RNA was mixed with *Superscript*II reverse transcriptase (RT) and random hexamer primers (Invitrogen) in a volume of 20 µL. One to two microliters of the reverse transcription reaction was used to amplify the *CALM-AF10* fusion with 23 µl of PCR Supermix High Fidelity (Invitrogen) (previously described), and 1 µl each of 10 µM of primers 5'TGTTCCTGTAATGACGCAACCAACC3' and 5'CTCTGGAATATACAGGGCACAAACA 3' and a thermal cycling profile of 94°C for 3 min; 34 cycles of 94°C for 30 seconds, 62°C for 30 seconds, 72°C for one min; followed by a terminal extension of 72°C for 10 min. To ensure quality control of the cDNA, one to two microliters of the reverse transcription reaction was also used to amplify the housekeeping gene β-actin using 1 µl each of 10 µM mouse primers 5'TGTTCCTGTAATGACGCAACCAACC3' and 5'CTCTGGAATATACAGGGCACAAACA3' (for mouse tissues) or the human primers 5'AGGCCGGCTTCGCGGGCGAC3' and 5'CTCGGGAGCCACACGCAGCTC3' (for the human cell line U937) and a thermal cycling profile of 94°C for 3 min; 34 cycles of 94°C for 30 seconds, 62°C for 30 seconds, 72°C for one min; followed by a terminal extension of 72°C for 10 min. PCR products were size fractionated by agarose gel electrophoresis and visualized under UV light (Eagle Eye II, Stratagene).

To verify that the *CALM-AF10* transgene was indeed expressed in γδ T-cells, purified γδ T-cells were extracted from total *CALM-AF10* transgenic spleen using a TCR $\gamma\delta^+$ T-cells isolation kit specific for mouse (Miltenyi Biotec, Auburn CA). First, splenocytes were physically extracted from the spleen and collected into PBS, pH 7.2, with 0.5% BSA. Following single cell suspension, cells were passed through a 30 µm nylon mesh to remove cell clumps and stromal elements. Next cells were centrifuged at 300xg for 10 min, the supernatant was removed, and cells were resuspended in 450 µl of buffer per 10^8 total cells. Fifty microliters of Non-T Cell Depletion Cocktail (Cocktail of Microbeads conjugated to monoclonal antibodies against mouse CD45R, mouse CD11b), and a biotin-conjugated monoclonal antibody against mouse TCR γ/δ cells, Miltenyi Biotec was added to the cells and incubated for 15 minutes at 4ºC. Following the incubation, the non-T cells were depleted using direct magnetic labeling with CD45R and CD11b Microbeads by passing the cell suspension through an LD magnetic column (Miltenyi Biotec), which retains the non-T cells. Note that the cells were simultaneously labeled with a biotin-conjugated monoclonal antibody against mouse TCR γ/δ cells for downstream collection of the γ/δ^+ T cells. The flow-through fraction of pre-enriched T-cells was collected, centrifuged at 300xg for 10 min, the supernatant was removed and the cells were resuspended in 450 µl of buffer. In order to positively select the γ/δ^+ T-cells, 50 µl of Anti-biotin Microbeads (Miltenyi Biotec) was added to the cell suspension, and incubated for 15 min at 4ºC. Following the incubation, the cells were washed by adding 10-20x labeling volume of buffer and centrifuged at 300xg for 10 min. The supernatant was removed completely and the cells were resuspended in 500 µl of buffer. The cell suspension

was applied to an MS Column (Miltenyi Biotec) and washed 3x with 500 µl of buffer. Once the column was empty of the final wash buffer, 1 ml of wash buffer was placed into the column and the TCR γ/δ^+ T-cells were flushed into a clean collection tube using the plunger supplied with the column. RT-PCR was performed on *DNase* treated RNA extracted from the TCR γ/δ^+ T-cells for the expression of *CALM-AF10* as described above. RT-PCR products were size fractionated on an agarose gel and transferred to a nitrocellulose membrane (Schliecher & Schuell) and then hybridized with a ^{32}P labeled *CALM-AF10* probe using procedures described above.

Evaluation of leukemic and healthy mice

A cohort of 38 transgenic (lines C10 and E6) and 33 wild-type littermate controls were housed together and observed daily for signs and symptoms of disease. Statistical analysis was done by chi-square with 1 df at 18 months of age. Whole blood was obtained from tail veins for complete blood counts (CBC) and morphological evaluation in attempts to detect leukemia in clinically healthy mice. Mice that showed signs of disease such as ruffled fur, hunched posture, or difficulty in breathing were euthanized for postmortem evaluation. Mice that were found dead were also dissected and tissues placed in formalin as below, unless the tissues were judged to be severely decomposed. Tissue samples including the liver, kidney, spleen, thymus, bone marrow, lung, and heart were fixed in 10% neutral buffered formalin (Sigma, St. Louis, MO), paraffin embedded, sectioned at 5 µm, and stained with hematoxylin and eosin (HE) or anti-myeloperoxidase (MPO; DAKO), CD3 (DAKO, Carpinteria, CA), F4/80 (Caltag, San Francisco, CA),and B220 (CD45R; Pharmingen, San Diego, CA). The Bethesda proposals for classifying nonlymphoid

hematopoietic and lymphoid neoplasms in mice were used as guides to evaluate tissues from ***CALM-AF10*** mice (Kogan, Ward et al. 2002; Morse, Anver et al. 2002). Single-cell suspensions were prepared from thymus, spleen, and/or bone marrow and incubated with fluorescein isothiocyanate (FITC), Phycoerythrin (PE) (Pharmingen, San Diego, CA), Allophycocyanin (APC) and Phycoerythrin-Cy5 (PE-Cy5) (eBioscience, San Diego, CA) and subsequently analyzed by three-color flow cytometry to determine immunophenotype. (FITC)–conjugated antibodies used were anti–mouse CD8, B220 and, Gr-1; (PE)–conjugated antibodies used were anti–mouse CD4, IgM, and Mac-1; (APC)-conjugated antibodies used were anti-mouse CD19, CD117, and IgM (eBioscience, San Diego, CA); and (PE-Cy5)-conjugated antibodies used were antimouse CD24. To identify Lin-/Sca-1+/c-Kit+ (“LSK”) cells, mouse bone marrow cells were resuspended with Hank’s balanced salt solution containing 2% FBS (HF2) at $1X10^7$ cells/mL. The cells were incubated with a biotin conjugated lineage antibody cocktail (CD5, TER119, B220, GR-1, Mac-1, Stemcell Technologies, Vancouver, Canada), Streptavidin conjugated to APC (Pharmingen), anti-cKit conjugated to FITC (Pharmingen) and anti-Sca-1 conjugated to PE (Pharmingen). The stained cells were resuspended with HF2 containing 1ug/mL of propidum iodide (Sigma). Four-color staining was used to identify LSK cells. Statistical differences between groups was done using a two-sided student’s t test.

Southern blot analysis for Tcrb, Tcrd, and Igh gene rearrangements

DNA extraction using proteinase K digestion

A three mm cubed section was cut from either liver, spleen, or thymus that had been previously snap frozen and stored at -80°C and placed into a 15-ml Falcon tube which contained six milliliters of DNA lysis buffer (200 mM NaCl, 20 mM EDTA, 40 mM TrisHCl, pH 8.0, 0.5% SDS) with 80 µg of proteinase K (20 mg/ml) (Invitrogen) and incubated at 50°C overnight (O/N) in a waterbath. On the next day (Day 2), 10 ug of RNaseA was added to the lysis solution and incubated at 37ºC. Next, three milliliters of saturated NaCl solution (approximately 6M) was added, shaken vigorously and incubated on ice for 20 minutes followed by centrifugation at 3313xg (4000 rpm) for 20 minutes. The supernatant (~ 7 ml) was removed and placed into a 50-ml Falcon tube (Becton Dickenson Labware, Franklin Lakes, NJ). Next, ~15 ml of 100% ethanol (Warner-Graham Company, Cokeysville, MD) was added to the supernatant and allowed to incubate at room temperature in order for DNA precipitation to occur. The precipitated DNA was removed using a Pastuer pipette, washed twice in 70% ethanol and air-dried. The DNA was resuspended in 100 µl of deionized H_2O and stored at 4ºC until further use.

Ten micrograms of genomic DNA from mouse liver, spleen, or thymus was digested with either 30 Units (U) of *Hin*dIII or *Sst*I (for ***Tcrb*** and ***Tcrd*** gene rearrangements), or 30 U of ***Eco***RI or ***Xba***I (for ***Igh*** rearrangements), size-fractionated on a 0.8% agarose gels over night. The following day the gel was denatured for one hour in 800 ml denaturing buffer (40 ml, 10N NaOH, 240 ml 5M NaCl, and 1720 deionized H_20), neutralized for one hour in 800 ml neutralizing buffer (240 ml, 5M NaCl and 1760 ml

1M Tris, pH 7.5) and transferred to nitrocellulose membranes (Schliecher & Schuell) O/N using 20X SSC buffer (Roche). The next day the membrane was removed and crosslinked with 1200 μ joules x100 UV UV light in a UV Stratalinker 1800 (Stratagene). Next, the membrane was washed briefly (30 seconds) in deionized H_2O and baked at 80ºC for 15 minutes and stored at room temperature (R/T) until hybridization. Nitrocellulose membranes were hybridized and probes were prepared by random priming as described above. The nitrocellulose membrane was hybridized to a ^{32}P-labeled *TCRB* probe that detects the constant region of both ***Tcrb1*** and *Tcrb2* gene or to a ^{32}P-labeled J 1 ***TCRD*** probe (Begley CG, Aplan PD et al. 1989) that detects the Jδ1 and constant regions of *Tcrd*, or to a ^{32}P-labeled murine *Igh* probe that hybridizes to the JH3-4 region of the mouse *Igh* locus which was provided as a gift from Dr. Michael Kuehl (Lang, Stanton et al. 1982).

Results

Generation of mice that express a CALM-AF10 fusion gene.

Transgenic *CALM-AF10* mice were generated by pronuclear injection of FVB/N single cell embryos, and eight potential founders were identified by Southern blotting of tail DNA. Four founders were bred and all four transmitted the transgene. F1 mice were euthanized to determine expression of the transgene. As expected, the *CALM-AF10* transgene was expressed in hematopoietic tissues (thymus, bone marrow, and spleen), but not in non-hematopoietic tissues (liver, kidney) (Figure. 2.1B, C). Complete blood counts (CBC) were obtained from clinically healthy offspring of the *CALM-AF10* founders aged 6-10 months; although the *CALM-AF10* transgenic mice had increased numbers of atypical lymphocytes (data not shown),

there were no statistical differences in, white blood cell, neutrophil, lymphocyte, hemoglobin, or platelet counts (Table 2.1).

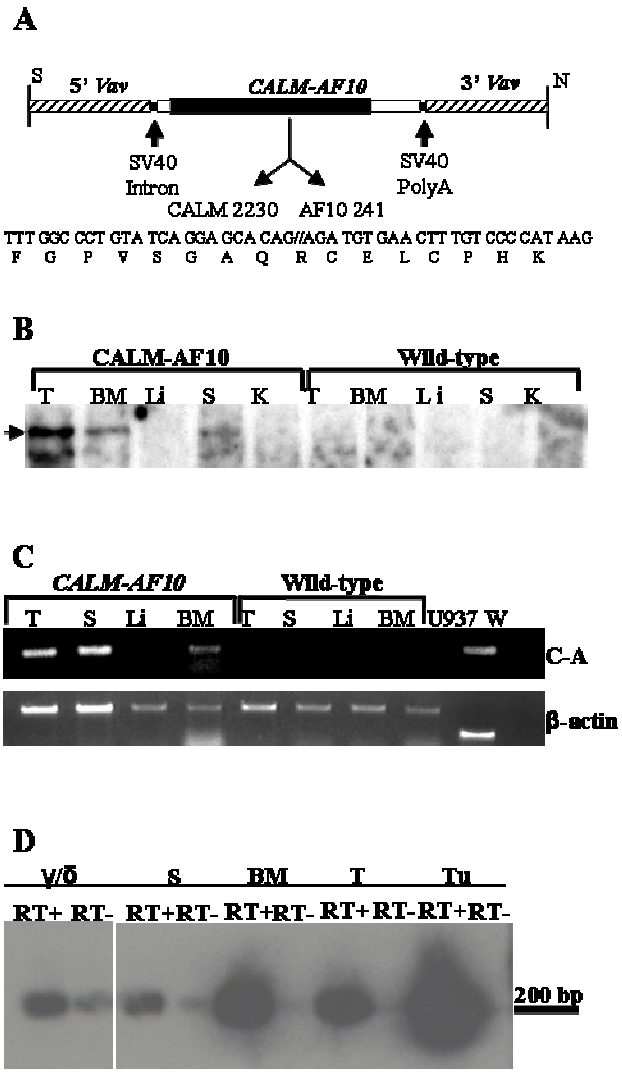

Figure 2.1. Expression of a *CALM-AF10* transgene. (***A***) Map of the construct used to generate *CALM-AF10* transgenic mice. 5' and 3' *vav* regulatory sequences are indicated. The fusion between *CALM* nucleotide 2230 and AF10 nucleotide 241 is indicated. (***B***) Northern blot of tissues from *CALM-AF10* mouse (line E6) and wild-type littermate. T, thymus; BM, bone marrow; Li, liver; S, spleen; K, kidney. The *CALM-AF10* fusion transcript is shown with an arrow. (***C***) RT-PCR analysis of tissue from *CALM-AF10* line C10. W, deionized H2O control. Human β-actin primers were used as a RNA quality control for the U937 cell line; C-A, *CALM-AF10*. (***D***) Hybridization blot of RT-PCR products from purified γδ T-cells; S, spleen; BM, bone marrow; T, thymus; Tu, tumor. The template used to generate the cDNA from γδ T-cells was 10 ng and 2 µg from S, BM, T, and Tu. Ten microliter equivalents of a 20 µl reaction was loaded onto the gel.

Table 2.1. CBC from clinically healthy and leukemic *CALM-AF10* mice

Mouse	Line	Genotype	Status	WBC	NE	Ly	Mo	Hgb	Plt
2953	C10	pos	healthy	6.06	2.09	3.63	0.29	12.5	1243
2954	C10	pos	healthy	8.82	1.85	6.32	0.58	13.7	807
2948	C10	pos	healthy	6.38	1.76	4.24	0.35	10.9	1759
2950	C10	pos	healthy	4.78	1.72	2.68	0.36	10.5	2078
7081	C10	pos	healthy	5.06	1.46	3.34	0.24	11.4	1520
2952	C10	pos	healthy	11.36	3.78	5.62	1.72	8.2	578
7058	C10	pos	healthy	5.86	2.2	3.35	0.23	12.3	769
			Avg ± STD	6.9 ± 2.3	2.12 ± 0.77	4.1 ± 1.3	0.54 ± .53	11.3 ± 1.8	1251 ± 562
2968	E6	pos	healthy	4.16	0.96	2.89	0.3	13.4	802
7019	E6	pos	healthy	6.36	1.2	4.74	0.38	10.8	1409
7095	E6	pos	healthy	7.96	3.08	4.63	0.2	13.1	992
7087	E6	pos	healthy	16.22	4.98	8.28	1.23	7.1	1048
7088	E6	pos	healthy	2.86	0.38	2.04	0.39	8.9	761
7089	E6	pos	healthy	5.5	1.62	3.6	0.22	10.9	1403
7104	E6	pos	healthy	4.6	1.91	2.37	0.26	12.3	856
			Avg ± STD	6.9 ± 4.5	2.02 ± 1.56	4.1 ± 2.1	0.43 ± 0.36	10.9 ± 2.3	1039 ± 270
2949	C10	neg	healthy	9.86	2.89	6.28	0.47	13.4	924
2955	C10	neg	healthy	7.68	2	5.11	0.35	13	867
7080	C10	neg	healthy	8.82	2.8	5.67	0.29	12.9	973
7113	C10	neg	healthy	5.36	1.04	4.11	0.2	13.4	831
7003	E6	neg	healthy	9.04	2.04	6.32	0.65	12.6	899
7020	E6	neg	healthy	7.72	1.85	5.34	0.5	12.1	965
7096	E6	neg	healthy	8.28	1.59	6.23	0.41	14.1	1090
			Avg ± STD	8.1 ± 1.4	2.03 ± 0.65	5.58 ± 0.81	0.41 ± 0.15	13.1 ± 0.6	936 ± 85
2952	C10	pos	leukemic	11.4	3.8	5.6	1.7	8.2	578
2953	C10	pos	leukemic	18.1	3.6	1.6	12.1	2.6	106
7081	C10	pos	leukemic	96.7	14	4.4	51.5	4.4	555
9001	C10	pos	leukemic	92.2	19.7	57.6	12.9	9.2	867
9014	C10	pos	leukemic	17.5	3.3	11.3	2.6	9.6	886
9043	C10	pos	leukemic	43.8	8.2	26	8.9	3	781
7026	E6	pos	leukemic	2.7	0.4	1.3	0.9	2.8	871
7087	E6	pos	leukemic	16.2	5	8.3	1.2	7.1	1048
7124	D3	pos	leukemic	45.9	5	4.5	33.2	2.6	671
			Avg ± STD	38.3 ± 34.9	7 ± 6	13.4 ± 18.2	13.9 ± 17.4	5.5 ± 3.0	707 ± 276

WBC, white blood cell count x 10^3 per uL; NE, neutrophil count x 10^3 per uL; Ly, lymphocyte count x 10^3 per uL; Mo, monocyte count x 10^3 per uL; Hgb, hemoglobin measured in g/dL; Plt, platelet count x 10^3 per uL.

Myeloid and T-cell differentiation in clinically healthy CALM-AF10 mice.

Given that the human disease most often associated with *CALM-AF10* fusions is pre-T LBL, it was somewhat surprising that the majority of the mice in this series had myeloid leukemia (although a minority of these leukemias had T-cell features such as CD3 staining and/or clonal *Tcrb* or *Tcrd* gene rearrangements). Since previously published models of pre-T LBL have often shown evidence of perturbed thymocyte differentiation prior to the onset of pre-T LBL, thymocyte subsets in 8 *CALM-AF10* transgenic and 8 wild-type control littermates were studied. Figure 2.2A shows that 4 of 8 transgenic mice had significantly decreased numbers of double positive CD4+/CD8+ (hereafter DP) cells (1-36 %), coinciding with dramatically increased numbers of more immature CD4-/CD8- (hereafter DN) cells (27-90%). Consistent with this finding, a mouse with >80 % DN cells (mouse # 9045) had *Tcrb* alleles that were exclusively in the germline configuration, in contrast to control mice with normal (<10%) numbers of DN cells, and transgenic mice with less marked (<30%) increases in DN cells, who demonstrated polyclonal *Tcrb* gene rearrangements (Figure 2.2B). As shown in Figure 2.2, the degree of impaired thymocyte differentiation was quite variable, indicating that the penetrance of this phenotype was incomplete.

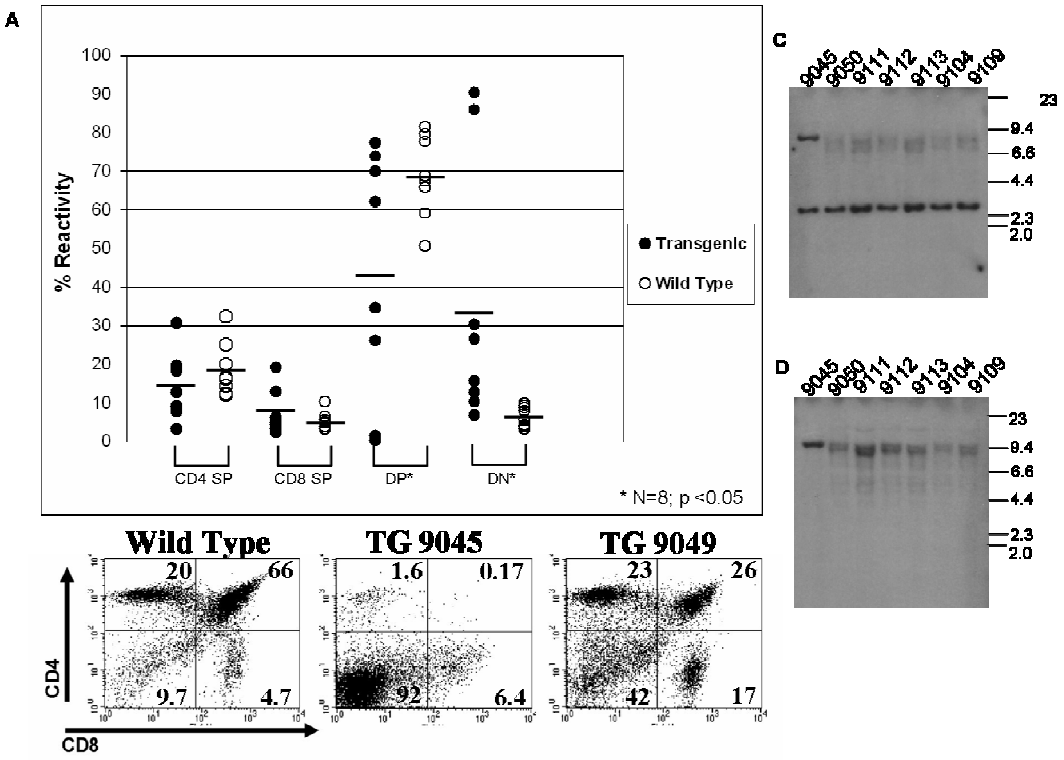

Figure 2.2. Aberrant thymocyte differentiation in *CALM-AF10* mice. **(A)** Scatter plot of CD4 SP, CD8 SP, DP, and DN thymocytes. Asterisk indicates statistical significance. **(B)** FACS plots from transgenic *CALM-AF10* mice with normal, dramatically increased, and moderately increased numbers of DN thymocytes. **(C and D)** Southern blot analysis of *Tcrb* gene rearrangements using *Hin*dIII **(C)** or *Sst*I **(D)**. Note polyclonal "smear" indicating polyclonal *Trcb* gene rearrangements in all lanes except 9045, which has a germline *Tcrb* gene configuration. Mice 9045, 9050, 9111, 9112, and 9113 are transgenic; 9104 and 9109 are wild-type mice. DP is Double Postive; DN is Double Negative; and SP is Single Positive.

Since the mice developed primarily myeloid leukemias, the proportion of Mac1+/Gr1+ cells in the bone marrow were assayed to determine if there was an expansion of this population in clinically healthy mice. Although there were increased numbers of Mac1+/Gr1+ cells in the *CALM-AF10* transgenic mice (68.7 ±12.4) compared to wild-type littermates (54.2±6.8), this difference did not reach statistical significance (Figure 2.3). The bone marrow from clinically healthy mice was evaluated to determine if there was expansion of LSK cells in bone marrow. Although there was a trend toward decreased LSK cells in *CALM-AF10* mice (0.03± 0.007%) compared to wild-type controls (0.08± 0.003%), this difference was not statistically significant.

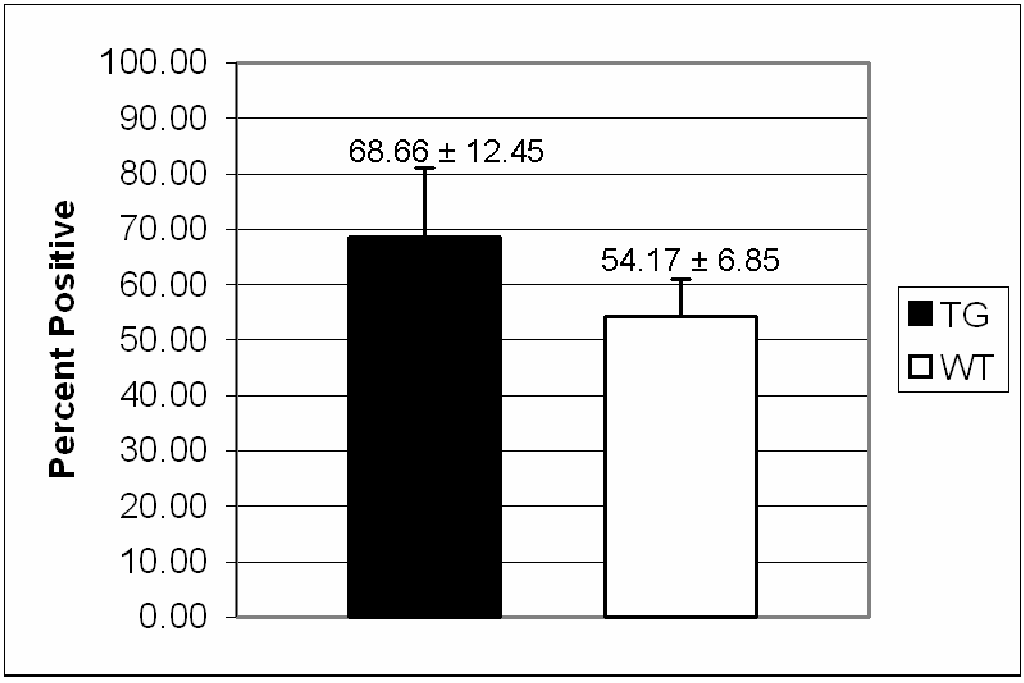

Figure 2.3A. Mac1+/Gr1+ cells in bone marrow from *CALM-AF10* mice. Bone marrow FACS with Mac1 and Gr1. Values represent the mean ± standard deviation from 4 transgenic (TG) and wild-type (WT) mice.

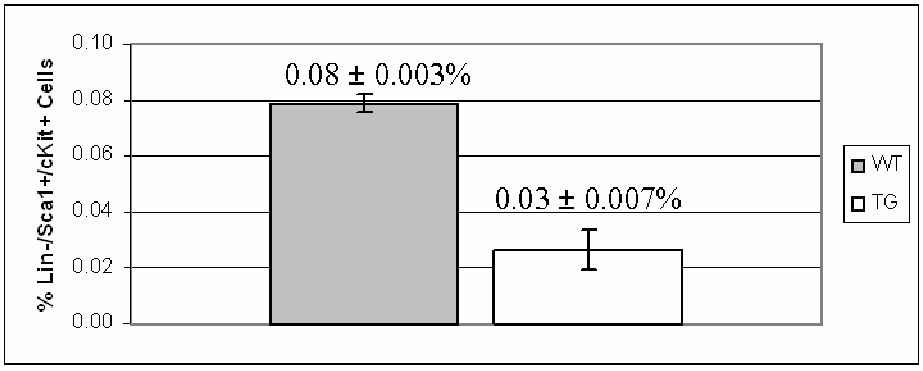

Figure 2.3B. LSK cells in bone marrow from *CALM-AF10* mice. Values represent the mean ± standard error of the mean from 3 wild-type (WT) and 3 transgenic mice (TG).

CALM-AF10 *mice develop acute leukemia*.

A cohort of transgenic offspring from four founder lines, C10, E6, D5, and D3 were observed for signs of disease for 18 months. Of these founder lines, offspring from C10 and E6 developed clinical signs of diseases. These mice were euthanized when signs and symptoms of leukemia, such as tachypnea, lethargy, ruffled fur, hunched posture, or lymphadenopathy were detected. Additionally, mice that were found dead in their cage were necropsied when possible, and tissues harvested for histology. As shown in Figure 2.4, 83% of the E6 transgenic mice and 70% of the C10 transgenic mice died by 18 months of age. At least 9 of the 18 (50%) E6 mice and 8 of the 20 (40%) C10 mice had clear signs of leukemia; six additional mice were found dead but were too autolytic to analyze. Wild type mice that died during the study showed no evidence of leukemia. In addition to the E6 and C10 offspring, one potential founder mouse, D5, developed a myeloid leukemia, and one of six offspring of a fourth founder (D3) died of a myeloid leukemia.

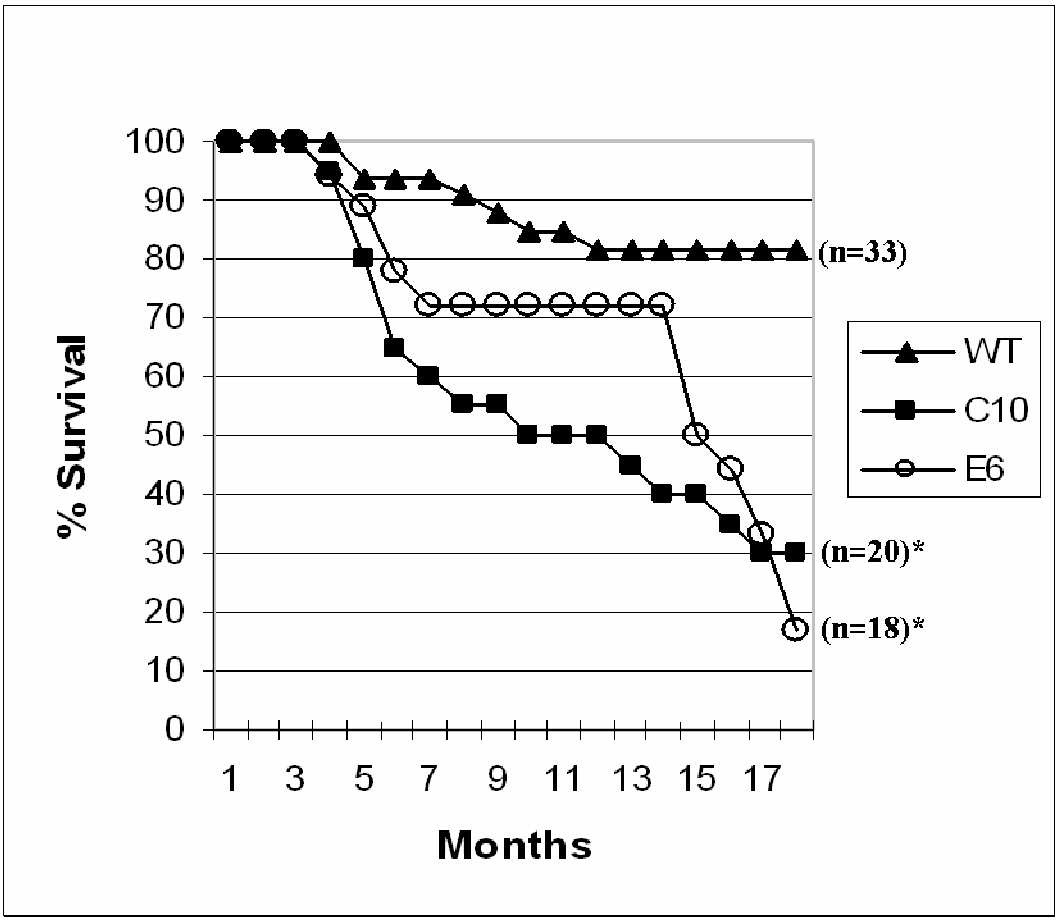

Figure 2.4 Survival of *CALM-AF10* mice. Transgenic mice from line C10 (20) and E6 (18), along with 33 wild-type littermate controls were followed for 18 months. *, $p<1x10^{-08}$ compared to littermate controls.

Leukemic mice typically had hunched posture, ruffled fur, and tachypnea. Gross examination revealed marked splenomegaly and hepatomegaly, with prominent scattered white foci. Histologically, the splenic red pulp was effaced by an expanding myeloid infiltrate accompanied by follicular atrophy. Peripheral blood examination showed circulating blasts with a high nuclear/cytoplasmic ratio, and the bone marrow was replaced by cells with a similar appearance (Figure 2.5). In addition to the spleen, parenchymal organs such as liver, lung, kidney and brain were infiltrated with malignant cells. Involved tissues were evaluated by immunohistochemical stains including the myeloid marker myeloperoxidase (MPO), the B-cell marker B220, the T-cell marker CD3, and the monocytic marker F4/80 (Table 2.2). CBCs, FACS, and antigen-receptor gene rearrangements were also analyzed on a subset of leukemic mice.

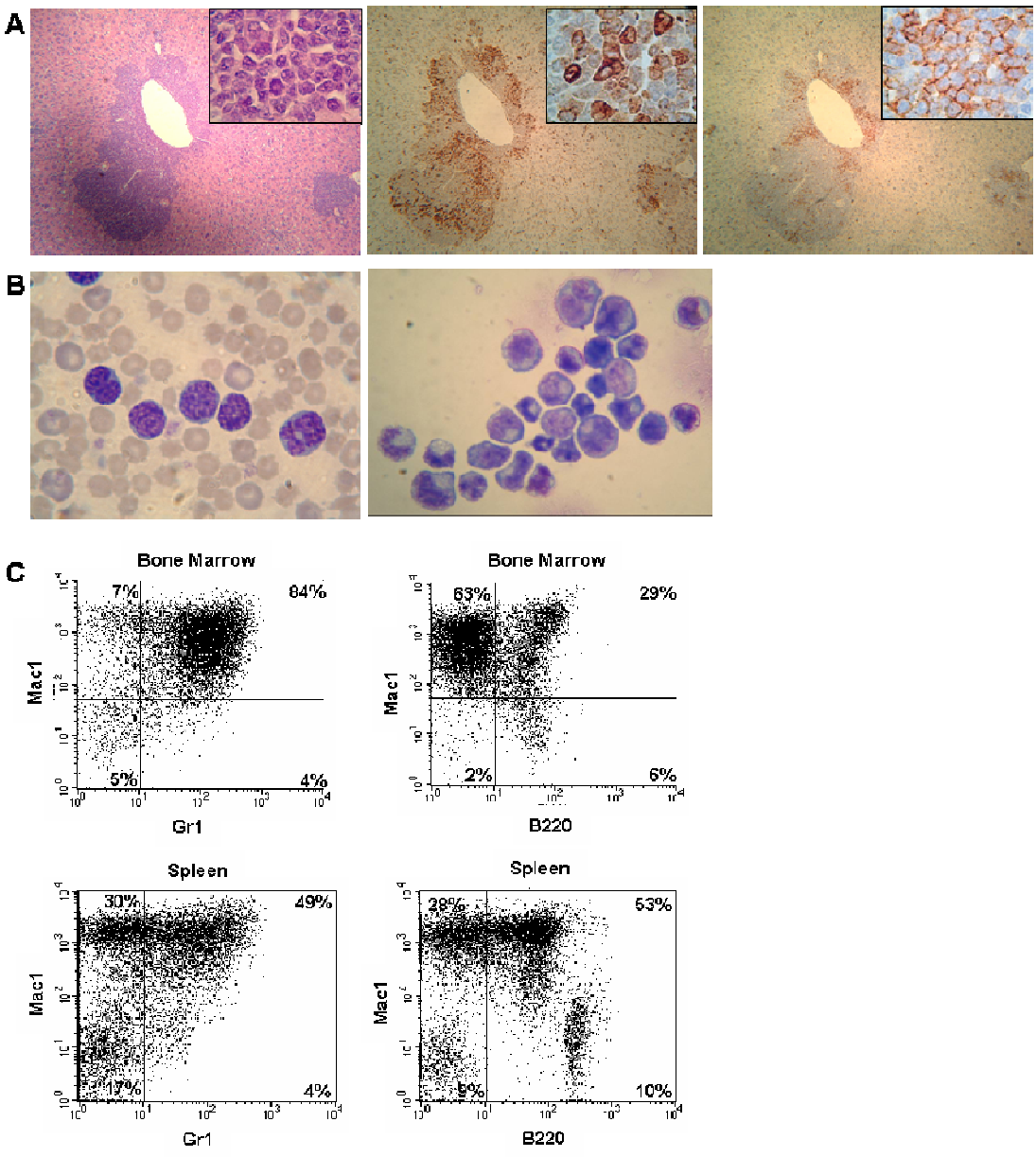

Figure 2.5. Myeloid leukemia in *CALM-AF10* mouse 9001. **(A)** Liver stained with H&E (left panel), MPO (middle panel), or B220 (right panel). Original magnification x 200 (inset x 1000). **(B)** Peripheral blood (left panel) or bone marrow cytospin (right panel) stained with May-Giemsa. Note increased numbers of blasts in the peripheral blood and bone marrow. Original magnification x 1000. **(C)** Bone marrow and spleen stained with the indicated antibodies, note the Mac-1+/B220+ population in bone marrow and spleen

As shown in Table 2.2, all 17 of the analyzable leukemias from the E6 and C10 lines were MPO positive, indicating that these mice had a myeloid leukemia. Three additional mice (7004, 7092 and 7061) were found dead and showed leukemic infiltration of parenchymal organs including the liver, kidney, and spleen, but did not stain positively for MPO, B220, CD3, or F4/80, raising the possibility that these mice had undifferentiated leukemias. However, given the phenotype of the other leukemic mice, it is likely that these were also myeloid leukemias, but that the MPO antibody was non-reactive because the tissues were partially autolytic. Nine of these analyzable leukemias were also B220+, and FACS analysis performed on a subset of these mice showed a population of leukemic cells that were Mac1+/B220+ (Figure 2.5). Eight of the MPO+ leukemias were negative for B220; a subset of these were analyzed by FACS and shown to be Mac1+/B220- (Figure 2.6). Two mice (7026 and 2953) developed myelomonocytic leukemia as evidenced by both MPO and F4/80 immunohistochemical staining; one of these also stained positive for CD3 (Figure 2.7). Taken together, these findings demonstrate that expression of a *CALM-AF10* fusion gene leads to an acute leukemia, with a long latency period and incomplete penetrance.

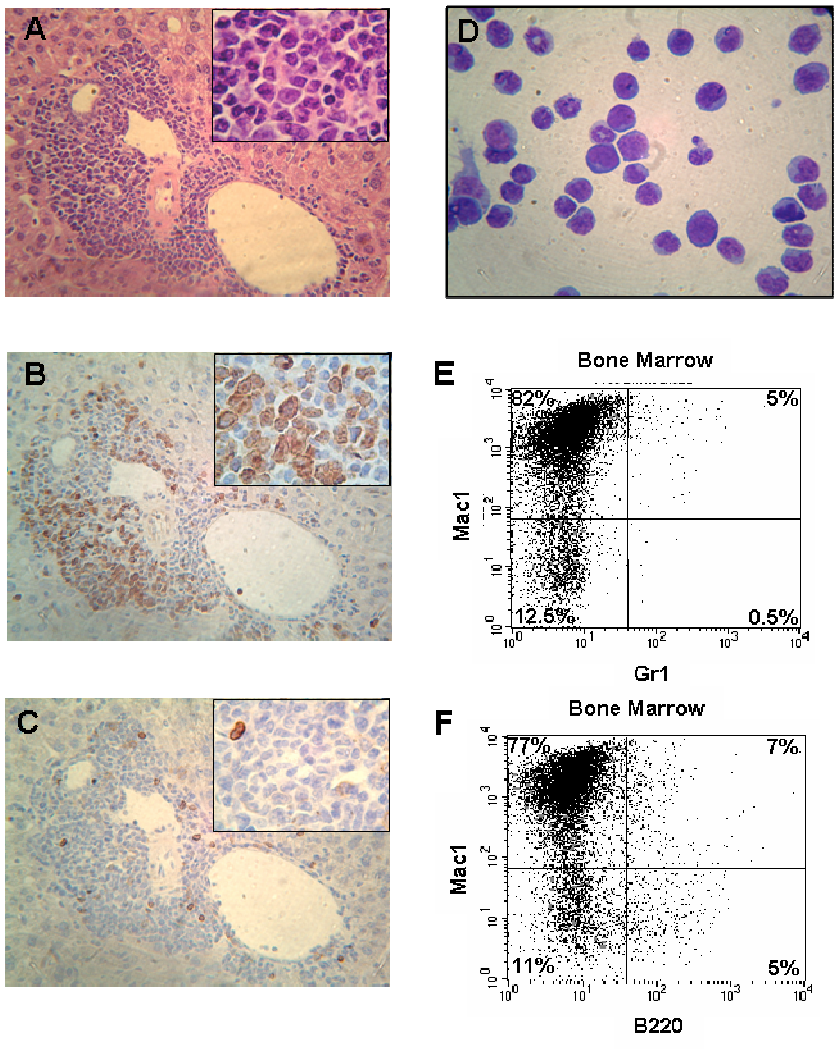

Figure 2.6. Myeloid leukemia in a *CALM-AF10* mouse 7160. H&E stained liver (***A* and *insert***), MPO labeled liver (***B* and *insert***) and B220 labeled liver (***C* and *insert***). (***D***) Bone marrow cytospin. Note increased numbers of blasts in the bone marrow and invasion of the liver with MPO+, B220- cells. (***E* and *F***) Bone marrow showing Mac1+/B220- population. Original magnification, x400 (*A, B*, and *C*); x1000 (*inserts* and *D*)

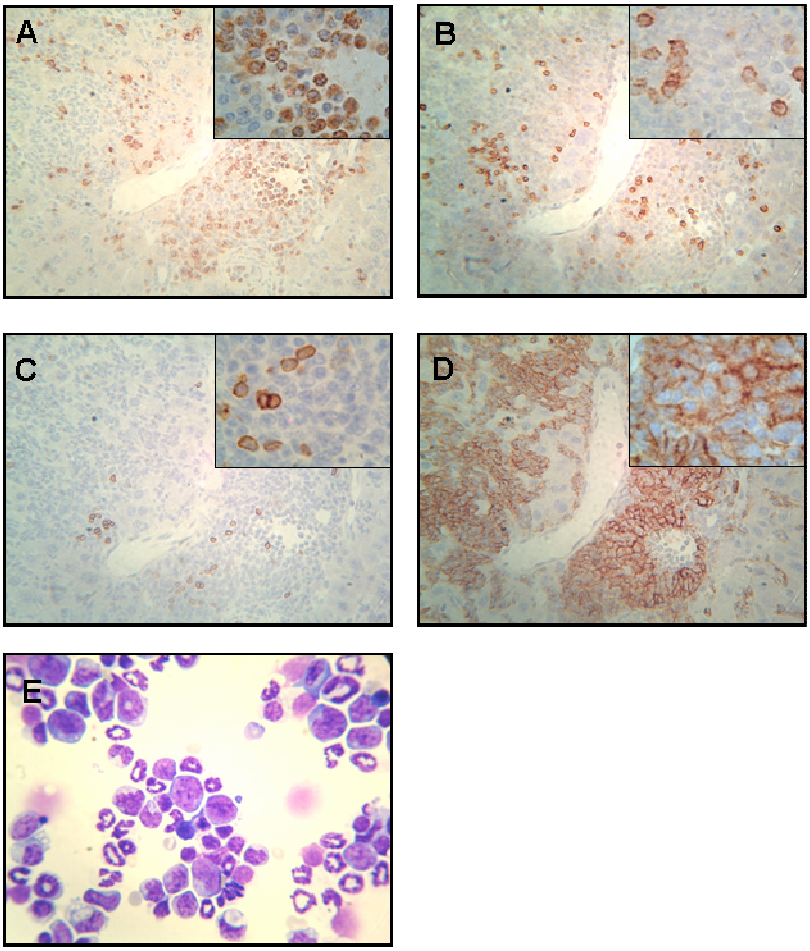

Figure 2.7. Mixed lineage leukemia in *CALM-AF10* mouse 2953. MPO labeled liver **(*A* and *insert*)**, CD3 labeled liver **(*B* and *insert*)**, B220 labeled liver **(*C* and *insert*)** and F4/80 labeled liver **(*D* and *insert*)**. **(*E*)** Bone marrow cytospin. Original magnification X400 (*A, B, C*, and *D*); x1000 (*E* and *inserts*)

Table 2.2. Summary of *CALM-AF10* Transgenic Mice with Leukemia

ID	Age (mo)	Diagnosis	Clinical Features	Histology	IHC				TCR β	TCR δ	IgH HC
					MPO	B220	CD3	F4/80			
E6											
2968	15	Myeloid leukemia	FD	Invasion of liver, kidney	+	-	-	-	nd	nd	nd
7001	15	Myeloid leukemia	FD, splenomegaly	Invasion of liver, kidney, spleen	+	-	-	-	nd	nd	nd
7004	5	Leukemia, NOS**	FD; marked autolysis	Invasion of bone marrow, liver, kidney, spleen	-	-	-	-	nd	nd	nd
7019	6	Myeloid leukemia	FD,	Invasion of bone marrow	+	-	-	-	-	-	-
7026	18	Myelomonocytic leukemia	ruffled fur, splenomegaly	Invasion of liver and spleen	+	-	-	+	-	-	-
7087	14	Myeloid leukemia	clinically healthy*	Invasion of bone marrow	+	-	-	-	-	-	-
7088	17	Myeloid leukemia	ocular discharge, ruffled fur, splenomegaly	Invasion of liver, kidney, spleen	+	-	-	-	-	-	-
7092	14	Leukemia, NOS**	FD; mildly autolytic, hepatosplenomegaly	Invasion of liver, kidney, spleen	-	-	-	-	+	-	+
7095	18	Myeloid leukemia	FD; splenomegaly	Invasion of liver, kidney, spleen, lung	+	-	-	-	+	-	+
C10											
2948	18	Myeloid leukemia	FD	Invasion of bone marrow, liver, kidney, lung	+	-	-	-	-	-	nd
2952	16	Myeloid leukemia	Clinically healthy*		+	+	-	-	-	-	+
2953	14	Myelomonocytic leukemia	lethargy, tachypnea, hepatomegaly	Invasion of bone marrow, lung, liver, kidney, spleen	+	+	+	+	+	+	+
7060	17	Myeloid Leukemia	FD	Invasion of bone marrow	+	-	-	-	nd	nd	nd
7081	14	Myeloid leukemia	ruffled fur, splenomegaly	Invasion of liver, lung, heart, kidney, pancreas, meninges, sinuses, spleen, bone marrow	+	-	-	-	-	-	-
7083	9	Myeloid leukemia	FD	Invasion of bone marrow, lung, kidney	+	-	-	-	nd	nd	nd
7160	17	Myeloid leukemia	hunched, ruffled fur, splenomegaly	Invasion of bone marrow, liver, lung, kidney, spleen	+	-	-	-	-	-	+
7161	12	Leukemia, NOS**	FD, splenomegaly	Invasion of liver, kidney, spleen, lung	-	-	-	-	-	-	+
9001	12	Myeloid leukemia	Clinically healthy*, splenomegaly, lymphadenopathy	Invasaion of bone marrow, lung, liver, kidney, spleen lymph nodes	+	+	-	-	-	nd	+
9014	12	Myeolid leukemia	Clinically healthy*, splenomegaly, lymphadenopathy	Invasion of bone marrow, lung, liver, kidney, spleen, lymph nodes	+	+	-	-	-	nd	-
9043	17	Myeolid leukemia	Lethargy, ruffled fur, hunched posture, splenomegaly, lymphadenopathy	Invasion of bone marrow, lung, liver, kidney, spleen, lymph nodes	+	+	-	-	-	nd	+
D3											
7124	16	Myeloid leukemia	ruffled fur, splenomegaly, lymphadenopathy	Invasion of liver, kidney, spleen, lung, bone marrow	+	-	-	-	nd	nd	nd
7098	14	Leukemia, NOS	FD, autolysis, splenomegaly, lymphadenopathy	Invasion of liver, kidney, lung, spleen, bone marrow	nd	nd	nd	nd	nd	nd	nd
D5	5	Myeloid leukemia	FD	Invasion of liver and kidney	+	-	-	-	nd	nd	nd

FD = Found Dead

NOS = Not otherwise specified

nd = not done

*Mouse euthanized due to CBC that showed an increased WBC, decreased HGB, and circulating blasts

**No clonal rearrangements identified, but genomic DNA was partially degraded

***9001, 9014, and 9043 were not part of the initial cohort shown in figure 2.1

****Mouse foud dead and partially autolytic. IHC stains were negative

Immunophenoptype analysis

It was observed that over half of the leukemic mice had either MPO+/B220+ cells within tumor infiltrates or were Mac1+/B220+ by FACS analysis. The possibility was considered that these B220+ leukemic cells might have other properties of B cells, or that they may be more immature bi-phenotypic cells, suggesting that the leukemia had arisen in a common early progenitor cell with the potential to differentiate along the myeloid or lymphoid lineages. Therefore, the leukemic Mac1+/B220+ population was assayed for the expression of either cKit (CD117), CD19, CD24, or IgM. As shown in Figure 2.8, although the leukemias were consistently positive for Mac1, the B220 staining was quite variable (compare #9001 and #7160, Figure 2.8). The Mac1+/B220+ cells were typically positive for CD24, negative for IgM and CD19, but showed variable expression of CD117, ranging from 23-72% positive cells. Of note, some of the mice (such as 9001, see Figure 2.8A) had a distinct B220+ population that was distinct from the Mac1+/B220+ population (gate R4 in Figure 2.8A). This "bright" B220+ population was not present in bone marrow from the leukemic mouse (Figure 2.8B), and these cells were positive for CD19 and IgM (Figure 2.8C), leading us to conclude that the Mac1-/ B220 "bright" population in the spleen represented contaminating normal B cells. The B220 "dim" population (gate R5 in Figure 2.8A) from these same mice was negative for both IgM and CD19 (Figure 2.8D)

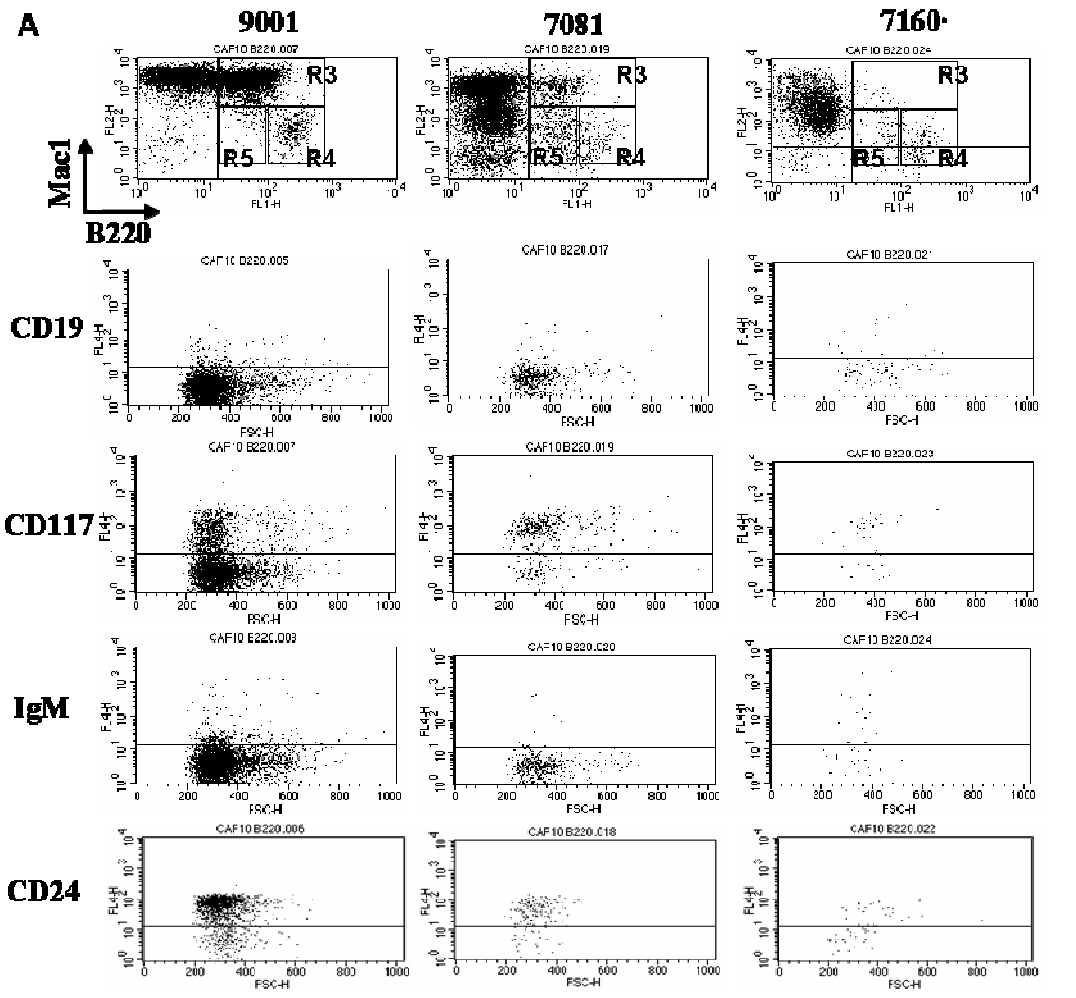

* Represents 30000 total events scored

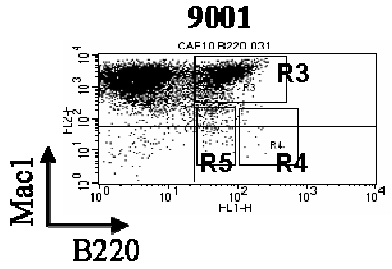

C

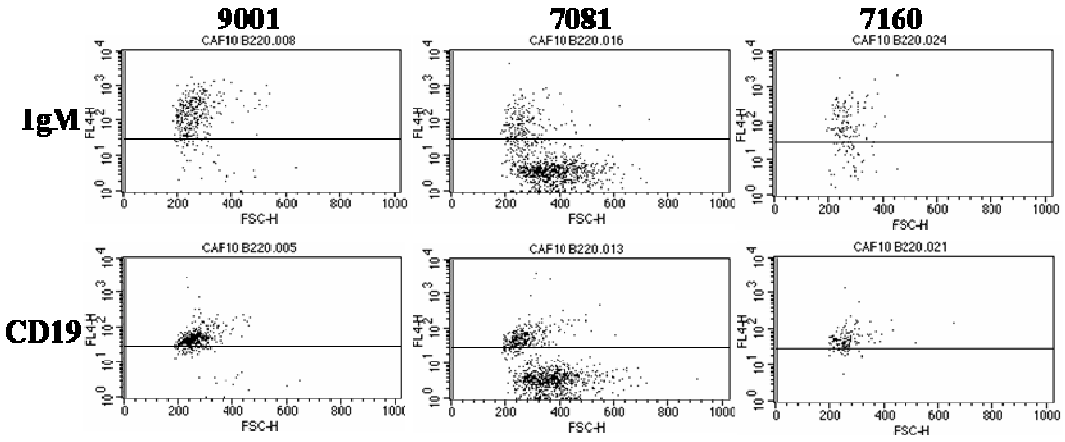
9001
7081
7160
IgM
CD19
CAF10 B220.008
CAF10 B220.016
CAF10 B220.024
CAF10 B220.005
CAF10 B220.013
CAF10 B220.021
FL4-H
FSC-H

D

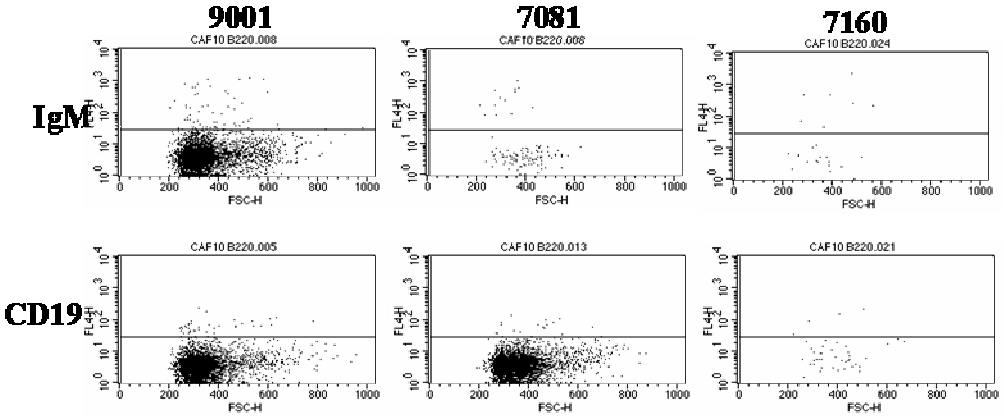
9001
7081
7160
IgM
CD19
CAF10 B220.008
CAF10 B220.024
CAF10 B220.005
CAF10 B220.013
CAF10 B220.021
FL4-H
FSC-H

E **Immunophenotype of *CALM-AF10* mice with leukemia**

Animal ID	Spleen						
	Mac1	B220	Mac1/B220	Mac1/B220			
				CD19	CD117	IgM	CD24
9001	51.4	2.0	41.9	3.3	23.0	6.4	86.1
9014	71.0	2.5	23.0	8.4	27.1	11.1	70.6
9043	27.0	7.4	42.8	2.8	29.2	6.6	94.0
7081	77.2	4.5	4.3	3.2	76.9	3.5	82.2
7160	87.3	5.0	1.6	22.1	72.1	39.0	46.4

Data for 7160 based on 3000 gated events

Figure 2.8. Immunophenotype of *CALM-AF10* leukemia. (***A***) Cells isolated from leukemic *CALM-AF10* mouse spleens were labeled with the indicated antibodies, and 10,000 total events scored. Gates R3, R4, and R5 are shown. Cells in gate R3 were scored for CD19, CD117, IgM, and CD24. (***B***) Cells isolated from leukemic CALM-AF10 mouse bone marrow and labeled with the indicated antibodies, and 10, 000 total events scored. Note the absence of a B220 "bright" population compared to spleen (R4) in A. (***C***) Cells from R4 in A indicating that the B220 "bright" population was positive for the markers IgM and CD19. (***D***) Cells from R5 in A indicating that the B220 "dim" population was negative for the markers IgM and CD19. (***E***) Summary of five *CALM-AF10* mice with AML; the cells in gate R3 were scored for CD19, CD117, IgM, and CD24.

Antigen receptor gene rearrangements

Because some of the leukemic mice stained for either the B-cell marker B220 or the T-cell marker CD3 in addition to myeloid markers, the possibility was considered that some of these cells might have additional features of T or B lymphocytes, such as clonal *Tcrb, Tcrd*, or *Igh* gene rearrangements. As shown in Figure 2.9, some of these leukemias had clonal T-cell and/or immunoglobulin gene rearrangements; indeed one mouse (2953) had clonal rearrangements of *Tcrb, Tcrd*, and *Igh*. In all, 3 of 15 mice analyzed had clonal *Tcrb* gene rearrangements, 1 of 15 had a clonal *Tcrd* gene rearrangement, and 8 of 15 mice analyzed had clonal *Igh* gene rearrangements.

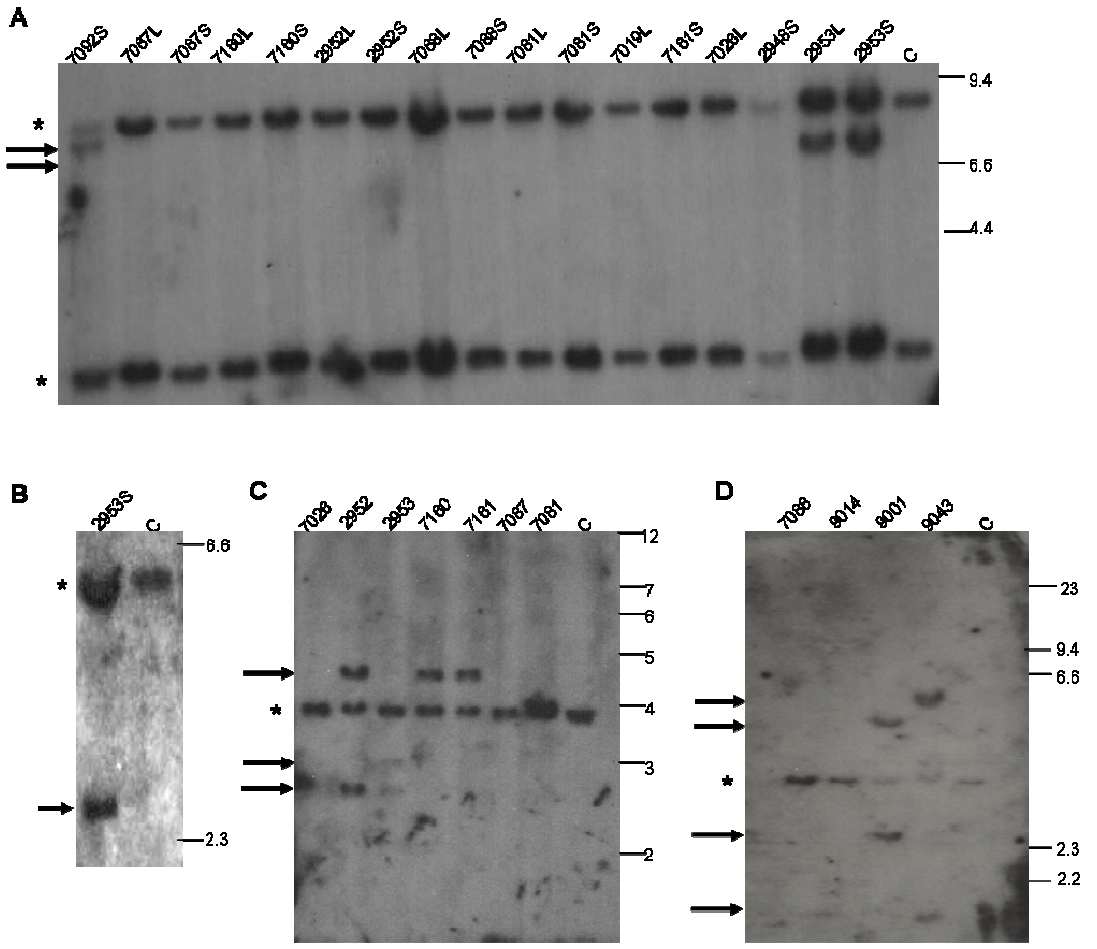

Figure 2.9. Clonal *Igh* and *TCR* gene rearrangements. (***A***) Southern blot of *Hin*dIII digested genomic DNA hybridized to a *TCRB* probe. Mouse numbers are indicated, a number followed by S indicates the infiltrated tissue was spleen, L indicates the tissue was liver. C is germline control tissue. Asterisk indicates germline bands, arrows indicate clonal rearrangments. Size standards are in kb. **(*B*)** Same as in (A), except the probe was *TCRD*. **(*C* and *D*)** Same as (*A*) except the digest was *Xba*I and the probe was *Igh*.

Discussion

To develop a mouse model for *CALM-AF10* leukemia, transgenic mice were generated that expressed the *CALM-AF10* fusion gene under control of *vav* regulatory elements. These mice developed acute leukemia, after an extended latent period (median 12 months), with an incomplete penetrance (40-50%). In addition, a substantial number of mice were found dead in their cages and were unable to be characterized as leukemic or non-leukemic. If all of these mice were leukemic, then the penetrance of the disease would rise to 70-83 %, depending on the founder line, over the 18-month study period.

The acute leukemias that developed in *CALM-AF10* transgenic mice were predominantly myeloid leukemias. Unexpectedly, half of these myeloid leukemias stained positive for B220. Although B220 is often regarded as a pan-B cell marker, B220 expression has also been detected on NK, dendritic, and myeloid progenitors (Rolink, ten Boekel et al. 1996; Balciunaite, Ceredig et al. 2005). The Mac1+/B220+ leukemic cells were negative for more specific B-cell markers, such as CD19 and IgM, but were positive for CD24 and heterogeneous for CD117 expression. *Igh* gene rearrangements were studied as an additional marker of B-cell differentiation; over half of the mice analyzed had clonal *Igh* rearrangements. Interestingly, the B220 staining did not correlate well with clonal *Igh* rearrangements, for instance, mouse # 7160 was negative for B220 and had clonal *Igh* gene rearrangements, and mouse #9014 was positive for B220 and did not have clonal *Igh* gene rearrangements. In addition, two mice had a myelomonocytic leukemia, one of which stained weakly

positive for CD3 and had both *Tcrb* and *Tcrd* rearrangements as well as an *Igh* rearrangement, and one mouse (#7160) had a myeloid leukemia with both *Tcrb* and *Igh* rearrangements.

Although *CALM-AF10* fusions have been identified in patients with myeloid, monocytic, and megakaryocytic leukemia (Dreyling, Schrader et al. 1998; Kumon, Kobayashi et al. 1999; Bohlander, Muschinsky et al. 2000; Carlson, Vignon et al. 2000; Jones, Chaplin et al. 2001), it was somewhat surprising that the mice in this study developed myeloid leukemia, since *CALM-AF10* leukemia in humans is primarily γ/δ pre-T LBL. The observation that over half (8/15) of the leukemias assayed had clonal *Tcr* or *Igh* gene rearrangements, and over half (9/17) stained positively for B220 suggests that the transformed cell, at least in some cases, was derived from a progenitor capable of lymphoid as well as myeloid differentiation. This finding is consistent with reports that clonal *TCRD* and/or *IGH* gene rearrangements are often detected in patients with *CALM-AF10* fusion and myeloid leukemia (Asnafi, Radford-Weiss et al. 2003; Deshpande, Cusan et al. 2006). Alternatively, the difference in leukemia phenotype may be due to use of the pan-hematopoietic *vav* regulatory elements to direct *CALM-AF10* expression. In humans, it is possible that *CALM-AF10* translocations occurs only rarely in myeloid progenitors, and more commonly in lymphoid progenitors. However, in *CALM-AF10* mice, the *vav* transgene cassette directs expression to all hematopoietic cells (Adams, Harris et al. 1999; Ogilvy, Metcalf et al. 1999), including those in the myeloid compartment, allowing the *CALM-AF10* fusion an opportunity to exert its oncogenic

potential in myeloid cells. Finally, it is possible that a *cis* effect present in *CALM-AF10* pre-T LBL patients is missing in these transgenic mice, where the *CALM-AF10* construct has integrated randomly.

CALM-AF10 mice were studied to determine if signs of impending leukemic transformation could be identified, however, CBCs from *CALM-AF10* mice were not significantly different than those of their wild-type littermates (Table 2.1). However, careful analysis of CBC data revealed clues of an emerging leukemia. This is evident in the case of mouse 2952 and 7087 (Table 2.1) that had a high white blood cell count, a high monocyte count and a low hemoglobin value. Although these mice were clinically healthy, the CBC values suggest bone marrow failure as a result of infiltrating or expanding leukemic blasts cells. Abnormalities of thymocyte differentiation were detected, as half (4/8) of the *CALM-AF10* mice had reduced numbers of DP thymocytes and increased numbers of more immature DN thymocytes. This impaired differentiation was reinforced by the observation that the mouse with the most dramatic increase in DN cells had not rearranged *Tcrb.* Since most of the *CALM-AF10* mice developed myeloid leukemia, it was reasoned that clinically healthy mice might have an increase in the proportion of Mac1+/Gr1+ cells in the bone marrow. However, although there was an increased proportion of Mac1+/Gr1+ cell in the bone marrow of the *CALM-AF10* mice compared to wild-type controls, this difference did not reach statistical significance.

Deshpande and colleagues reported the use of retroviral transduction and transplantation of primary bone marrow cells to show that expression of *CALM-AF10* in mouse bone marrow cells led to myeloid leukemia (Deshpande, Cusan et al. 2006). They noted that the myeloid leukemia cells were invariably B220+, with clonal *Igh* gene rearrangements, whereas in our study, only half of the myeloid leukemias were B220+, and only half had clonal *Igh* gene rearrangements. Similar to our findings, they found that the Mac1+/B220+ cells lacked specific B-cell markers such as CD19 and IgM. In contrast, the Mac1+/B220+ cells in their study lacked CD117 expression, whereas a variable (as high as 70%) percentage of Mac1+/B220+ leukemic cells from *CALM-AF10* transgenic mice expressed CD117. Intriguingly, they noted that transplantation of Mac1-/B220+ leukemic cells led to myeloid leukemia in recipient mice, and that the leukemic stem cell was likely to be a Mac1-/B220+ cell. In the current study, two distinct populations of Mac1-/B220+ cells were noted in some of the *CALM-AF10* leukemic mice (see Figure 2.9). The "bright" Mac1-/B220+ population (Fig. 2.8A, box R4) likely reflected contaminating normal B-cells, as these cells were positive for CD19 and IgM, and were only seen in leukemic spleen but not leukemic bone marrow, whereas the "dim" Mac1-/B220+ cells (Fig. 2.8A, box R5) were negative for CD19 and IgM, and may represent part of the leukemic clone, similar to the B220+ cells transplanted by Deshpande and colleagues (Deshpande, Cusan et al. 2006). Given the absence of other B lineage markers on the "dim" B220 population, along with reports of B220 expression on progenitor cells (20, 21), it is important to consider the possibility that the "dim"

B220 expression detected in these leukemic samples does not indicate B-lineage commitment.

In this chapter, it has been demonstrated that *CALM-AF10* expression is strongly leukemogenic. An emerging paradigm in leukemia biology predicts that most, if not all leukemic cells must undergo at least two collaborative events to produce a fully transformed cell. One of these events leads to impaired differentiation, and the second event results in increased proliferation and/or decreased apoptosis. The long latency period and incomplete penetrance of the leukemic phenotype supports the hypothesis that at least one additional event is required to fully transform these cells. The impaired differentiation that was observed in the thymus, along with previous reports that *HOX* gene overexpression is associated with impaired blood cell differentiation (Abramovich and Humphries 2005), is consistent with a model in which overexpression of the *CALM-AF10* gene impairs differentiation of hematopoietic cells. It seems likely that secondary, as yet undefined events which lead to increased proliferation and/or decreased apoptosis collaborate with the impaired differentiation caused by *CALM-AF10* expression and result in a completely transformed, leukemic cell.

Chapter 3: Cloning and identification of potential collaborating genes using retroviral insertional mutagenesis

Introduction

The rare but recurring chromosomal translocation [t(10;11)(p13;q21)] results in a *CALM-AF10* fusion that occurs in patients with both acute lymphoblastic leukemia (ALL) and acute myeloid leukemia (AML) (Asnafi, Radford-Weiss et al. 2003). It was shown in chapter two that *CALM-AF10* transgenic mice develop AML with lymphoid features. In this model, mice develop leukemia after a long latency period (median 12 months) with incomplete penetrance (40-50%). These findings suggest that additional genetic events are needed to complement the *CALM-AF10* transgene and complete the process of leukemic transformation. Identification of these genetic events as potential collaborating events with *CALM-AF10* could support an emerging paradigm, which predicts that most, if not all leukemic cells, must undergo at least two collaborative events to produce a fully transformed cell (Kelly and Gilliland 2002). As a consequence of these cumulative genetic and epigenetic events, the affected cell has a clonal advantage of progressing to a fully malignant cell.

Recent development of genetic screens to detect mutations seen in cancer have proven to be a useful tool for identifying important cancer associated genes and/or their associated pathways, as well as therapeutic targets. Retroviral insertional mutagenesis (RIM) is a large-scale, whole-genome screening technique used to

identify genes, many of which have been associated with a variety of human diseases including hematopoietic malignancies (Li, Shen et al. 1999; Suzuki, Shen et al. 2002; Castilla, Perrat et al. 2004).

To better understand this method, it is important to first review the retrovirus life cycle and its mechanisms that lead to celluar transformation (Wolff 2006; Slape 2008). In order for retrovirus infection to occur, the virus must first recognize and attach to the host cell membrane receptor that binds to viral specific receptors. Following attachment and entry, viral RNA undergoes reverse transcription into DNA using viral *reverse transcriptase* encoded by the viral gene *pol*. Next, the newly formed linear viral DNA provirus integrates into the host's genomic DNA through the use of *integrase* also encoded by the *pol* gene. After stable integration of the proviral DNA, production of new viral RNA begins through the use of host transcriptional and mRNA processing machinery. Finally, after RNA processing, new virions are released from the host cell through a process known as "budding". Following infection of the host cell, the retrovirus integrates into the genome and transforms cells through several different mechanisms (Dudley 2003; Wolff 2006; Slape 2008). First, the provirus can integrate into an endogenous promotor that results in replacement of the host's promotor with that of the viral promotor in the 3' UTR. This mechanism commonly occurs in the c-myc locus. Secondly, activation of nearby genes occurs when the provirus inserts near a host gene and exerts its influence over a long distance using proviral enchancer elements. A third mechanism of proviral activation occurs when the provirus inserts in either an exon or intron of a host gene.

This mechanism results in a truncated protein that gives rise to posttranscriptional dysregulation. Finally, the provirus can insert within a tumor suppressor gene and result in gene inactivation or truncation. Transformation of the cell leads to a growth advantage and clonal expansion which results in tumor formation. Integration of the provirus into the host's DNA serves as a tag by which nearby genes can be identified through ligation-mediated PCR (Li, Shen et al. 1999; Mikkers, Allen et al. 2002). Identification of these candidate disease genes provides insightful clues into their role in cancer.

One example of RIM involved the cloning of integrations from wild type mice. Recombinant inbred BXH2 mice are known to develop spontaneous retrovirally induced myeloid leukemia (Bedigian, Johnson et al. 1984) and the AKXD inbred mouse is susceptible to lymphoma development (Mucenski, Taylor et al. 1988; Gilbert, Neumann et al. 1993). The cloning of these retroviral integration sites from mouse tumor DNA led to the discovery of important disease genes, namely *Evi1* and *Meis1* (Mucenski, Taylor et al. 1988). In addition, *Nf1*, which is associated with the human disease Neurofibromatosis, type 1 and its associated myeloid disease, Juvenile myelomonocytic leukemia (JMML) (Korf 2000), was also identified using RIM (Buchberg, Bedigian et al. 1990; Cho, Shaughnessy et al. 1995). In a larger study, Li and colleagues used RIM in BXH2 and AKXD recombinant inbred mice to induce myeloid, B-cell or T-cell leukemia (Li, Shen et al. 1999). This was followed by large scale cloning of the proviral integration sites to identify several disease associated genes.

As shown above, RIM is a powerful tool by which to identify disease associated genes. This tool has broader application when combined with "sensitized" or genetically engineered mice to interrogate collaborating genes and/or their associated pathways. The first study to use RIM to identify collaborating genes in sensitized mice was conducted in *Cbfb-MYH11* knock-in chimeric mice infected with the 4070LTR retrovirus (Castilla, Perrat et al. 2004). In that particular study, 54 candidate genes and 4 CIS were identified; these included *Plag1,* and *Plagl2*, in addition to *Runx2, Myb, H2T24*, and *D6Mm5e*. Additional studies since then identified *PRUNX1* and *RUNX3* in a mouse model for CML/AML as a collaborating gene with *BCR-ABL* (Miething, Grundler et al. 2007). *Hoxa* genes have been identified as target genes in an *E2a-PBX1* mouse model for B-cell leukemia (Bijl, Sauvageau et al. 2005). Lymphoma was induced using M-MuLV in *p27*-null mice, and as a consequence *Myc* was identified as a target as well (Hwang, Martins et al. 2002). In another study that involved *NUP98HOXA9*, retroviral insertional mutagenesis was used to identify a large set of cofactors including the transcription regulator, *Meis1* (Iwasaki, Kuwata et al. 2005). Finally, a more recent study using MOL4070LTR-infected *NUP98HOXD13* transgenic mice identified candidate genes that included *Meis1*, *Mn1*, *Gata2*, and miR29a and b respectively (Slape, Hartung et al. 2007).

In this chapter demonstrates that retroviral insertional mutagensis can be used in *CALM-AF10* transgenic mice to accelerate the onset of acute leukemia and that genes

can be identified that potentially collaborate with the *CALM-AF10* fusion gene in the leukemic transformation process.

Materials and Methods

Retroviral Infection

The MOL4070LTR retrovirus was propagated at NCI-Frederick using a previously published protocol (Wolff, Koller et al. 2003). In order to propagate the MOL4070LTR retrovirus, 10^5 NIH3T3 cells chronically infected with virus were co cultured with an equal number of uninfected NIH3T3 cells in a 100-mm dish. The cells were propagated for 4 days in medium, which was replaced with fresh medium, and on day 5, the virus-containing medium was harvested, and titer was determined by the XC assay (Rowe, Pugh et al. 1970). A total of 76 two day-old mouse pups of undetermined genotype were inoculated intravenously into the tail vein with 4×10^4 infectious particles in 0.05 mL of culture medium.

Two months after infection the genotype was determined on the mice as previously described. In all, there were 45 *CALM-AF10* transgenic mice and 31 FVB wild-type mice. The mice were housed at NCI-Frederick and evaluated daily under the ACUC *Guidelines for the Care and Use of Animals*.

Evaluation of leukemic mice

Mice were observed daily for signs and symptoms of leukemia, which included ruffled fur, lethargy, labored breathing, lymphadenopathy, or abdominal swelling.

Mice that showed these signs of disease were humanely euthanized (as previously described) for postmortem evaluation. Mice that were found dead were also dissected and tissues placed in formalin as described below, unless tissues were severely autolytic. Whole blood was collected in EDTA for CBC analysis. Bone marrow cells were viably harvested by flushing a dissected femur with Dulbellco's medium with 2% Fetal calf serum (Invitrogen), hereafter referred to as HF2. Blood smears and cytospin preparations of bone marrow cells were stained with May-Grunwald-Giemsa and evaluated microscopically. Sections of tissue including liver, spleen, kidney, lymph nodes, thymus, and sternum were fixed in 10% neutral buffered formalin (Sigma), paraffin embedded, sectioned at 5µm, and stained with H&E or incubated with antiperoxidase (MPO; DAKO), CD3 (DAKO), F4/80 (Caltag), and B220 (CD45R; PharMingen). The Bethesda proposals for classifying nonlymphoid hematopoietic and lymphoid neoplasms in mice were used as guides to evaluate tissues from *CALM-AF10* mice (Kogan, Ward et al. 2002; Morse, Anver et al. 2002). Single-cell suspensions derived from spleen and/or bone marrow were incubated with FITC-conjugated antimouse CD8, B220, and Gr1; phycoerythrin-conjugated antimouse CD4 and Mac1 (PharMingen). The stained cells were resuspended in HF2 containing 1 µg/mL propidium iodide (Sigma) and analyzed by three-color flow cytometry to determine immunophenotype.

Ligation mediated PCR

One microgram of genomic DNA extracted from infiltrated spleens was digested with *Mse*I (10 units) (New England Biolabs, Ipswich, MA) or *Nla*III (10 units) (New

England Biolabs) in a total reaction volume of 40 µl for 6 hr at 37°C followed by heat inactivation at 70°C for 10 min. Digested fragments of DNA were ligated to linkers constructed by annealing the oligonucleotides 5'-GTAATACGACTCACTATAGGGCTCCGCTTAAGGGAC-3' and 5'-Phos-TAGTCCCTTAAGCGGAG-C3spacer-3' for *Mse*I-digested DNA and 5'-GTAATACGACTCACTATAGGGCTCCGCTTAAGGGACCATG-3' and 5'-Phos-GTCCCTTAAGCGGAG-C3spacer-3' for *Nla*III-digested DNA (Integrated DNA Technologies) in a 20 µl volume using 2000 units T4 DNA ligase (New England Biolabs) and 10mM ATP at 4°C overnight. The ligation was heat inactivated at 70°C for 10 minutes followed by a second digestion with *EcoR*V (20 units) (New England Biolabs) for one hr and heat inactivated at 70°C for 10 min. Primary PCR was performed using 2 µl of DNA template, 10 µmol/L deoxynucleotide triphosphate, 0.4 µmol/L of primer complementary to the linkers (5'-GTAATACGACTCACTATAGGGCTCCG-3' and the LTR of the MOL4070LTR retroviral sequence 5'-GCTAGCTTGCCAAACCTACAGGTGG-3'),

and 2.5 units of Taq enzyme (Invitrogen). Following a 1:50 dilution of the primary PCR product a secondary PCR was performed using nested primer sets for the MOL4070LTR retroviral sequence, 5'-CCAAACCTACAGGTGGGGTCTTTC-3', and complementary to the linkers, 5'-AGGGCTCCGCTTAAGGGAC-3'. Both the primary and secondary PCR reactions were performed on a PTC-200 Petltier Thermal Cycler (MJ Research, Watertown, MA) at the following conditions: a denaturing step at 94˚C for 2 minutes followed by 25 cycles of amplification (each cycle included 94˚C for 15s, 60˚C for 30s annealing, and extension at 72°C for 60s) and a final

extension at 72°C for 5 min. PCR products were purified through PCR columns (Quiagen), ligated into pGEM-T Easy (Promega), and transformed into DH5α *E. coli* cells (Invitrogen). Plasmid DNA was isolated from a total of 12-18 ampicillin-resistant colonies using a QIAprep Spin Miniprep Kit (Qiagen) and digested with *Eco*RI. Plasmids that were determined to contain unique insertions were sequenced using an SP6 primer with BigDye Terminator reagents and analyzed on a 3730 DNA Analyzer (Applied Biosystems) by Retrogen (Retrogen, Inc, San Diego, CA). Sequences were compared to the genomic build of February 2006 (National Center for Biotechnology Information Build 34) using the UCSC genome browser (http://genome.ucsc.edu/).

Southern blot analysis for virus integrations or Igh, Nf1, *and* Zeb2 *gene rearrangements.*

Genomic DNA from either transgenic or wild-type mouse spleens was isolated as previously described and digested with either *Eco*RI (10 units) (Ivitrogen) (for virus integrations or *Igh* gene rearrangements), *Xba*I (10 units) (Invitrogen) (for *Igh* gene rearrangements), *Stu*I (10 units) (Invitrogen) (for *Zeb2* gene rearrangements), *BamH*I (10 units) (Invitrogen) or *Hind*III (10 units) (Invitrogen) (*Nf1* gene rearrangements) size fractionated on either 0.65% or 0.8% agarose gels and transferred to nylon membranes (Schliecher & Schuell) as previously described. The nylon membrane was prehybridized using ULTRAhyb (Ambion) and hybridized to either MOL4070LTR envelope, murine *Igh*, murine *Zeb2*, or murine *Nf1* probes. The MOL4070LTR probe provided as provided as a gift by Dr. Chris Slape (Slape,

Hartung et al. 2007). The murine *Igh* probe was provided as a gift by Dr. Michael Kuehl.

The 803 bp *Zeb2* probe was generated using primers 5'TGAGCATCATTAAGCAGTGAGCAG3' and 5'AGTTGACTGTAGGTGGACTTGGTG3'. A second 613 bp *Zeb2* probe was generated using primers 5'AAGCGTTTGCGGAGACTTCAAGG3' and 5'AAAGAAAGCCTGCCACCAAAGAGC3'. The 527 bp *Nf1* probe was generated using primers 5'TTCAAGGCCTTGAAAACGTTAAGC3' and 5CTATATGTTCAGCCAGCTTCCCAGG3'. The following thermocycling conditions were used to generate the *Zeb2* and *Nf1* probes: 94°C for 3 min; 34 cycles of 94°C for 30 seconds, 60°C for 30 seconds, 72°C for one min; followed by a terminal extension of 72°C for 10 min. All probes were ^{32}P-labeled by random priming as described in Chapter 2.

Real Time PCR

Total RNA (1 µg) from spleen and bone marrow was reverse transcribed using 1-µg total RNA with *Superscript*II reverse transcriptase and random hexamer primers (Invitrogen) in a volume of 20 µL. Real-time RT-PCR was performed on a 7500 Fast Real-time TaqMan PCR system (Applied Biosystems, Fosters City CA) using aliquots of 1 of first-strand cDNA as templates for mouse *Zeb2b,* and *k-Ras*, with Applied Biosystems primer and probe sets. The expression of the 18S ribosomal RNA was used as an endogenous control. All reactions were done in triplicate with 20 µl

PCR reactions using the Applied Biosystems default thermalcycling conditions (an activation step at 95˚C for 20 sec followed by 40 cycles of amplification at 95˚C for 0.03 sec, followed by an annealing and extension step at 60˚C for 30 sec). The $-\Delta\Delta C_T$ mean and SE were calculated for each sample. Values for the transcript of interest were normalized to the 18S rRNA value and compared with the expression in wild-type bone marrow.

Real-time RT-PCR was performed for mouse *Nf1*, with specific primers 5'TTCAAGGCCTTGAAAACGTTAAGC3' and 5'CTATATGTTCAGCCAGCTTCCCAGG3' that spanned exons 36 and 37 of *Nf1*. SYBER Green was used as a detector and the expression of actin was used as an endogenous control. All reactions were done in triplicate with 20 µl PCR reactions using the Applied Biosystems default thermalcycling conditions (an activation step at 50˚C for 1 min then 95ºC for 10 min followed by 40 cycles of amplification at 95˚C for 0.15 sec, followed by an annealing and extension step at 60˚C for 1 min). The $-\Delta\Delta C_T$ mean and SE were calculated for each sample. Values for the transcript of interest were normalized to the actin value and compared with the expression in wild-type bone marrow.

Reverse transcription-PCR

In order to determine if there was an *Mn1*-retrovirus fusion in mice with an *Mn1* retrovirus integration, first-strand cDNA templates were generated as previously described. A forward *Mn1* primer (5'TACCTTCAACCCCTGACAGCTATGG-3') and a reverse *Moloney pol* primer (5'CTCCCGATCTCCATTGGTTACCTC3') were

used to amplify the fusion product. The thermocycling conditions were as follows: a denaturing step at 94˚C for 3 min followed by 35 cycles of amplification (each cycle included 94˚C for 30 s, 60˚C for 30 s annealing, and extension at 72°C for 90s) and a final extension at 72°C for 5 min. PCR products were evaluated using agarorse gel electrophoresis.

An EST is located 250 kb 5' of *Zeb2* and is ~75 kb from the region that contains most of the viral integrations detected by PCR (see map). In order to evaluate whether or not this was expressed in samples that contained *Zeb2* insertions, RT-PCR (as previously described) was performed using the following primer pairs (5'GCA GCC GGC GCT CAC CTT CC3' and 5'AAT GTT GTA AGA AAT GTG CC3'; 5'CTC ACC TTC CCT TAA ATC C3' and 5'AAT CGT TGT GGA CAA ATT AAG C3') The thermocycling conditions were as follows: a denaturing step at 94˚C for 3 minutes followed by 35 cycles of amplification (each cycle included 94˚C for 30 s, 60˚C for 30 s annealing, and extension at 72°C for 90s) and a final extension at 72°C for 5 min.

Results

MOL4070LTR infection accelerates acute leukemia in CALM-AF10 *transgenic mice*

In the previous chapter it was observed that *CALM-AF10* transgenic mice developed leukemia after a long latency period with incomplete penetrance. In order to accelerate the leukemia mice were infected with MOL4070LTR retrovirus. The MOL4070LTR is a recombinant retrovirus derived from the Moloney murine

leukemia virus (Mo-MuLV) and the 4070A virus. The majority of the U3 region of the long terminal repeat region from Mo-MuLV has been replaced with those from the 4070A virus. This NB tropic retrovirus is reported to cause myeloid leukemia in approximately half of the mice infected, in contrast to Mo-MuLV, which is associated with a predominately lymphoid phenotype in newborn mice. A previous study showed that infection of wild-type FVB mice with MOL4070LTR retrovirus results in leukemia after a mean latency of 31.7 weeks (Wolff, Koller et al. 2003). In this current study, 45 *CALM-AF10* and 31 wild type littermate control mice were infected on day two of life and monitored them for signs of leukemic diseases. Complete blood counts were obtained from a subset of 24 *CALM-AF10* mice at the time they developed disease; results are shown in table 3.1. Acute leukemia developed more rapidly in *CALM-AF10* infected mice than in either the FVB wild type mice infected with retrovirus ($P < 0.004$) or *CALM-AF10* mice not infected with retrovirus ($P < 0.037$); Figure 3.1 The mean latency of disease onset in *CALM-AF10* infected mice was 5.5 months. Transgenic and wild-type mice that developed leukemia were reported as pale, tachypneic, listless, hunched, and often had distended abdomens. Gross examination of the internal organs of these mice revealed marked splenomegaly, lymphadenopathy, hepatomegaly, pale kidneys, and invariably, enlarged thymuses. In three cases, mice were reported as being found dead (FD) in their cages. By nine months of age, all 45 transgenic mice had died.

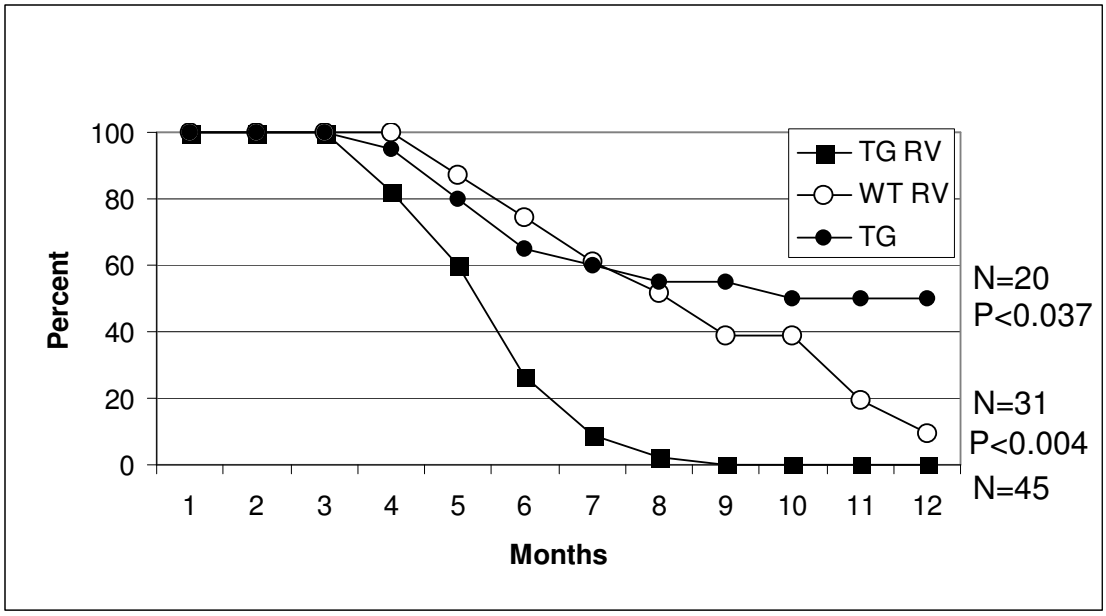

Figure 3.1. MOL4070LTR infection accelerates leukemic transformation in *CALM-AF10* mice. Survival of MOL4070LTR-infected *CALM-AF10* mice (■ n=58), MOL4070LTR-infected wild-type (○ n=30), and noninfected *CALM-AF10* transgenic mice (● n=10).

Table 3.1. Summary of Clinical and Immunphenotypic Findings in Retroviral-Infected *CALM-AF10* Mice with Leukemia

				CBC				IHC†					Flow Cytometry				Gene Insertion		
ID	Age	Dx	Clinical Features	WBC (K/ul)	Hgb (g/dL)	Plt (K/ul)	Histology	MPO only	B220 only	MPO/ B220	F4/80	CD3	BM M/G	BM M/B	Sp M/G	Sp M/B	*Igh*	*Zeb2*	*Nf1*
2*	4	Biclonal	FD, splenomegaly, enlarged thymus, mottled liver	np	np	np	Invasion of thymus, spleen, bone marrow, liver, kidney	-	-	+	-	-	np	np	np	np	np	np	np
17	6	B-ALL	Labored breathing, pale, dist abd, splenomegaly, mottled liver	> 200*	7	465	Invasion of spleen, bone marrow, liver, kidney	-	+	-	-	-	28.52	66.99	6.98	81.57	y	y	y
21	5	B-ALL	Pale, enlarged thymus, splenomegaly, lymphadenopathy, pale kidneys	159.04	10.2	450	Invasion of spleen, bone marrow, liver, kidney	-	+	-	-	-	1.23	9.16	2.42	9.48	y	y	n
23	4.5	B-ALL	Splenomegaly, lymphadenopathy	44.78	10.1	1589	Invasion of spleen, bone marrow, liver, kidney	-	+	-	-	-	4.26	24.26	5.69	25.88	y	y	y
25	6	B-ALL	Pale, dist abd, splenomegaly, lymphadenopathy	182.78	11.9	456	Invasion of spleen, bone marrow, liver, kidney	-	+	-	-	-	np	np	np	np	y	y	n
26	5	B-ALL	Pale, hunched posture, lethargy, splenomegaly, lymphadenopathy	38.22	6.6	216	Invasion of spleen, bone marrow, liver, kidney	-	+	-	-	-	7.13	51.66	4.25	35.14	y	y	y
8	6	B-ALL	Pale, hunched posture, splenomegaly, lymphadenopathy	5.06	6	228	Invasion of spleen, bone marrow, liver, kidney	-	+	-	-	-	22.79	29.11	16.67	26.65	y	n	n
14	5	B-ALL	Pale, dist abd, splenomegaly, lymphadenopathy	6.5	14.2	126	Invasion of spleen, bone marrow, liver	-	+	-	-	-	22.22	15.58	11.35	15.88	y	n	n
29	4	Biclonal	Pale, labored breathing, splenomegaly, lymphadenopathy	> 200	6.98	95	Invasion of spleen, bone marrow, liver, kidney	-	-	+	-	-	9.32	53.56	9.22	59.35	y	n	n

Table 1. Summary of Clinical and Immunphenotypic Findings in Retroviral-Infected *CALM-AF10* Mice with Leukemia (Cont.)

				CBC				IHC†					Flow Cytometry				Gene Insertion		
ID	Age	Dx	Clinical Features	WBC (K/ul)	Hgb (g/dL)	Plt (K/ul)	Histology	MPO	B220	MPO/ B220	F4/80	CD3	BM M/G	BM M/B	Sp M/G	Sp M/B	*Igh*	*Zeb2*	*Nf1*
42	5	Biclonal	Splenomegaly, lymphadenpathy, enlarged thymus	125.86	8.9	540	Invasion of thymus, spleen, bone marrow, liver, kidney	-	-	+	-	-	16.24	12.34	14.17	20.21	y	n	y
80	4	Biphen.	hind limb paralysis, splenomegaly	23.36	7	600	Invasion of spleen, bone marrow, liver, kidney	-	+	-	+	-	57.85	4.98	27.53	14.96	y	y	n
6	4	ANLL	Distended abd, pale Splenomgegaly, lymphadenopathy, hepatomegaly	36.48	5.4	288	Invasion of spleen, bone marrow, liver, kidney	+/-	+/-	-	-	-	44.78	22.4	25.31	16.69	n	n	n
10	4	Biphen.	Pale, hunched posture, labored breathing, splenomegaly, lymphadenopathy	44.78	11.3	1235	Invasion of spleen, bone marrow, liver, kidney	-	-	+	-	-	44.9	44.95	35.65	40.66	n	n	n
13	5	ANLL	Pale, dist abd, splenomgegaly, lymphadenopathy,	87.46	5	966	Invasion of spleen, bone marrow, liver	+	-	-	-	-	84.62	3.74	49.06	1.99	n	n	y
15	4	ANLL	Listless, labored breathing, pale hemoabdomen, splenomegaly, lymphadenopathy, pale kidneys	21.38	1.8	184	Invasion of spleen, bone marrow, liver, kidney	+/-	+/-	-	-	-	82.61	10.44	9.58	10.57	n	n	n
30	4	ANLL	Dist abd, pale, splenomegaly, lymphadenopathy, hepatomegaly	16.72	5.4	429	Invasion of spleen, bone marrow, liver	-	-	-	-	-	59	14			n	n	n
31	5	ANLL	labored breathing, splenomegaly, enlarged thymus, lymphadenopathy	126.46	7.3	332	Invasion of thymus, spleen, bone marrow, liver, kidney	+	-	-	-	-	72.59	2.22	48.46	6.98	n	n	y
35	5	ANLL	Splenomegaly, lymphadenopathy	12.02	5.82	979	Invasion of spleen, bone marrow, liver, kidney	+	-	-	-	-	41.84	13.61	16.88	12.71	y	n	n

Table 3.1. Summary of Clinical and Immunphenotypic Findings in Retroviral-Infected *CALM-AF10* Mice with Leukemia (Cont.)

				CBC				IHC†					Flow Cytometry				Gene Insertion		
ID	Age	Dx	Clinical Features	WBC (K/ul)	Hgb (g/dL)	Plt (K/ul)	Histology	MPO	B220	MPO/ B220	F4/80	CD3	BM M/G	BM M/B	Sp M/G	Sp M/B	*Igh*	*Zeb2*	*Nf1*
36	5	ANLL	Pale, dist abd, labored breathing, splenomegaly, lymphadenopathy, hepatomegaly	16.78	8.2	395	Invasion of spleen, liver, kidney	+	-	-	+	-	46.12	19.95	13.76	20.95	n	y	y
27	4	B-ALL	Ruffled fur, hunched, labored breathing, splenomegaly, lymphadenopathy	np	np	np	Invasion of spleen, bone marrow, liver, kidney	-	+	-	-	-	np	np	np	np	y	y	n
28	3	ANLL	Pale, labored breathing, dist abd, splenomegaly, hepatomegaly	97.78	4.6	757	Invasion of spleen, liver	-	-	-	-	-	np	np	np	np	n	n	n
32*	3	B-ALL	FD Mild to moderate splenomegaly	np	np	np	Invasion of liver	-	+	-	-	-	np	np	np	np	np	np	np
38	4	B-ALL	Pale, dist abd, splenomegaly, lymphadenopathy, hepatomegaly	73.66	5.2	800	Invasion of spleen, bone marrow, liver	-	+	-	-	-	31.86	22.34	1.02	np	n	n	n
39	4	B-ALL	Pale, dist abd, labored breathing, splenomegaly, lymphadenopathy	164.58	6.5	616	Invasion of spleen, bone marrow, liver, kidney	-	+	-	-	-	15.23	43.56	3.57	15.47	n	n	n
46	4	ANLL	Pale, dist abd, labored breathing, splenomegaly, lymphadenopathy	114.64	5.2	674	Invasion of spleen, bone marrow, liver, kidney	-	-	-	-	-	9.07	36.31	0.07	np	n	n	n
88	3	ANLL	Pale, dist abd, Hemoabdomen, ovarian mass, splenomegaly, hepatomgegaly	105.32	5.2	771	Invasion of spleen, liver, kidney	+	-	-	-	-	np	np	np	np	n	n	n
96*	3	ANLL	FD	np	np	np	Invasion of spleen, liver	-	-	-	-	-	np	np	np	np	n	n	y

Table 3.1. Summary of Clinical and Immunphenotypic Findings in Retroviral-Infected *CALM-AF10* Mice with Leukemia (Cont.)

				CBC				IHC†					Flow Cytometry				Gene Insertion		
ID	Age	Dx	Clinical Features	WBC (K/ul)	Hgb (g/dL)	Plt (K/ul)	Histology	MPO	B220	MPO/ B220	F4/80	CD3	BM M/G	BM M/B	Sp M/G	Sp M/B	*Igh*	*Zeb2*	*Nf1*
52*	4	NL	FD dried blood, saliva around muzzle	np	np	np	autolytic	-	-	-	-	-	np	np	np	np	n	n	n
5	7	B-ALL	Pale, distended abdomen, labored breathing, splenomgegaly, lymphadenopathy, pale kidneys	np	np	np	Invasion of spleen, bone marrow, liver, kidney	-	+	-	-	-	np	np	np	np	y	y	n
98	4	B-ALL	Pale, labored breathing, splenomegaly, lymphadenopathy	np	np	np	Invasion of spleen, bone marrow, liver, kidney	-	+	-	-	-	np	np	np	np	y	y	y
47	5	ANLL	Pale, labored breathing, dist abd	np	np	np	Invasion of spleen, bone marrow, liver	+	-	-	-	-	np	np	np	np	n	n	n
102	4	ANLL	Pale, labored breathing, dist abd	np	np	np	Invasion of spleen, bone marrow, liver	-	-	-	-	-	np	np	np	np	n	n	n
18	6	Biclonal	Pale, splenomegaly, lymphadenopathy	np	np	np	Invasion of spleen, bone marrow, liver	-	-	+	-	-	np	np	np	np	y	n	n
76	5	ANLL	Pale, labored breathing, dist abd	np	np	np	Invasion of spleen, bone marrow, liver	+	-	-	-	-	np	np	np	np	n	y	n
74	5	ANLL	Pale, labored breathing, splenomegaly, lymphadenopathy	np	np	np	Invasion of spleen, bone marrow, liver	+	-	-	-	-	np	np	np	np	y	y	n
9	7	Biphen.	Pale, labored breathing	np	np	np	Invasion of spleen, bone marrow, liver	-	-	+	-	-	np	np	np	np	y	n	n
72	5	Biphen.	Ruffled fur, pale, labored breathing	np	np	np	Invasion of spleen, bone marrow, liver	-	-	+	-	-	np	np	np	np	y	n	n
20	6	ANLL	Pale, dist abd	np	np	np	Invasion of spleen, bone marrow, liver	+	-	-	-	-	np	np	np	np	y	n	n
66	5	T-ALL	Pale, labored breathing, dist abd	np	np	np	Invasion of spleen, bone marrow, liver	-	-	-	-	+	np	np	np	np	y	n	n
70	6	Biphen	Splenomegaly, lymphadenopathy	np	np	np	Invasion of spleen, bone marrow, liver	-	-	+	-	-	np	np	np	np	n	n	n

Table 3.1. Summary of Clinical and Immunphenotypic Findings in Retroviral-Infected *CALM-AF10* Mice with Leukemia (Cont.)

				CBC				IHC†					Flow Cytometry				Gene Insertion		
ID	Age	Dx	Clinical Features	WBC (K/ul)	Hgb (g/dL)	Plt (K/ul)	Histology	MPO	B220	MPO/ B220	F4/80	CD3	BM M/G	BM M/B	Sp M/G	Sp M/B	*Igh*	*Zeb2*	*Nf1*
51	4	Biphen	Pale, dist abd, labored breathing	np	np	np	Invasion of spleen, bone marrow, liver	-	-	+	-	-	np	np	np	np	y	y	n
40	6	ANLL	Labored breathing, pale, anorexia, splenomegaly, lymphadenopathy	np	np	np	Invasion of spleen, bone marrow, liver	+	-	-	-	-	np	np	np	np	n	n	y
44	6	ANLL	Dist abd, labored breathing, splenomegaly, lymphadenopathy	np	np	np	Invasion of spleen, bone marrow, liver	+	-	-	-	-	np	np	np	np	n	n	y
69	4	ANLL	Pale, labored breathing	np	np	np	Invasion of spleen, bone marrow, liver	+/-	+/-	-	-	-	np	np	np	np	y	n	n
67	5	ANLL	Pale, labored breathing, dist abd	np	np	np	Invasion of spleen, bone marrow, liver, kidney	+	-	-	-	-	np	np	np	np	y	n	n

CBC, complete blood count; IHC, immunohistochemistry; WBC, white blood cell; NT, neutrophils; LM, lymphocytes; MO, monocytes
BM, bone marrow; Sp, spleen; B-ALL, B-cell acute lymphoid leukemia; ANLL, acute non-lymphoid leukemia; Hgb, hemoglobin; Plt, platlets; MPO, myeloperoxidase
M/G, Mac1/Gr1 double positive; M/B, Mac1/B220 double positive; *Igh* , Immunoglobulin heavy chain; y, yes; n, no; np, not performed
FD, Found dead
†IHC results based on degree of antibody labeling blasts in infiltrated liver, kidney, speen, and bone marrow
*CBC data generated on a Mascot 850 Hematology Analyzer, Drew Scientific Inc., Waterbury, CT. Linearity limits for WBC x 10^3 cells/mm^3 = 0.1-200

CALM-AF10 *develop B-ALL and ANLL*

As shown in Table 3.1 mice developed either acute lymphoid (B-cell or T-cell), nonlymphoid (Myeloid), or biphenotypic (Myeloid and B-cell) leukemia as determined by histologic and immunophenotypic analysis. Of the three mice that were found dead in their cages, only one mouse did not develop leukemia (mouse 52). Histologically the splenic red pulp was expanded and effaced by a leukemic infiltrate with simultaneous loss of the white pulp. There was marked perivascular accumulation and sinusoidal expansion by leukemic cells in the liver and kidney. Bone marrow elements were effaced by the expansive leukemic infiltrate. Peripheral blood examination revealed circulating lymphoid or myeloid blasts that often had large nuclear to cytoplasmic rations and open chromatin. Immunohistochemistry for the markers MPO, CD45 (B220), CD3, and F4/80 was also performed. The markers Mac1, Gr1, and B220 were used for flow cytometry. The Bethesda proposals described above were used as guides to classify the leukemias. In addition to the classification scheme used in the Bethesda proposal, biclonal and biphenotypic diagnoses were also applied to a subset of the leukemias. In this study, mice developed leukemias that represented a broader spectrum of phenotypes with respect to myeloid disease compared to mice that developed leukemia in Chapter 2. The predominant phenotype seen in mice in Chapter 2 was either AML or AML with B-lymphoid features. That is contrast to mice in this study that were infected with MOL4070LTR retrovirus that developed both well differentiated AML and poorly differentiated AML (these tumors did not label for the surface antigens MPO, F4/80, B220, and CD3). Because of this spectrum of myeloid disease, the term acute non-

lymphoid leukemia (ANLL) was used rather than AML. A subset of mice also developed AML with features of myeloid and/or B-lymphoid disease. These leukemias may represent either biphenotypic or biclonal leukemias. Biclonal leukemias represent two distinct clones with cell populations that express distinct surface antigens that are not expressed on cells from the other clone. This is in contrast to biphenotypic leukemias that are thought to arise in a multipotent progenitor cell capable of differentiating simultaneously into both myeloid and lymphoid lineages (Matutes, Morilla et al. 1997). The most common outcome are blasts cells that coexpress myeloid and B-cell surface antigens (Matutes, Morilla et al. 1997).

In this study, there was a large percentage of ANLL (45%) (Figure 3.2 and 3.3) and B-ALL (29%) (Figure 3.2 and 3.4) and biphenotypic (13%) or biclonal leukemias (9%) (Figure 3.2 and 3.5 and 3.6), and much smaller percentage of T-ALL (2%) (Figure 3.2 and 3.7) compared to the leukemias that developed in wild type mice. Figure 3.8 depicts the morphology of acute lymphoid leukemia in a *CALM-AF10* mouse infected with MOL4070LTR. This is in contrast to an acute nonlymphoid (myeloid) leukemia shown in Figures 3.9 and 3.10. These mice were evaluated for *Igh* gene rearrangements and 23 of 43 mice had *Igh* rearrangements as shown in Figure 3.11. Taken together, these findings demonstrated that *CALM-AF10* mice infected with retrovirus developed a broader spectrum of leukemias with respect to immunophenotype than did *CALM-AF10* mice not infected with retrovirus that developed predominately a myeloid leukemia (see Chapter 2, Table 2.2)

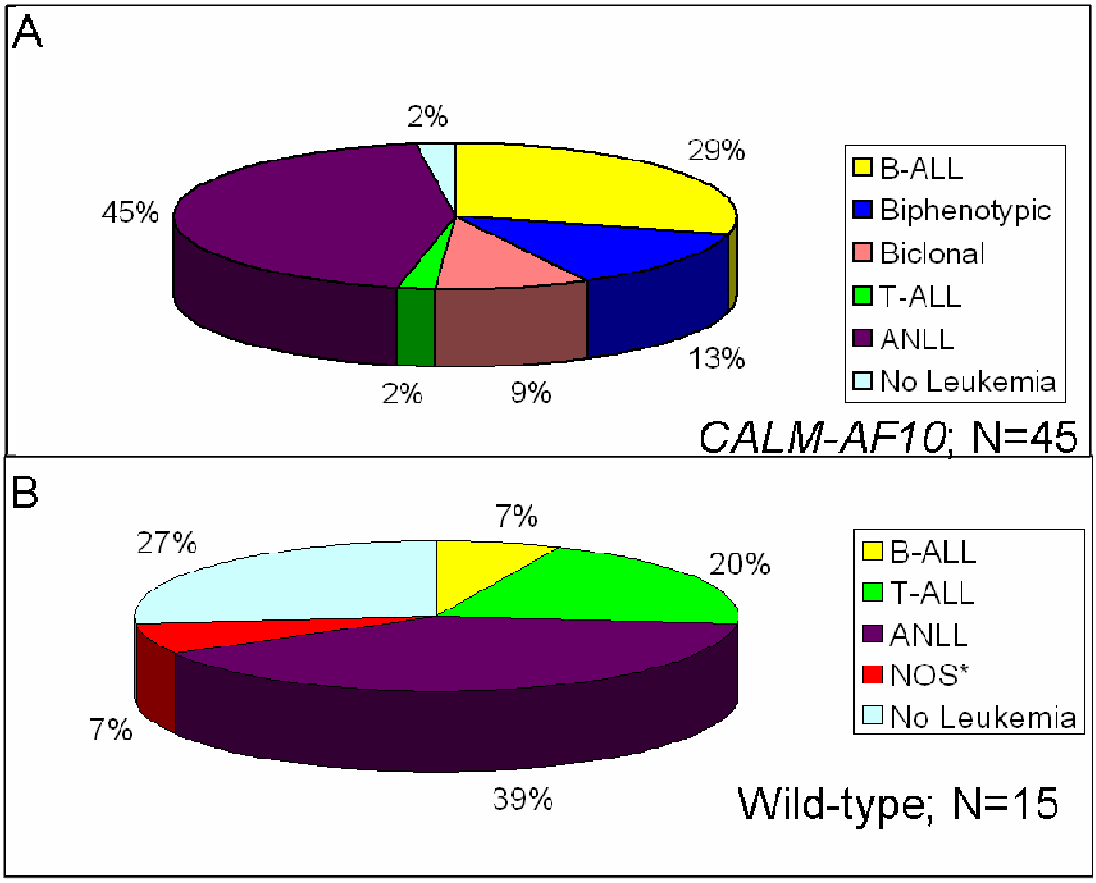

Figure 3.2. Distribution of leukemia by phenotype in *CALM-AF10* (A) and FVB wild-type control mice (B) infected with MOL4070LTR retrovirus. Note the predominance of B-cell and myeloid (ANLL) tumors, as well as the biphenotypic tumors, in the *CALM-AF10* mice compared to the wild-type control mice. *NOS is not otherwise specified. This represents mouse 71 that developed leukemia; however tissues were not available for histological and immunphenotype analysis.

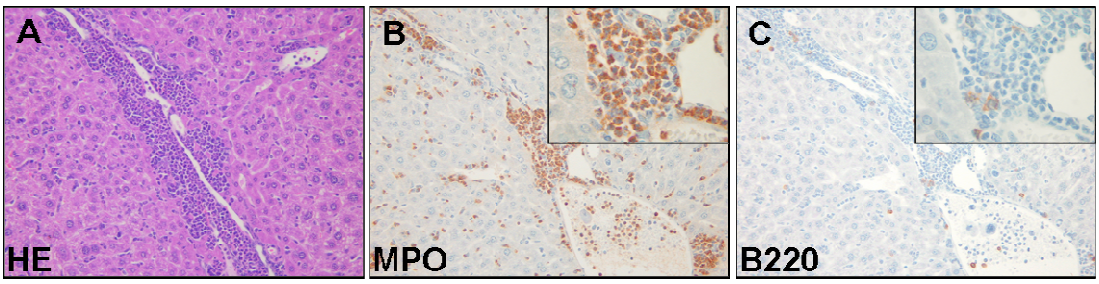

.

Figure 3.3. Acute myeloid leukemia in *CALM-AF10* mouse 13 infected with MOL4070LTR. H&E stained liver (***A*** and ***insert***), MPO labeled liver (***B*** and ***insert***) and B220 labeled liver (***C*** and ***insert***). Note the invasion of liver with MPO+, B220- cells. Original magnification, x200 (A, B, and C); x1000 (inserts).

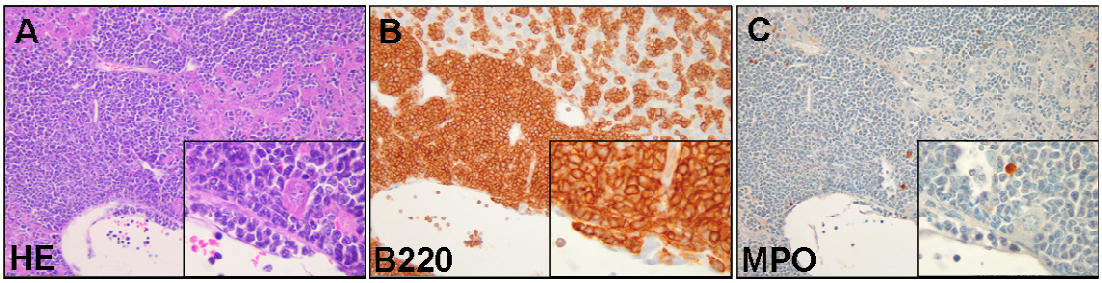

Figure 3.4. Acute lymphoid leukemia (B-ALL) in *CALM-AF10* mouse 17 infected with MOL4070LTR. H&E stained liver (***A*** and ***insert***), B220 labeled liver (***B*** and ***insert***) and MPO labeled liver (***C*** and ***insert***). Note the invasion of liver with B220+, MPO- cells. Original magnification, x200 (A, B, and C); x1000 (inserts).

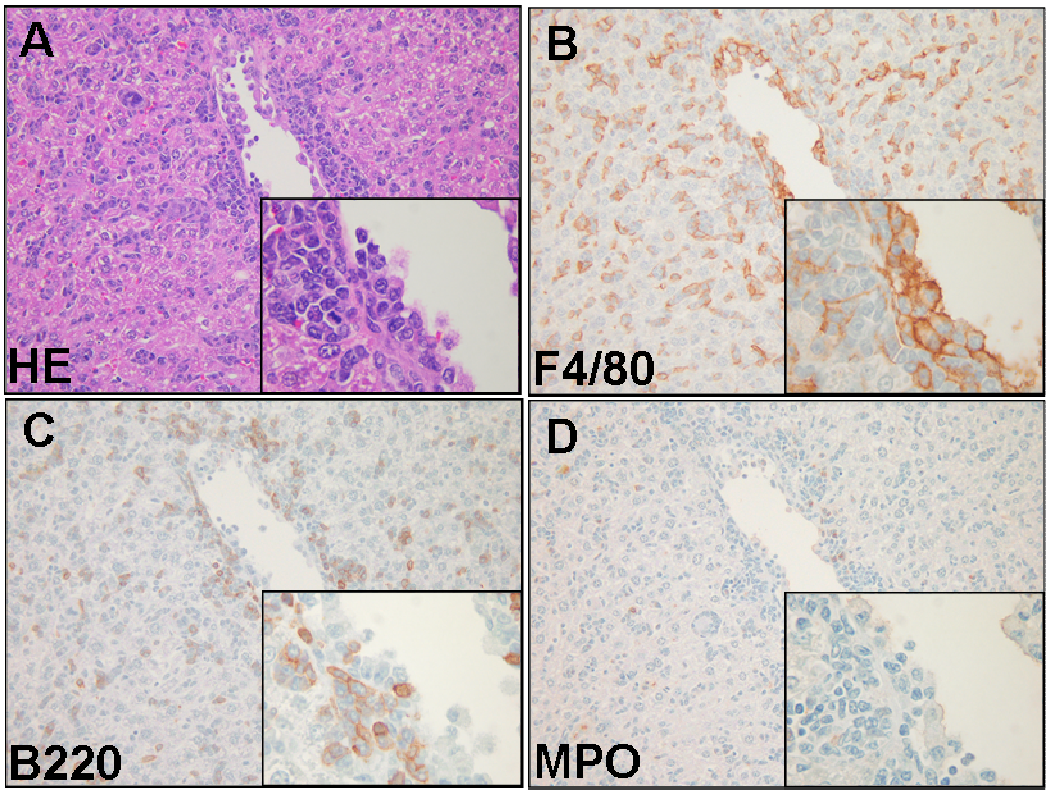

Figure 3.5. Acute myeloid leukemia (Biphenotypic) in *CALM-AF10* mouse 80 infected with MOL4070LTR. H&E stained liver (***A*** and ***insert***), F4/80 labeled liver (**B** and ***insert***), B220 labeled liver, (***C*** and ***insert***), and MPO labeled liver (***D*** and ***insert***). Original magnification, x200 (A, B, C, and D); x1000 (inserts)

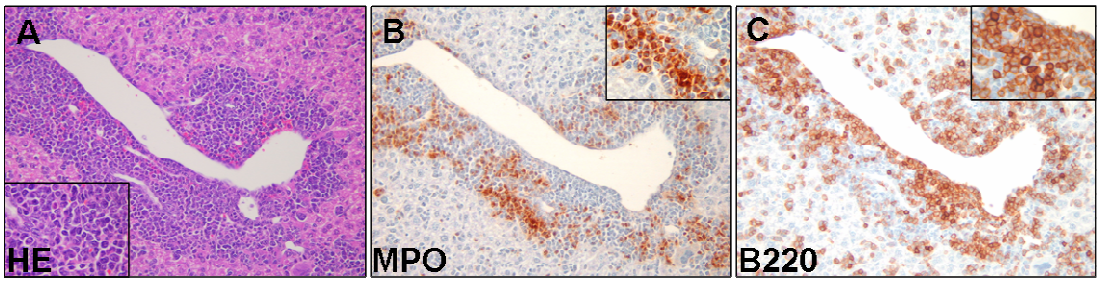

Figure 3.6. Acute myeloid leukemia (Biclonal in *CALM-AF10* mouse 42 infected with MOL4070LTR. H&E stained liver (***A*** and ***insert***), MPO labeled liver, (***B*** and ***insert***), B220 labeled liver (***C*** and ***insert***). Note the mutually exclusive areas of immunoreactivity in the perivascular infiltrates. Original magnification, x200 (A, B, and C); x1000 inserts).

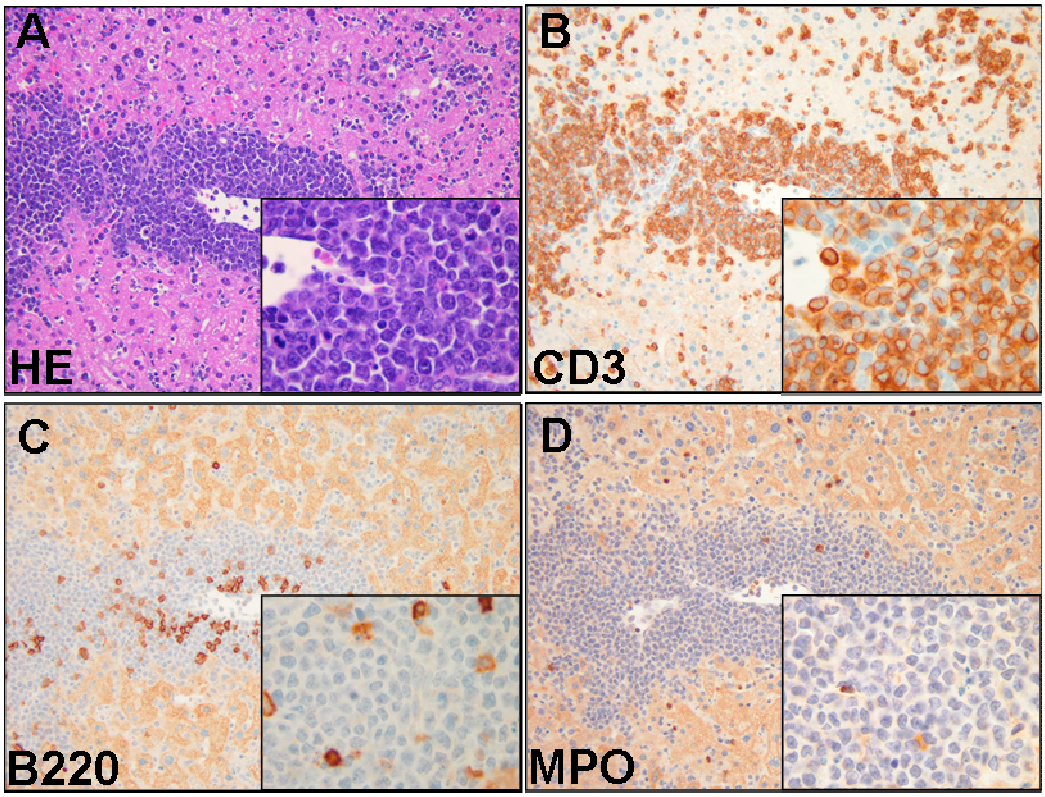

Figure 3.7. Acute lymphoid leukemia (T-ALL) in *CALM-AF10* mouse 66 infected with MOL4070LTR. H&E stained liver (***A*** and ***insert***), CD3 labeled liver (***B*** and ***insert***), B220 labeled liver, (***C*** and ***insert***), and MPO labeled liver (***D*** and ***insert***). Original magnification, x200 (A, B, C and D); x1000 (inserts).

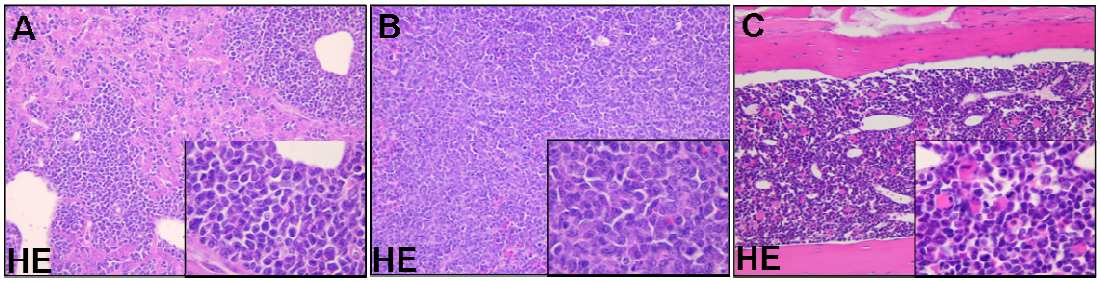

Figure 3.8. Acute lymphoid leukemia in *CALM-AF10* mouse 17 infected with MOL4070LTR. H&E stained liver (***A*** and ***insert***), spleen (***B*** and ***insert***), bone marrow (***C*** and ***insert***). Note the perivascular accumulation of lymphoblasts in the liver and the marked expansion by lymphoblasts in spleen and bone marrow. Original magnification, x200 (A, B, and C); x1000 (inserts).

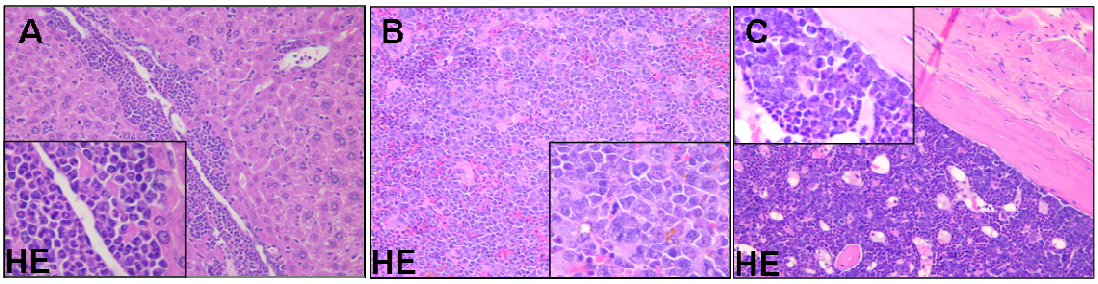

Figure 3.9. Acute myeloid leukemia in *CALM-AF10* mouse 13 infected with MOL4070LTR. H&E stained liver (***A*** and ***insert***), spleen (***B*** and ***insert***), bone marrow (***C*** and ***insert***). Note the perivascular accumulation of myeloblasts in the liver and the marked expansion by blasts in spleen and bone marrow. Original magnification, x200 (A, B, and C); x1000 (inserts).

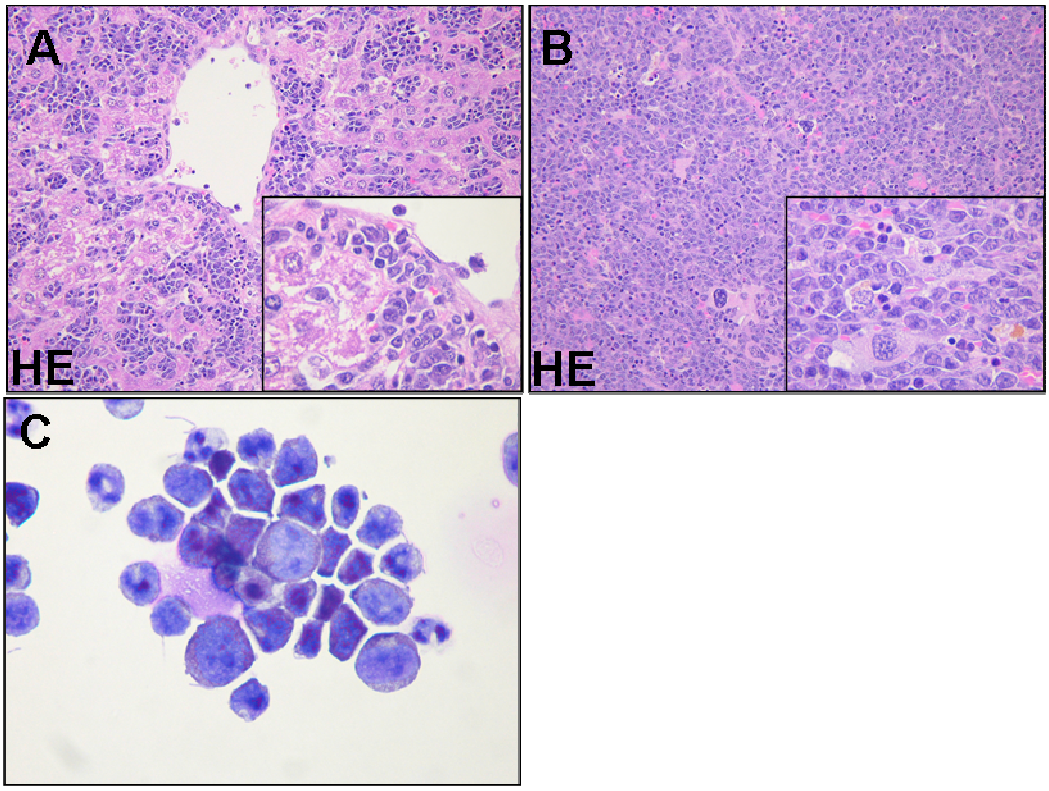

Figure 3.10. Acute myeloid leukemia in *CALM-AF10* mouse 80 infected with MOL4070LTR. H&E stained liver (***A*** and ***insert***), spleen (***B*** and ***insert***), bone marrow cytospin (***C*** and ***insert***). Note the perivascular accumulation of myeloblasts in the liver and infiltration into hepatic sinusoids, and the marked expansion by blasts in spleen. Original magnification, x200 (A, B,); x1000 (C and inserts).

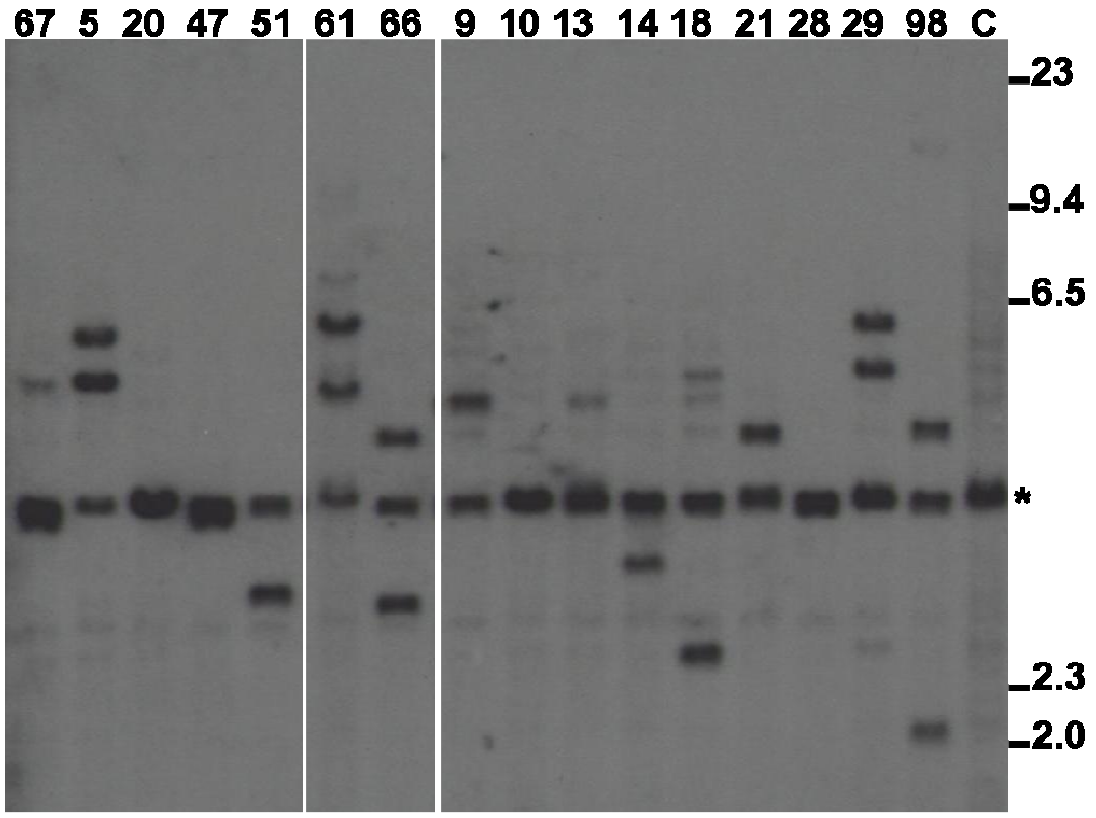

Figure 3.11. Clonal Igh gene rearrangements. Southern blot of *Eco*RI digested genomic DNA from spleen hybridized to an *IgH* probe. Mouse numbers are indicated. C is germline control tissue. Asterisk denotes germ-line band. Size standards are in kb.

Tumors are either clonal or oligoclonal.

Leukemic samples from the infected *CALM-AF10* mice were evaluated using Southern blot analysis to determine the clonality of tumors (Figure 3.11). There were between one and ten integrations per tumors suggesting the tumors were clonal to oligoclonal. These findings in our study suggest a number of possibilities. First, a single dominant band (such as mouse #5 in Figure 3.12) suggests that the tumor developed from a single integration event and is therefore clonal. In the case of mouse 9 (Figure 3.12), there are five unique bands, all of equal intensity suggesting that the tumor was comprised of one major clone with five insertions. Mouse 13 developed a tumor that contains two prominent bands and two-three bands that are less intense; this tumor is likely oligoclonal, comprised of a major clone (represented by the two intense bands) and a minor clone (represented by the three fainter bands). There were between one and ten integrations in WT mice. Interestingly, one *CALM-AF10* mouse and three WT mice did not have detectable integrations suggesting that these mice did not get infected with the retrovirus; there was no evidence of leukemia in these mice at the time of death.

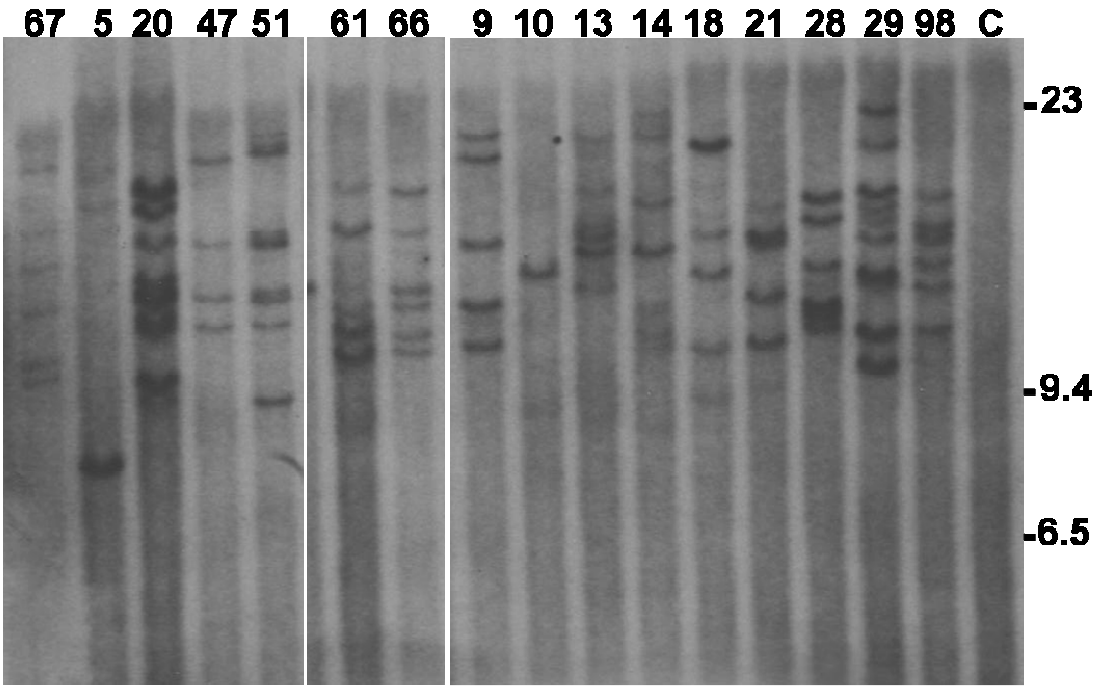

Figure 3.12. Retroviral integration analysis. Southern blot analysis of *EcoR*I-digested genomic DNA from spleens of transgenic mice infected with MOL4070LTR hybridized to probe that targets the *env* viral genome. Mouse identifications are indicated; C, germ-line control tissue; Size standards are given in kilobases. Note the variation of band intensity within each sample; this suggests the tumors are oligoclonal.

Identification of unique retrovirus insertions

Ligation-mediated PCR was attempted on all 42 mice. A total of 255 unique insertions were identified in 39 mice (See Appendix V). Seventeen common insertion sites (CIS); defined as an insertions within 100 kb of a nearby gene and occurring in two or more mice were identified; Table 3.2. Nonrecurrent integrations were also identified that are of interest due to the function of nearby genes or because they were previously identified in other mutagenesis screens.

Inbred strains of mice are known to harbor proviral DNA derived from retroviral infections. Because of this biological phenomenon, the possibility was considered that the primers used in the linker-mediated PCR assay were not specific to the MOL4070LTR and therefore could amplify non-MOL4070LTR provirus. As shown in Figure 3.13, the primers used in the PCR assay were indeed specific for MOL4070LTR and did not amplify the LTR region of evolutionarily conserved provirus.

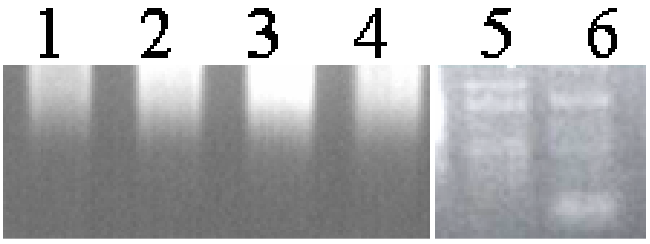

Figure 3.13. PCR to validate LTR primer specificity. PCR showing that primers used to amplify the LTR of MOL4070LTR retrovirus were specific. 1 is FVB wild-type mouse spleen, 2 is FVB wild-type mouse spleen, 3 is *CALM-AF10* mouse with tumor, 4 is *CALM-AF10* mouse with tumor, 5 is *CALM-AF10* mouse infected with MOL4070LTR, 6 is *CALM-AF10* mouse infected with MOL4070LTR. Note bands in lanes 5 and 6 are from a mouse infected with MOL4070LTR.

Table 3.2. Common integration sites in *CALM-AF10* mice infected with MOL4070LTR retrovirus[a]

CIS	Incidence	Mouse Identification	Chromosome	Occurrence in RTCGD[b]
Zeb2	6 (5)[c]	5, 17, 21, 27, 36, 98	2	13
Mn1	6	25, 38, 39, 46, 67, 80	5	8
Evi1	5	6, 14, 29, 31, 36	3	7
Nf1	4 (7)	17, 23, 36, 98	11	28
Ift57	3	14, 36, 69	16	0
Mllt3	3	14, 47, 69	4	0
Plag1	2	21, 42	4	8
Mpl	2	10, 80	4	0
Prkcz	2	17, 31	4	0
Foxp1	2	35, 88	6	0
Kras	2	20, 27	6	7
AK212323	2	25, 23	7	0
Rras2	2	21, 39	7	32
Phb	2	69, 96	11	0
Erg	2	6, 69	16	3
Vav1	2	15, 74	17	0
Gata1	2	14, 47	X	0

[a]Common integration sites determined by ligation-mediated PCR and sequence analysis

[b]RTCGD data derived from transposon insertion studies are not included

[c]Numbers in parenthesis represent number of additional mice with an integrations as identified by Southern blot analysis

Zeb2 *(*Zfhxx1b *or* Sip1*) is a potential collaborating gene with* CALM-AF10

Zeb2 was identified by PCR in six mice. This gene has been reported 13 times in the RTCGD. Five of the *Zeb2* integrations determined by PCR occurred within a 12 kb cluster 164 kb 5' of *Zeb2*; the sixth integration was 106 kb 5' of *Zeb2*. All six integrations were determined to be in the reverse orientation of *Zeb2* transcription; Figure 3.14. Southern blot analysis was performed using a probe that targeted a 9.5 kb region within the clustered region on all 45 *CALM-AF10* mice to screen for *Zeb2* rearrangements. Four out of six mice that had a *Zeb2* insertion by PCR (17, 21, 23, 31, 36, and 98) also had a gene rearrangement as determined by Southern blot analysis (17, 23, 31, and 98); mouse 21 and 36 were not confirmed by Southern blot analysis because their integration event was outside the range of the Southern blot probe. Five additional mice (5, 27, 51, 70, and 80) were also detected with a gene rearrangement for *Zeb2*. Since the germ-line and rearranged bands were of approximate equal intensity, it is likely that the *Zeb2* insertion represented a major clone in each tumor, except mouse 98; Figure 3.15. There was a second cluster of viral integrations from the RTCGD associated with the first exon of *Zeb2,* it was hypothesized that there might also be additional integrations in the *CALM-AF10* mice not previously identified by the initial Southern blot analysis. A second Southern blot analysis was performed using a probe that covered a 16.7 kb region of the first exon of *Zeb2* and identified two additional mice (25 and 26) with gene rearrangements; Figure 3.15.

An EST was also observed 200kb from *Zeb2* and ~75 kb from the cluster of integrations located 160kb from *Zeb2*. It was hypothesized that because the viral integrations were in close proximity to the EST, they could be altering the expression of the EST. The expression of the EST was assayed using RTPCR and determined that its expression was negative. Next, we assayed the expression of *Zeb2* was assayed in leukemic spleens by real time PCR and showed that tumors as a 3-10 fold higher level of *Zeb2* expression than did wild-type bone marrow (Figure 3.16) All of the mice with *Zeb2* insertions developed either B-cell or biphenotypic leukemia except for mouse 36; all of the mice in this sub cohort had an *Igh* gene rearrangement except mouse 36.

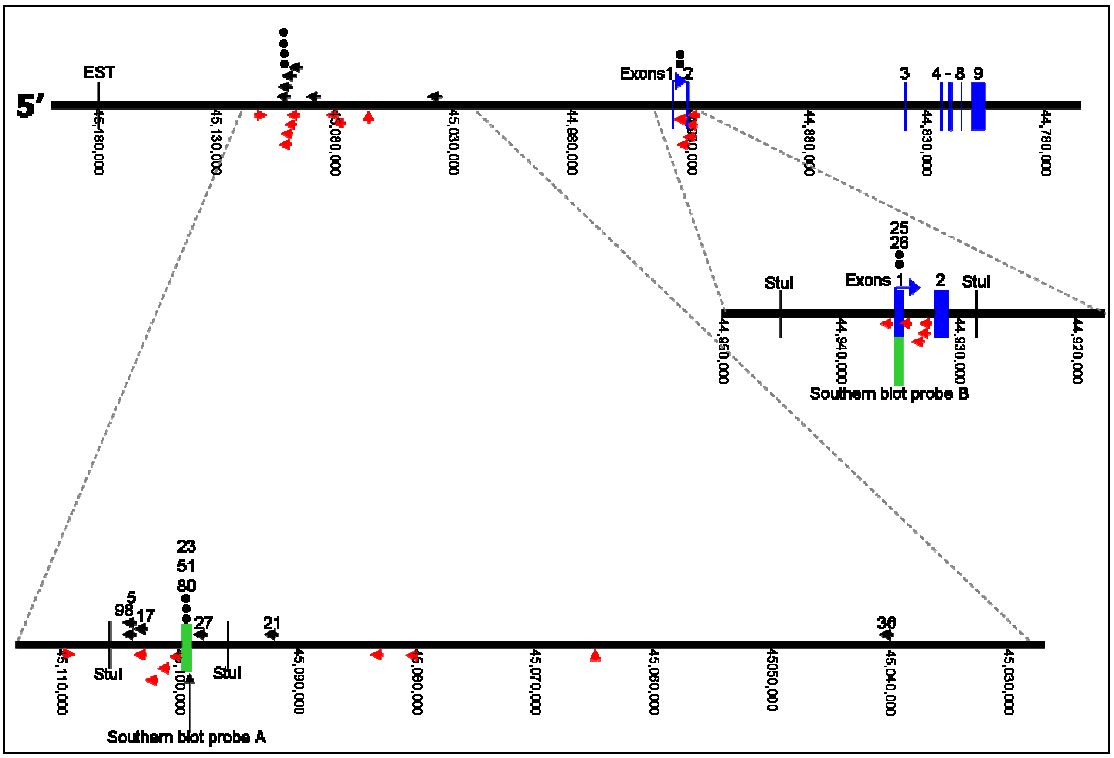

Figure 3.14. Gene map of *Zeb2* viral insertion events. Viral insertions identified by PCR in *CALM-AF10* mice are indicated by black arrows. Insertions events reported in the RTCGD are indicated by red arrows. The vertical red arrows represent insertion events for which the integration orientation was not reported in the RTCGD. Black circles indicate insertion events identified by Southern blot analysis. Probes used for Southern blot analysis are indicated by green bars.

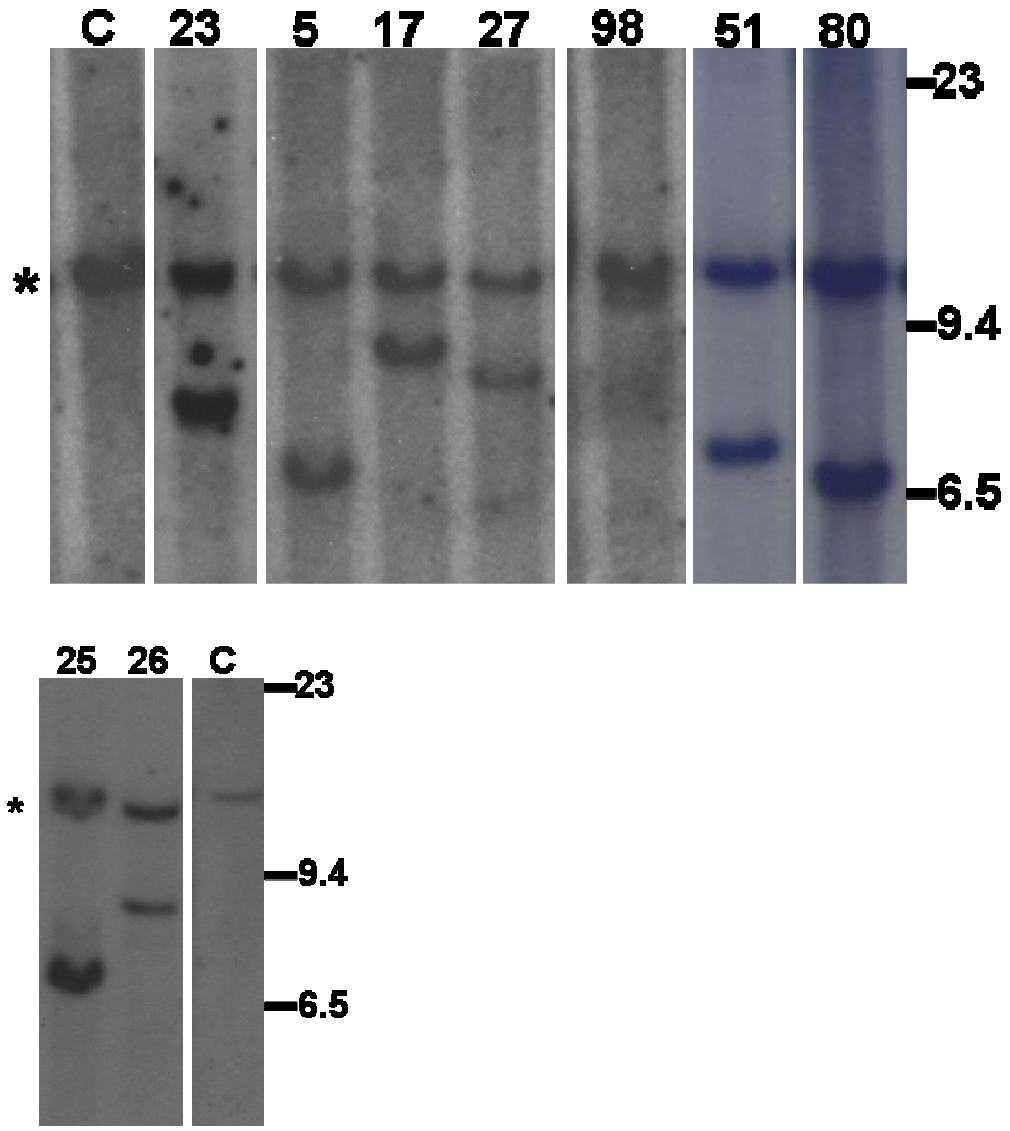

Figure 3.15. *Zeb2* gene rearrangements. Southern blot of *Stu*I-digested genomic DNA extracted from leukemia-infiltrated spleen and hybridized with *Zeb2* probe *A* (upper blot) or *Zeb2* probe *B* (lower blot). Mouse numbers are indicated; C is germ-line control tissue. Asterisks, germ-line bands. Size standards are given in kilobases. Note the equal intensity of germline and rearranged bands indicating that the leukemias were predominately clonal, except for #98.

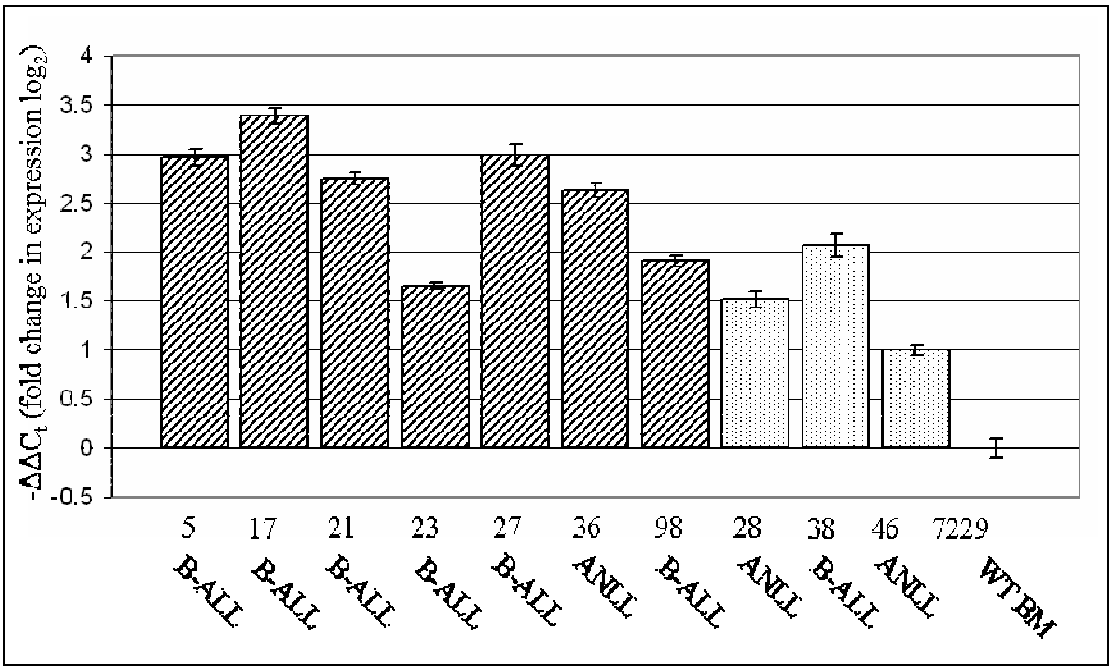

Figure 3.16. *Zeb2* expression in *CALM-AF10* mice infected with MOL4070LTR. RNA transcript analysis by real time RT-PCR of leukemia –infiltrated spleen from transgenic mice with *Zeb2* retrovirus insertions (mice 5, 17, 21, 23, 27, 36, and 98), in mice without a known *Zeb2* insertion (28, 38, and 46), and in addition to wild-type bone marrow (7229).

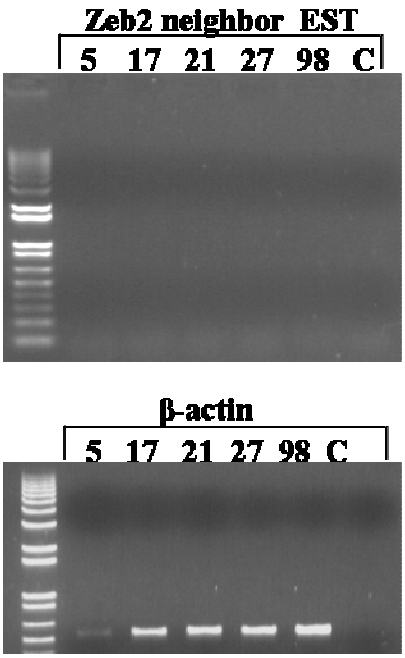

Figure 3.17. Expression of EST associated with *Zeb2*. RT-PCR analysis of leukemic spleen from *CALM-AF10* mice infected with MOL4070LTR that had viral integrations associated with *Zeb2*. Numbers represent individual mouse IDs, C is deionized H20 control. Primer pairs are shown above the brackets. Mouse β-actin primers were used as RNA quality control for each sample shown in lower panel which represents 25 cycles of DNA replication.

Nf1 *is a potential collaborating gene with* CALM-AF10

Retroviral integrations were identified within intron 36 of the tumor suppressor gene *Nf1* in four mice by ligation-mediated PCR (17, 23, 36, and 98); Figure 3.18. The retroviral integrations determined by PCR were confirmed by Southern blot analysis Additional integrations were identified by Southern blot analysis in an additional seven mice (13, 26, 31, 40, 42, 44, and 96). Of note, there was loss of the germ line allele in mice 17 and 23. Next, the tumors from these mice were evaluated using real time RTPCR and showed that there was a decreased expression in samples 17, 23, 26, and 96.

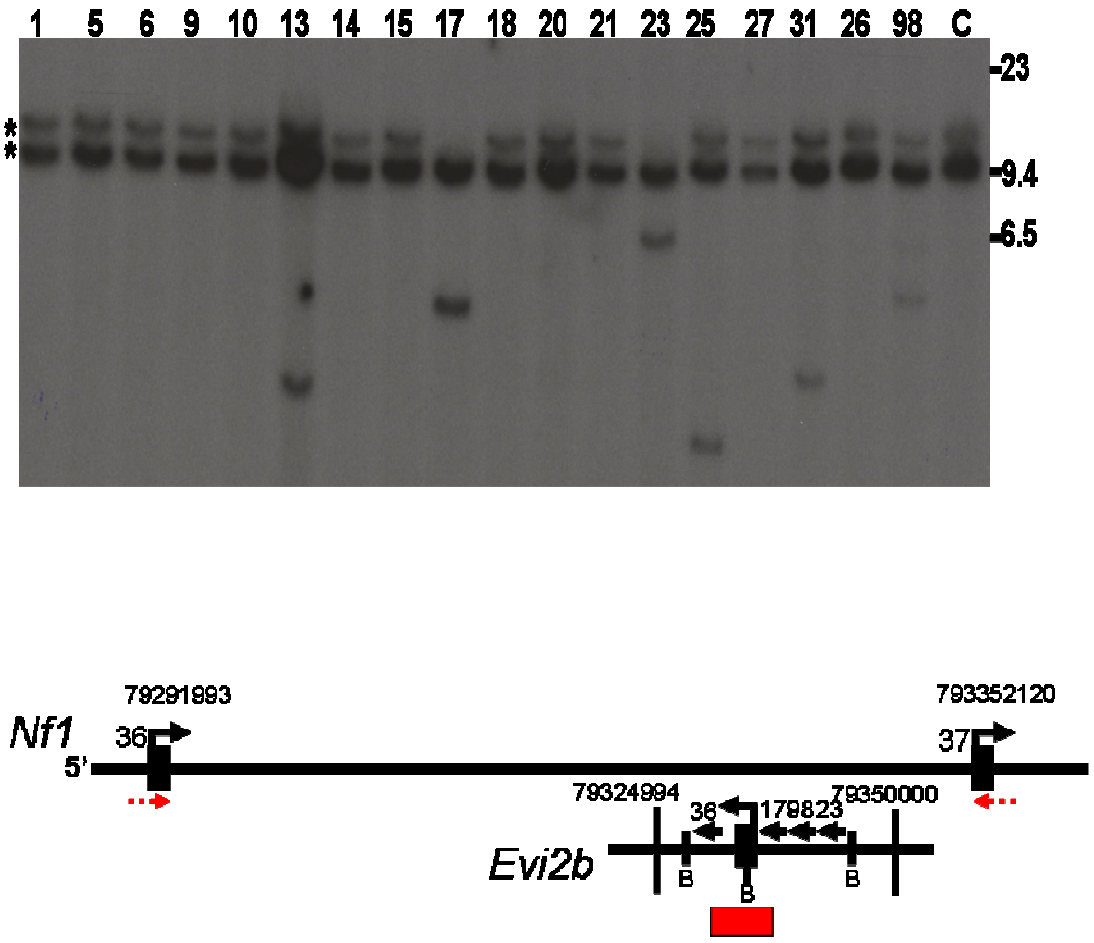

Figure 3.18. ***Nf1*** **integration analysis.** *Nf1* gene rearrangements (upper panel). Southern blot of *BamH*I-digested genomic DNA extracted from leukemia-infiltrated spleen and hybridized with an *Nf1* probe (see map) Mouse numbers are indicated; C is germ-line control tissue. Asterisks, germ-line bands. Two germ-line bands are seen as the probe is split by a *BamH*1 site. Size standards are given in kilobases. Note the loss of germ-line allele in # 17 and 23. Gene map of *Nf1* viral insertion events (lower panel). Viral insertions identified by PCR in *CALM-AF10* mice are indicated by black arrows. The red arrows indicate the position of primers used in the real time PCR gene expression assay. The red box represents the probe used for the Southern blot assay.

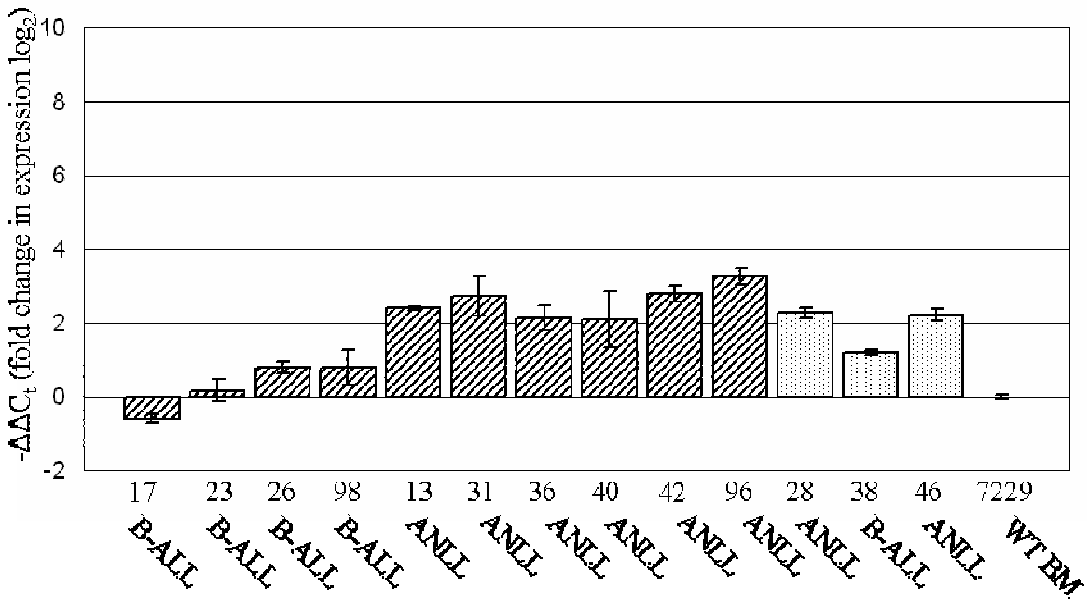

Figure 3.19. *Nf1* expression in *CALM-AF10* mice infected with MOL4070LTR. RNA transcript analysis by real time RT-PCR of leukemia–infiltrated spleen from transgenic mice with *Nf1* retrovirus insertions (mice 17, 23, 26, 98, 13, 31, 36, 40, 42, and 96); in mice without a known Nf1 insertion (28, 38, and 46); and in wild-type bone marrow (7229).

Table 3.3. Summary of *CALM-AF10* mice with *Zeb2* and/or *Nf1* Insertions

ID	Age (months)	Diagnosis	*Igh* Rearrangement	Gene Insertion
5	7	B-ALL	yes	*Zeb2*
21	5	B-ALL	yes	*Zeb2*
27	4	B-ALL	yes	*Zeb2*
80	4	Biphenotypic	yes	*Zeb2*
51	4	Biphenotypic	yes	*Zeb2*
25	6	B-ALL	yes	*Zeb2*
17	6	B-ALL	yes	*Zeb2, Nf1*
36	5	ANLL	no	*Zeb2, Nf1*
23	4	B-ALL	yes	*Zeb2, Nf1*
98	4	B-ALL	yes	*Zeb2, Nf1*
26	5	B-ALL	yes	*Zeb2, Nf1*
31	5	ANLL	no	*Nf1*
13	5	ANLL	no	*Nf1*
40	6	ANLL	no	*Nf1*
42	6	Biphenotypic	yes	*Nf1*
44	6	ANLL	no	*Nf1*
96	3	ANLL	no	*Nf1*

Mn1 *forms a fusion transcript with MOL4070LTR*

Mn1 was identified in six mice (25, 38, 39, 46, and 80). Three insertions were identified in the same intron of *Mn1*, all in the forward direction. *MN1-TEL* fusions have been identified in a subset of human leukemias. The three insertions that were detected occurred in the same breakpoint region as *MN1TEL* fusions, and in the same intron and orientation of integrations identified in *NUP98HOXD13* mice infected with MOL4070LTR (Slape, Hartung et al. 2007). RT-PCR analysis revealed an *Mn1*-retroviral fusion transcript in all three mice with the intronic insertion. Sequence analysis showed that the *Mn1* exon contained a cryptic splice acceptor that spliced to the viral *pol* gene which resulted in an in-frame *Mn1-pol* fusion; Figure 3.22. This fusion transcript encodes a protein that fuses the Mn1 N-terminus to the final 115 amino acid residues of the integrase peptide which is encoded by the viral *pol* gene (Accession number AAC98548) (Slape).

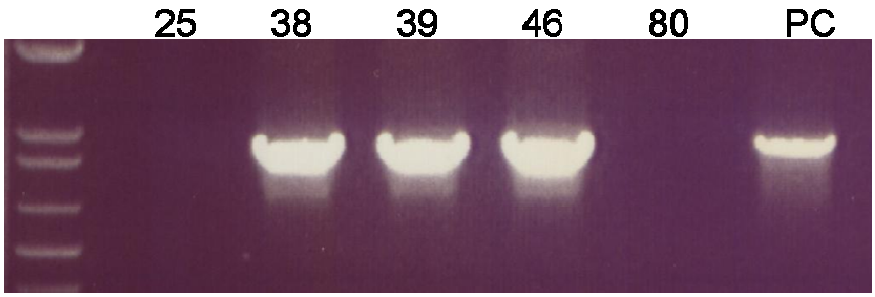

CAGAACCCCAACAACAAAGAAGctcacttacaggctctctacttagtccag

Q N P N N K E A h l q a l y l v q

Figure 3.20 RT-PCR analysis of *CALM-AF10* mice with *Mn1* integrations. Samples 38, 39, and 46, all had integrations that occurred within the first intron; samples 25 and 80 had integrations that occurred in the opposite orientation as Mn1 transcription and occurred after outside of 3' of intron one; PC is a positive control sample. Samples 38, 39, and 49 were sequenced and shown to form an *Mn1*-viral fusion as indicated.

Kras *is a CIS in* CALM-AF10 *mice and has a point mutation*

Kras was identified as a CIS in two mice (20 and 27). Point mutations have previously been reported in *KRAS* from patients with AML, among other malignancies (Reuter, Morgan et al. 2000; Bacher, Kern et al. 2005; Renneville, Roumier et al. 2008). In one of the samples with a *Kras* retroviral integration (27) there was a single point mutation that resulted in a glycine to aspartic acid amino acid change (Figure 3.21A). Next, the gene expression of *Kras* was assayed in the tumors from these mice and found that the expression was 3.5-27 fold higher in mice with *Kras* integrations when compared to wild-type bone marrow (Figure 3.21B). Of note, mouse 27 which had the point mutation also had the highest expression.

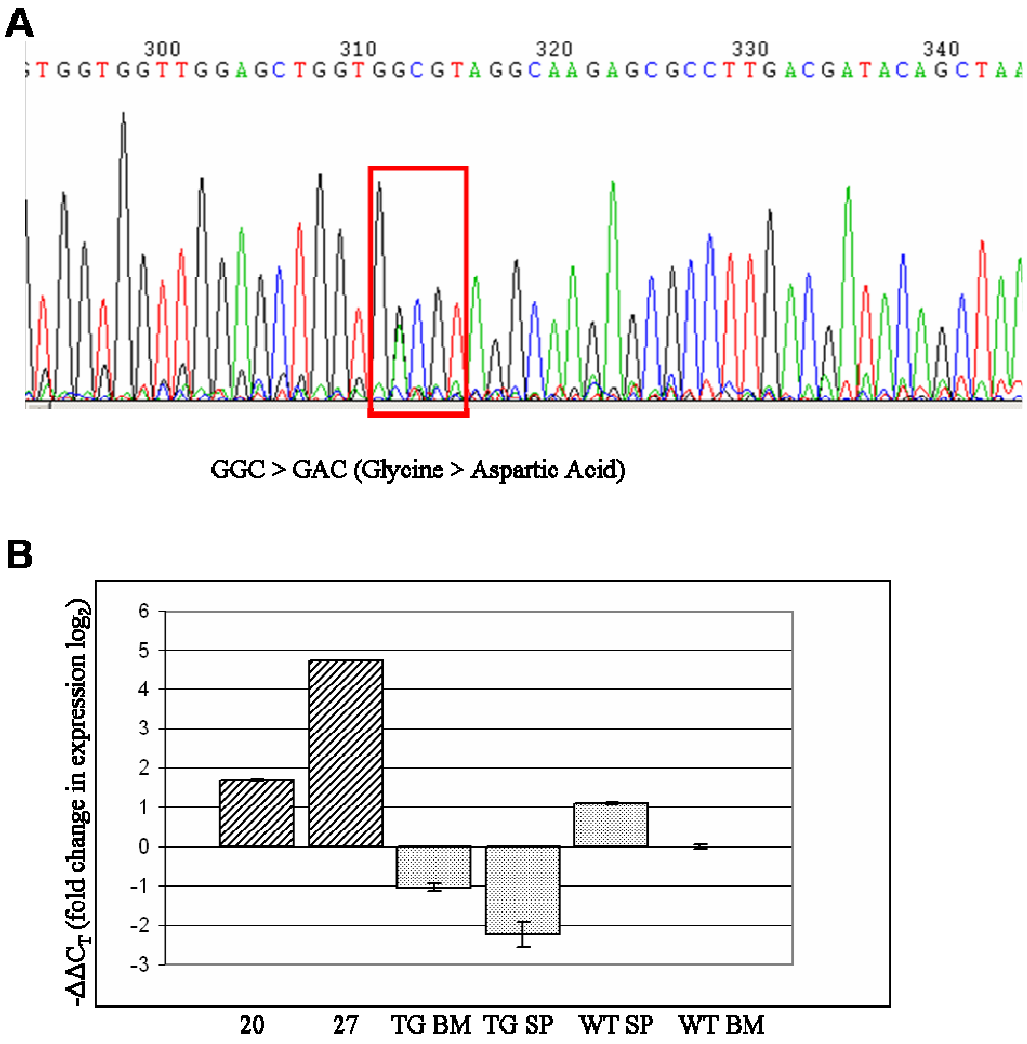

Figure 3.21. Analysis of *Kras* as a CIS. A. Chromatogram of DNA sequence analysis from mouse 27. Note the GGC>GAC point mutation that resulted in a glycine to aspartic acid amino acid change. B. RNA transcript analysis by real time RT-PCR of leukemia-infiltrated spleen from *CALM-AF10* mice (20 and 27), clinically healthy transgenic bone marrow (TG BM); transgenic spleen (TG SP); wild-type spleen (WT SP); and wild-type bone marrow (WT BM).

Meis*1 was not identified as a CIS in* CALM-AF10 *mice*

Meis1 is one of the genes most commonly identified by RIM, but was identified only once by PCR analysis in this study, therefore 43 tumor samples were screened using Southern blot analysis. However, additional insertion events for *Meis1* were not identified.

Discussion

In Chapter 2, a *CALM-AF10* fusion cDNA resulted in impaired thymocyte differentiation and AML when expressed in mice. The *CALM-AF10* mice develop leukemia after a long latency period and incomplete penetrance, which suggest the need for complementary events. A current concept in leukemic biology suggest that one mutation event results in impaired differentiation and a complementary mutation(s) increases cellular proliferation and/or decreased apoptosis (Kelly and Gilliland 2002). Retroviral insertional mutagenesis was used to identify candidate genes that complement a *CALM-AF10* fusion during the leukemogenic transformation.

A cohort of newborn *CALM-AF10* mice infected with MOL4070LTR developed acute leukemia after a median of 4.5 months. This is an acceleration of disease compared to wild type mice infected with retrovirus (median latency 10.5 months) or *CALM-AF10* mice not infected with retrovirus (median latency 13 months). These findings support our hypothesis that the retrovirus collaborates with *CALM-AF10* to accelerate leukemia in mice. Ligation-mediated PCR and sequence analysis was used

to identify a total of 17 CIS (two insertions that occur within 100 kb) (Hwang, Martins et al. 2002). Of these CIS, many had been reported in other retroviral mutagenesis studies as either proto-oncogenes or tumor suppressor genes. In some cases (*Mllt3*, *Ift57, Mpl, Foxp1, Phb, Vav,* and *Gata1*) the insertions have not been identified as CIS in retroviral mutagenesis screens.

To verify the retroviral insertions identified by PCR, Southern blot analysis and RQ-RTPCR were performed on a subset of CIS. A strong correlation was observed between certain CISs and immunophenotype. Gene expression analysis also correlated with immunophenotype again supporting the role of the CIS in that particular leukemia.

Zeb2 (*Sip1* or *Zfhx1b*) located on chromosome 2q22 encodes for Smad interacting protein 1, a member of the TGF-β family of cytokines. Much of what is known about this gene comes from studies in patients with Mowat-Wilson Syndrome (Mowat, Wilson et al. 2003). These patients have marked developmental disorders as a result of various mutations that occur in cells of neural crest origin (Dastot-Le Moal, Wilson et al. 2007). *Zeb2* also plays a role in epithelial to mesenchymal transition that is seen in certain types of cancers such as breast cancer and renal cell carcinoma (Krishnamachary, Zagzag et al. 2006; Lombaerts, van Wezel et al. 2006; Beltran, Puig et al. 2008; Gregory, Bert et al. 2008; Korpal, Lee et al. 2008). Previous retroviral mutagenesis screens in mice have identified this gene 13 times (RTCGD) in mouse models of leukemia supporting a role in leukemogenesis. Finally, *Zeb2* was

identified as being overexpressed by gene expression array analysis in pediatric AML patients with *MLL* gene rearrangements (Aoi Jo 2007). Here *Zeb2* was identified by either PCR or Southern blot in 12 mice and showed that the majority of the tumors with Zeb2 integrations were also clonal. When the tumor samples were assayed for expression of *Zeb2* it was not surprising, given the findings on Southern blot analysis that the tumors also had high levels of the *Zeb2* transcript. It was observed that a large percentage of mice with *Zeb2* insertions also developed B-cell or biphenotypic leukemia and that all of the mice except for mouse 36 had an *Igh* gene rearrangement. It should be noted that the integration site for mouse 36 was outside of the region assayed by either of the Southern blot probes. Therefore, it is possible that the leukemic clone containing a *Zeb2* insertion from mouse 36 represented a minor clone, providing a potential explanation for the lack of a B-cell phenotype in this mouse. These findings suggest that *Zeb2* collaborates with *CALM-AF10* to promote B-cell leukemia. Tumor samples from seven of the mice with a known *Zeb2* insertion event were assayed for gene expression. There was a 3 to 10 fold increase in *Zeb2*-associated tumors when compared to *Zeb2* expression in wild-type bone marrow.

Neurofibromatosis type 1 (NF1) is an autosomal disorder in humans which results in the development of peripheral nerve sheath tumors, neurofibromas (Korf 2000). Children with NF1 are at increased risk for developing malignant myeloid disease that includes AML, monosomy 7 syndrome, and juvenile myelomonocytic leukemia (JMML). Pediatric patients with NF1 share a variety of common clinical and molecular characteristics, including sex, early onset, marked hepatomegaly and

splenomegaly, leukocytosis and Nf1 loss of heterozygosity in myeloid progenitor cells. The prognosis is poor (O'Marcaigh and Shannon 1997; Tefferi and Gilliland 2007).

NF1 plays a crucial role in hematopoiesis, especially in myeloid cell development. *Neurofibromatosis, type1*, encodes a 327 kD protein known as neurofibromin. Neurofibromin serves as a GTPase-activating protein that accelerates Ras-GTP hydrolysis, converting Ras-GTP to its inactive form Ras-GDP (Braun and Shannon 2008). In health, granulocyte-macrophage colony stimulating factor, a growth promoting transmembrane signal induces $p21^{ras}$ activation by enhancing the levels of Ras-GTP (active) as opposed to Ras-GDP (inactive). The active Ras-GTP, in turn activates a series of downstream kinases that promote cellular proliferation. To further highlight the role of NF1 in hematopoiesis, studies have shown that a loss or deficiency in *Nf1* results in a hypersensitivity to granulocyte-macrophage colony stimulating factor resulting in aberrant hematopoietic cell growth and/or the development of chronic myeloid leukemia (Bollag, Clapp et al. 1996; Largaespada, Brannan et al. 1996).

Several lines of evidence from studies in mice further emphasize the role of *Nf1* in hematopoiesis and leukemia. Gene targeting strategies have been used to disrupt *Nf1* in the mouse. In one study, $Nf1^{+/-}$ heterozygous mice developed a myeloproliferative disease, in year two of life, which was associated with LOH in myeloid cells(Jacks, Shih et al. 1994). This particular model recapitulates the findings seen in JMML. In

a second model, *Nf1*$^{-/-}$ mice died in utero at E12.5-E13.5 from cardiopulmonary development disorders. The fetal liver is a rich source of hematopoietic cells. These cells were harvested from the *Nf1*$^{-/-}$ embryos on day 13.5 and used to reconstitute trilineage hematopoiesis in recipient mice. Following a short incubation period, the mice developed a myeloproliferative syndrome similar to that seen in patients with JMML (Largaespada, Brannan et al. 1996). Finally, the analysis of retroviral integration sites in BXH2 mice that developed spontaneous leukemias identified *Evi-2* as a candidate gene. Further analysis revealed that this gene was located in a large intron of *Nf1,* suggesting a role of *Nf1* in leukemia.

In this present study, *Nf1* was identified as a CIS in 11 mice by either ligation-mediated PCR or Southern blot analysis. This gene has been reported 28 times in the RTCGD. All four insertion events identified by PCR occurred in the same orientation within the *Evi2b* gene located within intron 36 of *Nf1*. In two mice (17 and 23) that had *Nf1* integrations, the loss of the germ line band on the Southern blot analysis suggests a reduction to homozygosity. The expression of *Nf1* was assayed in mice that evidence for *Nf1* insertions. In two samples (17 and 23), expression was decreased compared to wild-type bone marrow. The remaining samples had gene expression levels higher than that of wild-type bone marrow. Of note, the mice with the lowest levels of gene expression also developed B-ALL. We did not anticipate the high level of *Nf1* expression in tumor samples with an *Nf1* gene rearrangement. It is possible that an alternate splice variant is produced as a consequence of viral

integration into *Nf1*, and provides a mechanism by which *Nf1* can be overexpressed in myeloid cells (Largaespada, Shaughnessy et al. 1995).

Mn1 was identified six times as an insertion event by PCR. *MN1* was first cloned from a patient with meningioma(Lekanne Deprez, Riegman et al. 1995) and is a transcriptional coactivator that cooperates with retinoic acid to mediate transcription (van Wely, Molijn et al. 2003). *MN1* is implicated in leukmogenic transformation through two possible mechanisms. *MN1* forms a fusion transcript with *TEL*, a member of the ETS transcription factors and known oncogene in AML (Buijs, Sherr et al. 1995), 1995). It is likely that the MN1-TEL fusion produces an aberrant transcription factor that contains the ETS DNA binding-domain derived from TEL (Buijs, Sherr et al. 1995). In another study, 142 patients with AML with normal cytogentics were analyzed for the expression of MN1. Patients with high levels of MN1 had a poor response to induction therapy, a higher relapse rate, and a shorter relapse free period as well as decreased overall survival (Heuser, Beutel et al. 2006). In a recent retrovirus mutagenesis screen, *MN1* was reported eight times in *NUP98HOXD13* mice that were infected with MOL4070LTR. This finding suggests that *Mn1* collaborates with the *NUP98HOXD13* transgene to cause leukemia in mice.

The fact that *Mn1* was identified six times in *CALM-AF10* mice supports the role of *Mn1* as an oncogene in AML. Furthermore, three mice in this study had viral insertions in the first intron of *Mn1* that formed fusion transcripts with the viral gene, *integrase*. This finding highlights the previous observation of *MN1-TEL* fusions. A

previous study in mice showed that the *MN1-TEL* fusion collaborates with *HOXA9* to induce a myeloid malignancy. Slape and colleagues hypothesized that the *Mn1-integrase* fusions could collaborate with the *NUP98HOXD13* transgene in a way similar to *MN1-TEL* fusions to induce myeloid leukemia (Slape, Hartung et al. 2007). Intriguingly chapter 4 showed (Caudell, Zhang et al. 2007) that *Hoxa9* is up-regulated in *CALM-AF10* induced myeloid leukemias. Taken together these findings suggest a collaborative role between *CALM-AF10* and *Mn1* in leukemia.

Kras is one of three 21 kD protein members of the Ras family that binds quanine nucleotides and plays a central role in cell proliferation, survival, and differentiation (Ellis and Clark 2000; Adjei 2001). Activating mutations in *Kras* result in the constitutive activation of cell proliferation signals (Adjei 2001). Mutations involving *Kras* have been reported in five per cent of patients with AML, and when combined with mutations that involve *Nras*, can be seen in as many as 20% of all AMLs (Renneville, Roumier et al. 2008). Studies in mouse models have shown that the oncogenic form of *Kras* results in a myeloproliferative disease but not AML; this finding suggests that additional mutations are needed for mice to develop leukemia. Here *Kras* was identified as a CIS in two mice; *Kras* has been reported 7 times in the RTCGD. These findings prompted us to screen the samples for the presence of point mutations. Because point mutations occur at such a high rate in humans with leukemia, it was not surprising that a point mutation was identified in at least one of the mice (mouse 27). The expression of *Kras* was assayed and found that the

expression was higher than in wild-type bone marrow. Of note, sample 27 which had the highest gene expression was the same mouse with the point mutation.

Meis1 is a transcription factor that collaborates with *HOX* genes in leukemia (Moskow, Bullrich et al. 1995; Nakamura T, Largaespada DA et al. 1996; Kroon, Krosl et al. 1998; Thorsteinsdottir, Kroon et al. 2001; Pineault, Buske et al. 2003). *Meis1* has previously been identified as a CIS through a retroviral mutagenesis screens in mice (Iwasaki, Kuwata et al. 2005). In fact, in a recent study, *Meis1* was identified in 14 *NUP98HOXD13* transgenic mice that were infected with the MOL4070LTR(Slape, Hartung et al. 2007). In Chapter 4 it is shown that *Meis1* is up-regulated in *CALM-AF10* mice with leukemia along with *Hoxa9* in bone marrow from clinically healthy *CALM-AF10* mice and in mice with AML. *Meis1* was identified only once in a tumor sample by PCR in our study. Because *Meis1* is overexpressed in *CALM-AF10* sensitized mice it is an unlikely target by the retrovirus during infection and integration, and is not surprising that we identified it only once as an insertion event.

Recently, a similar study was published that used retroviral mutagenesis in *NUP98HOXD13* sensitized mice to screen for collaborating genes (Slape, Hartung et al. 2007). In that study, they found that many of the leukemias contained more than one CIS suggesting that multiple retroviral integrations complement the transgene. In retroviral-infected *CALM-AF10* mice, there was evidence by Southern-blot analysis that a single insertion was sufficient to complement *CALM-AF10* in a subset of the

mice. Other leukemias that developed in the *CALM-AF10* mice were indeed oligoclonal; some of these leukemias had a single intense integration with additional less intense bands, or multiple equally intense bands. This suggests that these tumors were composed of major and minor clones, or multiple dominant clones. Several insertions were also identified that occurred only once that are of interest either because of their known role in cancer biology or have been previously reported in the RTCGD. These single insertion events may have occurred due to the *CALM-AF10* transgene effect or the type of retrovirus used to accelerate the leukemia. Furthermore, although these events were detected, they represented "passenger mutations" i.e., events that occurred within hematopoietic cells but did not offer a selective advantage to the cell and thus leukemic transformation.

In Chapter 2 it was shown that *CALM-AF10* mice developed acute leukemia after a long latency and incomplete penetrance. These findings suggest that additional mutations were needed to complement the transgene. In this study, we used retroviral insertional mutagenesis to identify complementary genetic events that might collaborate with *CALM-AF10* during leukemic transformation. We identified several CIS that potentially collaborate with *CALM-AF10.* Of these CIS, *Zeb2* and *Nf1* are interesting and warrant further investigation into their role as collaborating genes with *CALM-AF10.* Overexpression of *Zeb2* in a retroviral-based bone marrow transduction and transplantion system would be one mechanism by which to study *Zeb2* collaboration with *CALM-AF10.* The role of *Nf1* in *CALM-AF10* leukemias could be studied by crossing *CALM-AF10* mice to $Nf1^{+/-}$ mice with the expectation

that mice would develop leukemia at an accelerated rate. Retroviral infection was shown here to accelerate the onset of acute leukemia, and genes were identified that potentially collaborate with the *CALM-AF10* fusion gene in the leukemic transformation process. This transgenic murine model serves as a model system for studying leukemogenesis similar to that observed in humans with leukemia.

Chapter 4: Evaluation of differentially expressed genes in hematopoietic precursor cells from *CALM-AF10* mice.

Introduction

This chapter will focus on experiments designed to gain insight into the consequence of *CALM-AF10* fusion transcript expression on potential gene targets in the *CALM-AF10* transgenic mouse model. In order to identify theses genes, two different approaches were taken to address this question, a candidate gene approach as well as a whole genome screen. A recently published study using gene expression profiling showed that human *CALM-AF10*+ T-ALLs are characterized by overexpression of *HOXA*, *MEIS1*, and *BMI1* oncogenes. Therefore, gene expression of these and other *Hox* genes were assayed in *CALM-AF10* positive leukemic cells compared to wild-type hematopoietic progenitors using real time RT-PCR. The second approach used to address this question involved gene expression profiles of bone marrow from *CALM-AF10* mice compared to the expression profiles of wild-type mouse bone marrow by microarray analysis.

Materials and methods

Real Time RT-PCR assay for Hoxa5, Hoxa7, Hoxa9 Hoxa10, Hoxa11, Hoxa13, Hoxb4, Hoxd13,*and* Meis1.

Total RNA (1ug) from transgenic or wild-type spleen, bone marrow, and thymus, as well as spleen infiltrated by leukemic cells was reverse transcribed as described in

chapter two. Real time RT-PCR was performed on a 7500 Fast Real Time Taqman PCR system (Applied Biosystem) using aliquots of first strand cDNA as templates for mouse *Hoxa5, Hoxa7, Hoxa9, Hoxa10, Hoxa11, Hoxa13, Hoxb4, Hoxd13,* and *Meis1* with Applied Biosystems primer and probe sets. All reactions were done in triplicate with 20 µl PCR reactions using the Applied Biosystems default thermalcycling conditions (an activation step at 95˚C for 20 sec followed by 40 cycles of amplification at 95˚C for 0.03 sec, followed by an annealing and extension step at 60˚C for 30 sec). The expression of the 18S ribosomal RNA was used as an endogenous control. All reactions were performed in triplicate, and the $-\Delta\Delta C_T$ mean and standard error were calculated for each sample. Values for the transcript of interest were normalized to the 18S rRNA value and compared to the expression in wild-type bone marrow.

RT-PCR

RT-PCR analysis was performed for the expression of *Bmi1* in tumors as well as transgenic and wild-type liver as previously described. The PCR was performed as previously descried using with the following primers 5'CCCAGTGCTAACCACCAATCTTCC3' and 5'GGAAGCAAACTGGACGACAGTCAC3' with the following thermocycling conditions 94°C for 3 min; 34 cycles of 94°C for 30 seconds, 62°C for 30 seconds, 72°C for one min; followed by a terminal extension of 72°C for 10 min.

Microarray analysis

Bone marrow, spleen, and thymus was harvested from three wild-type and three *CALM-AF10* mice and placed in either Hanks Balanced Salt Solution with 2% FCS or snap frozen and stored at -80°C. Whole blood was collected for CBC analysis. Single-cell suspensions prepared from thymus and bone marrow were incubated with fluorescein isothiocyanate (FITC)–conjugated anti–mouse CD8, B220, Gr-1, phycoerythrin (PE)–conjugated anti–mouse CD4, IgM, Mac-1 (Pharmingen) and analyzed by three-color flow cytometry to determine immunophenotype as described previously.

Microarray Hybridization

Total RNA was isolated from bone marrow samples by Trizol (Invitrogen) as described in Chapter 2, and three micrograms of total RNA was sent to the Laboratory of Molecular Technology (LMT), NCI-Frederick, Frederick, MD. To perform the Affymetrix microarray, 50 ng of total RNA was used for microarray hybridization following the Affymetrix protocol for 2-cycle cDNA synthesis (http://www.affymetrix.com/products/reagents/specific/cdna2.affx and http://www.affymetrix.com/support/technical/manual/expression_manual.affx)**.** First, Poly-A RNA controls, designed to provide exogenous controls that evaluate the total labeling process of the eukaryotic target, were prepared using the Poly-A RNA Control Kit (Affymetrix). These controls were mixed with the T7-Oligo(dT) Primer and added to the total RNA sample for the first cycle, first strand and second strand cDNA synthesis using the Affymetrix 2-cycle cDNA synthesis kit. Next**,** the first cycle in vitro transcription (IVT) reaction was performed overnight using a

MEGAscript T7 kit (Ambion). Afterwards, the first cycle RNA clean-up step was performed using a cRNA clean-up column. Next, the second cycle of first and second strand cDNA synthesis was performed using the Affymetrix 2-cycle cDNA synthesis kit. The second cycle cDNA clean-up was performed the following day using a column followed by an overnight IVT reaction that produced biotin-labeled cRNA. Next, biotin-labeled cRNA was fragmented followed by a final cleaned up step. This was followed by overnight hybridization of the fragmented cRNA, using the Affymetrix GeneChip Eukaryotic Hybridization Control Kit, to the mouse gene chip array (430 2.0 GeneChip® Array; Affymetrix, Santa Clara, CA). Finally, the arrays were washed and loaded into the Affymetrix GeneChip System scanner 3000 (Hewlett-Packard, Santa Clara, CA). Data files (.CEL, .DAT, .CDF and .CHP) were copied to a cd and returned for analysis. The fluorescence of the hybridized chips was analyzed using BRB array tools software, version 3.6.0. A comparison analysis based on ***CALM-AF10*** fusion was performed after normalization using standard settings of BRB array tool (experiment/baseline ratio higher or lower than 2)

Results

Hoxa cluster genes are up-regulated in CALM-AF10 mice

We assayed *Hoxa5*, *Hoxa7, Hoxa9*, *Hoxa10*, *Hoxa11, Hoxa13, Hoxb4, Hoxd13,* and *Meis1* expression by real time RT-PCR in leukemias from *CALM-AF10* mice to determine if the up-regulation of these genes was seen in this mouse model as well as in the human leukemias. As shown in Figure. 4.1, *Hoxa5*, *Hoxa7, Hoxa9, Hoxa10,* and *Meis1* were all up-regulated in hematopoietic tissue (bone marrow, spleen, thymus) from clinically healthy *CALM-AF10* mice. Myeloid leukemias from *CALM-*

AF10 mice also showed up-regulation of *Hoxa5*, *Hoxa7*, *Hoxa9*, *Hoxa10*, and *Meis1*, indicating that up-regulation of these genes occurs in myeloid as well as T-cell tumors associated with *CALM-AF10* expression. *Hoxb4* was modestly decreased in clinically healthy transgenic bone marrow, as well as in one of four leukemia samples. Expression of *Hoxa11*, *Hoxa13*, and *Hoxd13* was undetectable in all tissues and tumor samples after 35 cycles of amplification in contrast to the threshold of detection for the 18S ribosomal control at 18 cycles of amplification. In contrast to the upregulation of *Hoxa* cluster genes described above, conventional RT-PCR demonstrated that *Bmi1* was highly expressed in hematopoietic tissue and leukemias from both transgenic and non-transgenic mice, but not up-regulated (Figure 4.2)

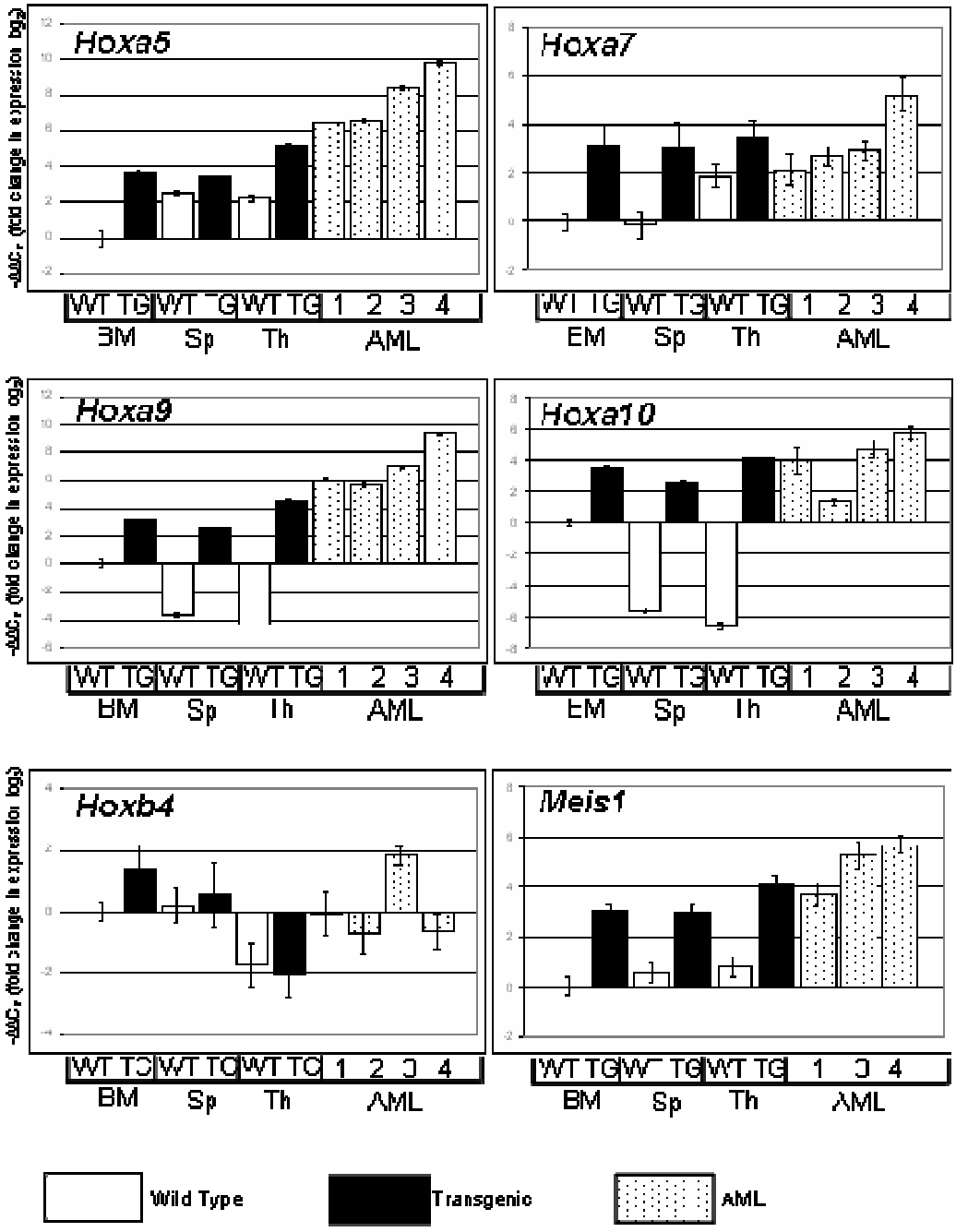

Figure 4.1. ***Hoxa*** **cluster and** ***Meis1*** **expression in** ***CALM-AF10*** **mice.** RNA transcript analysis by real time RT-PCR of bone marrow (BM), spleen (Sp), and thymus (Th) from clinically healthy wild type (WT) and transgenic (TG) mice in addition to mice 7088, 7180, 7160, and 9014 (samples 1,2,3,4) with AML. Expression of *Hoxa5, Hoxa7, Hoxa9, Hoxa10, Hoxa11, Hoxa13, Hoxb4, Hoxd13,* and *Meis1* was normalized to 18S rRNA expression and shown as mean fold change (log2) compared to WT BM.

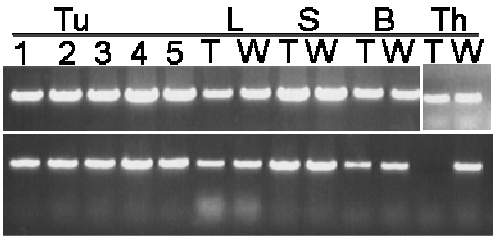

Figure 4.2. RT-PCR analysis of *Bmi1* expression. RT-PCR analysis of tumors (Tu 1,2,3,4, and 5) from *CALM-AF10* mice and Liver (L); Spleen, (S); Bone marrow (B); and Thymus (Th) from *CALM-AF10* transgenic (T) and wild-type (W) mouse, upper panel. Lower panel is β-actin loading control which represents 25 cycles of DNA replication.

Genes upregulated in CALM-AF10 *bone marrow*

In order to gain insight into the consequences of *CALM-AF10* gene expression on downstream gene targets we performed gene expression arrays on bone marrow samples from three *CALM-AF10* clinically healthy mice and three wild-type control mice. Analysis of the microarray set at a 2-fold change in expression identified 80 genes. Five genes were significantly ($P<0.05$) increased in *CALM-AF10* bone marrow compared to wild type controls. These genes included *Hoxa9, Meis1, Dsp (twice), Xlr4b, BB053468.* Of these five genes, Hoxa9 and Meis1 are the two genes most significantly associated with *CALM-AF10* expression (Table 4.1).

Genes downregulated in CALM-AF10 bone marrow

Microarray analysis showed that six genes that belonged to the immunoglobulin family (*Ighg*, *Igh-6*, *Igl-V1*, *Igh*, *Igkv14-111*, and *Igk-V28*) were significantly ($P<0.05$) down-regulated in *CALM-AF10* bone marrow samples compared to wild-type controls. The genes within this cluster that showed the most significant degree of downreguation were those that belong to the immunogbulin family. Specifically, *Igh-6*, which encodes for IgM was detected on four distinct probe sets and showed a 0.19 to 0.45 fold difference in gene expression between transgenic and wild type bone marrow.

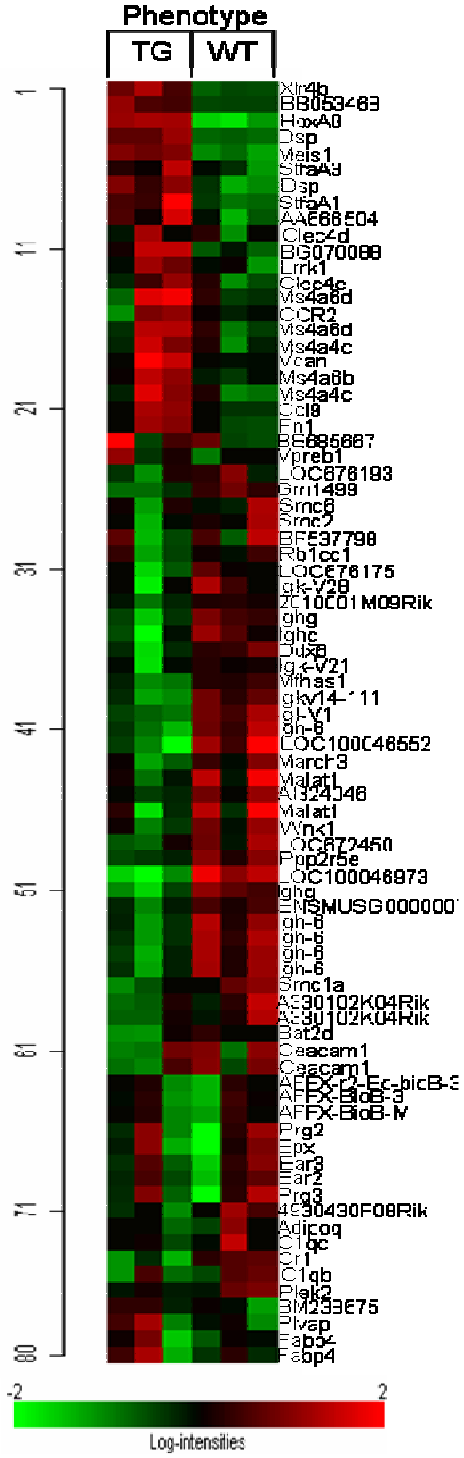

Figure 4.3 Heat map. This heat map depicts a 2-fold change between differentially expressed genes in *CALM-AF10* clinically healthy mouse bone marrow compared to wild-type controls. Samples are indicated at the top, gene abbreviations are indicated at the right. The heat map was generated using BRB array tools v3.6.0.

Table 4.1 Genes differentially upregulated in *CALM-AF10* transgenic mouse bone marrow

Gene symbol	Description	Biological or Molecular Function	Mean of log intensities for T	Mean of log intensities for W	Fold Diff	Probe set
Hoxa9	homeo box A9	transcription factor	6.81655	4.05052	6.80	1455626_at
Meis1	myeloid ecotropic viral integration site 1	transcription factor	6.01177	4.05436	3.88	1450992_a_at
Dsp	desmoplakin	intercellular adhesion	5.34648	3.64366	3.26	1435493_at
Dsp	desmoplakin	intercellular adhesion	5.24705	3.64951	3.03	1435494_s_at
Prg2	proteoglycan 2, bone marrow	immune response	9.74908	8.15596	3.02	1422873_at
BG070088	Unknown	unknown	4.32633	2.77767	2.93	1445773_at
Xlr4b	X-linked lymphocyte-regulated 4B	lymphocyte regulation	8.63156	7.12867	2.83	1449347_a_at
OTTMUSG00000000971	predicted gene, OTTMUSG00000000971	unknown	7.92819	6.46624	2.75	1436530_at
Ms4a4c	membrane-spanning 4-domains, subfamily A, member 4C	signal transduction	7.90808	6.48779	2.68	1450291_s_at
Vcan	versican	cell adhesion, heart development	4.09383	2.7888	2.47	1427256_at
BB053468	Unknown	unknown	3.46935	2.2425	2.34	1440431_at
Ms4a6d	membrane-spanning 4-domains, subfamily A, member 6D	signal transduction	6.84554	5.68744	2.23	1419599_s_at
Fn1	fibronectin 1	ECM-receptor interaction, focal	9.17377	8.0605	2.16	1426642_at
Ms4a6d	membrane-spanning 4-domains, subfamily A, member 6D	signal transduction	5.05986	3.94961	2.16	1419598_at
Ms4a4c	membrane-spanning 4-domains, subfamily A, member 4C	signal transduction	7.06742	5.95976	2.15	1420671_x_at
Stfa3	stefin A3	endopeptidase/ cysteine protease inhibitor activity	6.63602	5.53681	2.14	1419709_at
Ms4a6b	membrane-spanning 4-domains, subfamily A, member 6B	signal transduction	4.72428	3.63995	2.12	1439956_at
Ccl9	chemokine (C-C motif) ligand 9	chemotaxis, immune response, signal transduction	8.77605	7.73974	2.05	1417936_at
Lrrk1	leucine-rich repeat kinase 1	nuclease, ATP, ion binding	5.09694	4.06928	2.04	1451985_at

T is Transgenic; W is Wild-type

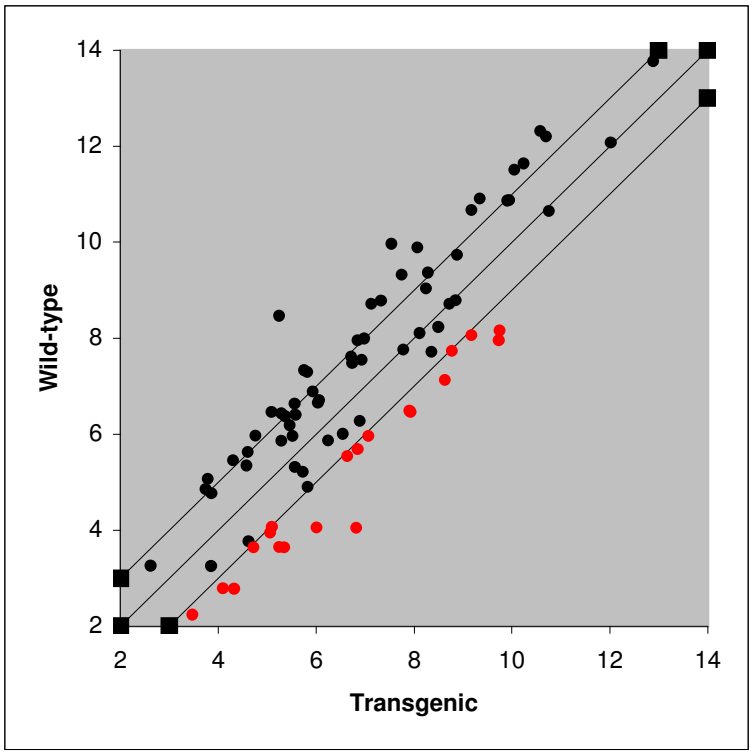

Figure 4.4. Scatter plot of differentially up-regulated genes from *CALM-AF10* bone marrow. The red dots below the linear regression line depict genes from Table 4.1 that were up-regulated in *CALM-AF10* transgenic mouse bone marrow compared to wild-type mouse bone marrow.

Table 4.2 Genes differentially downregulated in *CALM-AF10* transgenic mouse bone marrow

Gene symbol	Description	Biological or Molecular Function	Mean of log intensities for T	Mean of log intensities for W	Fold Diff	Probe set
Mfhas1	malignant fibrous histiocytoma amplified sequence 1	small GTPase mediated signal transduction	5.37112	6.37516	0.50	1436897_at
4930430F08Rik	RIKEN cDNA 4930430F08 gene	unknown	4.60125	5.63136	0.49	1453468_at
March3	membrane-associated ring finger (C3HC4) 3	ubiquitin cycle, endocytosis	5.56403	6.63243	0.48	1441643_at
Wnk1	WNK lysine deficient protein kinase 1	unknown	8.28331	9.36445	0.47	1436746_at
LOC672450	V(kappa) gene product	unknown	6.85216	7.9587	0.46	1451965_at
Ppp2r5e	protein phosphatase 2, regulatory subunit B (B56), epsilon isoform	signal transduction	3.74209	4.85734	0.46	1452788_at
Smc1a	structural maintenance of chromosomes 1A	cell cycle checkpoint, DNA repair, chrom. segregation	5.29126	6.43449	0.45	1417831_at
Gm1499	Gene model 1499, (NCBI)	unknown	4.30106	5.45504	0.45	1426201_at
Igk-V28 /// LOC213481	immunoglobulin kappa chain variable 28 (V28) /// immunoglobulin kappa light chain 17-1A	antigen binding	4.75719	5.97045	0.43	1451962_at
Ddx6	DEAD (Asp-Glu-Ala-Asp) box polypeptide 6	unknown	3.79017	5.06666	0.41	1424598_at
Malat1	Metastasis associated lung adenocarcinoma transcript 1 (non-coding RNA)	unknown	5.0933	6.46321	0.39	1418189_s_at
Ighg	Immunoglobulin heavy chain (gamma polypeptide)	antigen binding	10.23961	11.63655	0.38	1424631_a_at
Cr1	Ig kappa chain	complement cascade	7.32921	8.7828	0.37	1460423_x_at
Igh-6	Immunoglobulin heavy chain 6 (heavy chain of IgM)	ADCC, Type I, II hyper-sensitivity, antigen processing	10.05111	11.50638	0.36	1425247_a_at
Igkv14-111	Immunoglobulin kappa chain variable 14-111	unknown	5.82124	7.29228	0.36	1451951_at
Igh-6	Immunoglobulin heavy chain 6 (heavy chain of IgM)	ADCC, Type I, II hyper-sensitivity, antigen processing	9.17671	10.66721	0.36	1427756_x_at
Igh /// Ighg	immunoglobulin heavy chain complex /// Immunoglobulin heavy chain (gamma polypeptide)	antigen binding	10.69404	12.2014	0.35	1451632_a_at
Igh-6	Immunoglobulin heavy chain 6 (heavy chain of IgM)	ADCC, Type I, II hyper-sensitivity, antigen processing	9.34102	10.9124	0.34	1425324_x_at
Igh-6	Immunoglobulin heavy chain 6 (heavy chain of IgM)	ADCC, Type I, II hyper-sensitivity, antigen processing	7.74318	9.31974	0.34	1427870_x_at
Igl-V1	immunoglobulin lambda chain, variable 1	humoral immune response, antigen binding	5.75049	7.33528	0.33	1430523_s_at
Malat1	Metastasis associated lung adenocarcinoma transcript 1 (non-coding RNA)	unknown	7.12584	8.71402	0.33	1418188_a_at
Igh-6	immunoglobulin heavy chain 6 (heavy chain of IgM)	ADCC, Type I, II hyper-sensitivity, antigen processing	10.58038	12.31376	0.30	1427351_s_at
Ighg	Immunoglobulin heavy chain (gamma polypeptide)	antigen binding	8.07328	9.89093	0.28	1426174_s_at
LOC100046552	similar to Unknown (protein for MGC:103328)	unknown	7.53875	9.96831	0.19	1427837_at
LOC100046973	similar to [Human Ig rearranged gamma chain mRNA, V-J-C region and complete cds.], gene product	unknown	5.24322	8.46545	0.11	1425871_a_at

T is Transgenic; W is Wild-type

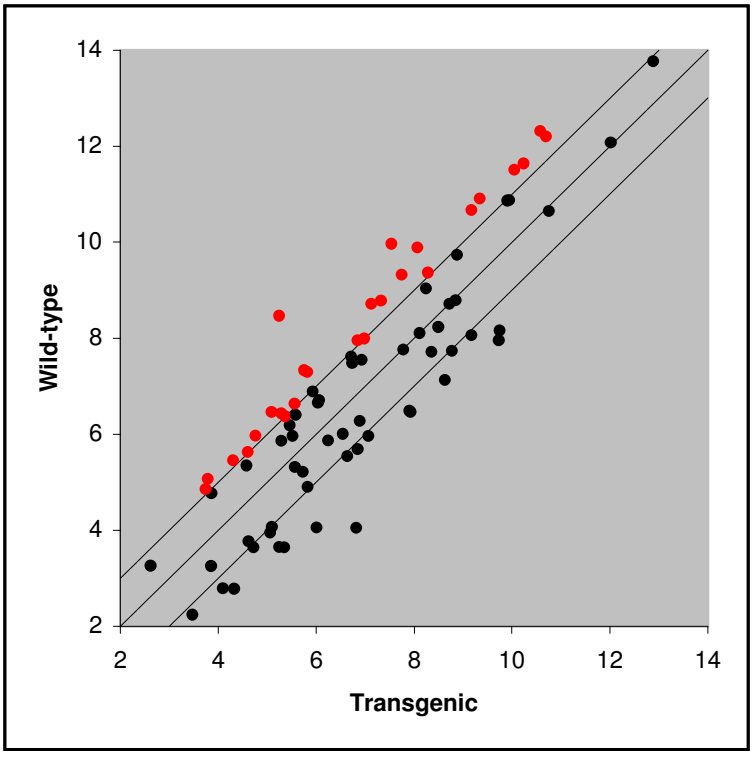

Figure 4.5. Scatter plot of differentially down-regulated genes from *CALM-AF10* bone marrow. The black dots below the linear regression line depict genes from Table 4.2 that were down-regulated in *CALM-AF10* transgenic mouse bone marrow compared to wild-type mouse bone marrow.

Discussion

Patients with *CALM-AF10* fusion are known to have differentially expressed genes that are thought to be targets as a consequence of *CALM-AF10* expression. These genes include *HOXA*, *MEIS1*, *and BMI1* oncogenes (Dik, Brahim et al. 2005). In order to gain insight the role of *CALM-AF10* on potential target genes, RT-PCR and whole genome arrays were used to identify differentially expressed genes in bone marrow of *CALM-AF10* transgenic mice. In this study, *Hoxa* and Meis1, but not *Bmi1* were differentially expressed in *CALM-AF10* mouse bone marrow. Several other genes known to be involved in B-cell development were also identified as being differentially expressed in *CALM-AF10* mice. These findings mimic those that have been reported in *CALM-AF10* patients with leukemia.

Several lines of evidence developed over the past several years have demonstrated the importance of *HOX* gene dysregulation during leukemic transformation. First, *HOX* genes are located downstream of MLL; their unscheduled expression has been observed in leukemias associated with MLL fusions(Ferrando and Look 2003). Second, multiple *HOX* genes have been identified as either fusion partners with *NUP98* or *TCRA* regulatory elements in chromosomal translocations associated with acute leukemia (Calvo, Sykes et al. 2002; Ferrando and Look 2003; Slape and Aplan 2004). Third, gene expression profile studies have shown that up-regulation of several *HOX* genes, especially *HOXA7* and *HOXA9,* occurs in both acute lymphoid and myeloid leukemia (Golub, Slonim et al. 1999; Abramovich and Humphries 2005; Soulier, Clappier et al. 2005). Fourth, *Hox* genes, again including *Hoxa7* and *Hoxa9*,

have been found to be up-regulated by retroviral insertion in mice with retroviral-induced myeloid leukemia (Nakamura, Largaespada et al. 1996). Finally, a number of investigators have reported that over-expression of *HOX* genes or *NUP98-HOX* fusion genes leads to acute myeloid malignancies in mice (Kroon, Thorsteinsdottir et al. 2001; Pineault, Buske et al. 2003; Pineault, Abramovich et al. 2004; Abramovich and Humphries 2005; Lin, Slape et al. 2005). Of note, recent reports demonstrated over-expression of *HOXA5, HOXA9,* and *HOXA10* in pre-T LBL patients who had *CALM-AF10* translocations (Dik, Brahim et al. 2005; Soulier, Clappier et al. 2005; Bergeron, Clappier et al. 2006).

In this study, expression of a *CALM-AF10* fusion gene lead to upregulation of *Hoxa5, Hoxa9*, and *Hoxa10* in hematopoietic tissues from clinically healthy and leukemic *CALM-AF10* transgenic mice. In contrast to previous studies that used retroviral transduction and transplantation to over-express *HOXA9* or *HOXA10* in mouse bone marrow, evidence for myeloproliferation was not detected in *CALM-AF10* transgenic mice (Thorsteinsdottir, Sauvageau et al. 1997; Kroon, Krosl et al. 1998; Calvo, Sykes et al. 2000; Buske, Feuring-Buske et al. 2001; Thorsteinsdottir, Kroon et al. 2001) This difference may be due to the relative levels of *Hox* gene expression, or to activation of multiple *Hox* genes by the *CALM-AF10* transgene, or to the technique employed to express *CALM-AF10* in hematopoietic cells (retroviral transduction and transplantation vs. transgenesis). Given the documented leukemogenicity associated with up-regulation of *HOX* genes, particularly those of the *abd-b* group (paralogs 9-

13) (Abramovich and Humphries 2005), it seems likely that the *CALM-AF10* transgene exerts its leukemic effect, at least in part, through *HOX* gene activation.

Previous studies have shown that *BMI1* is upregulated in patients with *CALM-AF10* pre T-ALL (Dik, Brahim et al. 2005). Presumably, in this case the upreguation of *BMI1* occurs through a *cis* effect as the *AF10* gene is located near *BMI1* on chromosome 10. It was hypothesized that this effect was absent in the transgenic mice and that the *CALM-AF10* mice would not up-regulate *Bmi1*. The results reported here demonstrate that expression of a *CALM-AF10* fusion gene does not result in overexpression of Bmi1 as it is was shown to be differentially expressed in both hematopoietic and nonhematopoietic tissues.

There was great interest in elucidating the role that *Hoxa9* might have on B-cell development. In one study, overexpression of *Hoxa9* in bone marrow resulted in enhanced granulopoiesis as well as a partial block in B-cell lymphopoiesis at the pre-B-cell stage (Thorsteinsdottir, Mamo et al. 2002). In this study, *Hoxa9* was overexpressed in transgenic bone marrow with a concomitant decrease in *Igh6*, which encodes for IgM. Furthermore, we showed here that mice, which developed AML, had overexpression of *Hoxa9* in tumors, and that there was evidence of *Igh* rearrangement by Southern blot analysis (chapter 2 and 3). Taken together, it is reasonable to suggest that an overexpression of *Hoxa9* impairs B-cell differentiation in *CALM-AF10* mice. It would also be reasonable to expect that these mice might

also be deficient in IgM. In this case, the mice would have impaired immunoglobulin class switching from IgM to IgG and thus have a deficient humoral immune system.

Gene expression analysis revealed that *Desmoplakin* (*Dsp*) was overexpressed in bone marrow from *CALM-AF10* mice. This is intriguing because *Dsp* encodes for desmoplakin, an intermediate filament found in tissues subject to mechanical stress (Sonnenberg and Liem 2007). Diseases such as pemphigus, an autoimmune skin disease that results in vesicle formation, as well as arrhythmogenic ventricular cardiomyopathy have been associated with mutations that involve desmoplakin (Lai Cheong, Wessagowit et al. 2005). Desmoplakin has also been studied in the context of cancer, particularly hepatocellular carcinoma, an epithelial cancer; however, there are no known reports citing a direct role of desmoplakin in leukemia (Cao, Chang et al. 2007).

In Chapters 2 and 3, *CALM-AF10* mice that developed leukemia also had a striking perivascular accumulation of neoplastic cells in peripheral tissues. The observation that desmoplakin is overexpressed in transgenic bone marrow, and that it is a known cell adhesion protein, warrants further investigation into its potential mechanistic role in the perivascular accumulation of leukemic cells.

Chapter 5: Conclusion and Discussion

Gross chromosomal rearrangements are molecular lesions observed in patients with hematological malignancies. A chromosomal translocation is the product of a reciprocal event whereby two chromosomes undergo double strand breaks and exchange their DNA as a consequence of misrepair. Evaluation of these genetic aberrations has proven to be a rich source of information regarding mechanisms of leukemogenesis, prognostic classifications, and therapeutic target identification. Understanding these events through mouse models would help identify and target molecular markers that would improve quality of life for patients.

The t(10;11) translocation was first identified in the U937 cell line derived from a patient with histiocytic lymphoma (Sundstrom and Nilsson 1976), and later was shown to result in a fusion gene product known as *CALM-AF10* (Kobayashi, Thirman et al. 1995; Shipley, Williams et al. 1995). This fusion has been observed in both adult and pediatric patients with a wide variety of hematological malignancies including AML, ALL, and histiocytic lymphoma (Caudell and Aplan 2008). A subset of patients with gamma/delta T-ALL have also been observed with the t(10;11) translocation; of the diverse phenotypes, this is the most striking association between phenotype and the t(10;11) chromosomal translocation (Asnafi, Radford-Weiss et al. 2003). This broad spectrum of phenotypes suggests that the original cell type affected by the translocation is an hematopoietic stem cell or early progenitor cell; however, the exact cell of origin remains unknown. At the inception of this work,

little was known about the mechanism of action of the *CALM-AF10*, fusion, and no biological models existed in which to study this genetic lesion. This generated a need for a mouse model in which to show that the *CALM-AF10* fusion was indeed leukemogenic, interrogate genes and their respective pathways associated with the biology of *CALM-AF10*, and identify potential therapeutic targets.

In order to express *CALM-AF10* in mice, we cloned a *CALM-AF10* fusion cDNA from the U937 cell line into a *Vav* vector, in order to achieve expression across the entire hematopoietic cellular compartment, and derived transgenic mice on an FVB background. In this model mice developed AML with lymphoid features including immunoglobulin gene rearrangements, and the B-cell surface marker B220. These findings suggested that the target cell was an early progenitor cell. Interestingly, the mice did not develop T-cell tumors; however, they did show evidence of clonal TCR-beta gene rearrangements in myeloid tumors, as well as a reduction in CD4/8 double positive cells in the thymus.

We also showed by gene expression analysis, using RQ-RTPCR, that *Hoxa* cluster genes and *Meis1* were upregulated in tumors from transgenic mice with AML as well as in spleen, bone marrow and thymus of clinically healthy transgenic mice. Using a whole-genome survey, we showed that two of the three most differentially upregulated genes (from a set of 80 genes) were *Hoxa9* and *Meis1*. These findings mimic previous results from studies that involved mouse models and patients with *MLL* and *NUP98* fusions, as well as some T-ALL-associated translocations. In those

studies, the fusion genes mediated their action, in part, through *HOX* genes, especially *HOXA9*. These findings in our mouse model warrant further biochemical studies such as chromatin immunoprecipitation (ChIP) assays to show how directly or indirectly *CALM-AF10* and *Hoxa* genes interact to transduce hematopoietic cell differentiation.

The current paradigm in leukemic biology is that Class I mutations (e.g. *RAS*, *FLIT3*, or c*KIT* mutations) lead to uncontrolled proliferation or impaired apoptosis and that Class II mutations target transcription factors, e.g. *HOXA* clusters, and result in impaired differentiation (Kelly and Gilliland 2002). The mice in our initial study developed leukemia after a long latency period (median 13 months) with incomplete penetrance. This suggested that additional mutations, namely those that would result in uncontrolled proliferation were likely needed as complementary events, which would collaborate with the *CALM-AF10* transgene in leukemia development.

To test our hypothesis that complementary events were needed to collaborate with the *CALM-AF10* transgene to produce leukemia, we infected two-day old *CALM-AF10* transgenic and wild-type control mice with MOL4070LTR retrovirus in order to accelerate the leukemia and identify collaborating genes. In this latter study, transgenic mice that were infected with retrovirus developed leukemia more quickly than retrovirus-infected wild-type mice or *CALM-AF10* mice not infected with retrovirus. The *CALM-AF10* retrovirus-infected mice developed leukemia that was predominately B-cell ALL or ANLL. This was in contrast to the wild-type retrovirus-

infected mice that, in addition to B-cell ALL and ANLL, also developed T-cell ALL. The B-cell ALL finding was also strikingly different than the noninfected *CALM-AF10* mice that developed AML with lymphoid features. These findings suggest that the retrovirus collaborates with the *CALM-AF10* transgene and targets a progenitor cell of B-cell origin, in at least a subset of the leukemias.

The second aim of this study was to identify collaborating genes and their pathways, which complement the *CALM-AF10* transgene. We used ligation-mediated PCR and sequence analysis to identify ~255 unique retroviral insertion sites. Seventeen common integrations were identified; of these, we focused on two genes in particular, *Zeb2* and *Nf1*.

ZEB2 (also known as *SIP1* or *ZFHX1B*) is a transcription factor associated with TGFβ that is involved in neurogenesis and Mowat-Wilson syndrome, a neurological developmental disorder (Mowat, Wilson et al. 2003). *Zeb2* has been identified by retroviral insertional mutagenesis in previous mouse models for T-cell, B-cell, and myeloid leukemia, in addition to AML pediatric patients with *MLL*-associated leukemias. In our study we observed that retroviral-infected *CALM-AF10* mice that had an identifiable insertion near *Zeb2*, either by PCR or Southern blot analysis also developed B-cell ALL suggesting an association between *Zeb2* and B-cell ALL. Although the insertions are 160 kb 5' of *Zeb2*, it is possible that retroviral enhancer elements lead to dysregulation of *Zeb2* and uncontrolled proliferation through some,

as yet, unidentified mechanism. Taken together, these findings strongly suggest that *Zeb2* collaborates with *CALM-AF10* to produce leukemia in mice.

Nf1, a tumor suppressor gene that plays a critical role in the RAS signaling pathway of myeloid cells, is associated with myeloid leukemia. In this present study, *Nf1* was identified as a potential collaborating gene with *CALM-AF10*. A subset of tumors with *Nf1* retroviral integration events had evidence of LOH; B-ALL tumors with *Nf1* retroviral integrations also had decreased *Nf1 gene* expression.

In this two-part study a transgenic mouse model for the t(10;11) translocation was developed that recapitulates the disease observed in patients with leukemia. In addition to confirming the oncogenicity of the *CALM-AF10* fusion, it was shown that this mouse model produces a myeloid leukemia with lymphoid features. Furthermore, it was shown that the transgenic mice have impaired differentiation, which is possibly mediated through overexpresion of *Hoxa* and *Meis1*. Through the use of retroviral insertional mutagenesis genes and pathways were identified that potentially complement the *CALM-AF10* fusion. Because of these findings, this model lends itself as a useful model for studying early hematopoietic progenitor or stem cells as a target of the t(10;11) translocation.

The potential candidate genes that we identified are of interest either because of their established role in leukemia, or because they were previously identified through whole genome screens. These findings warrant further investigation into their

collaborative role with the *CALM-AF10* fusion. A first approach would be to express the genes of interest, e.g. *Zeb2* in retroviral vectors and conduct retroviral bone marrow transduction and transplantation studies. Similar experiments could also be performed for some of the other CIS such as *Mpl*, *Foxp1*, or *Plag1*. *Nf1* is interesting because of its role as a tumor suppressor gene. Two approaches could be taken to better understand the role of this gene in the *CALM-AF10* mouse model. First, decreasing the expression of *Nf1* in *CALM-AF10* transgenic bone marrow using RNA interference (RNAi) would allow for the study of gene dosage effect on myeloid cells. A second approach would be to cross $Nf1^{+/-}$ mice with *CALM-AF10* transgenic mice with the anticipation that offspring would develop leukemia at a faster rate than either of the individual genotypes.

Class I mutations are frequently associated with point mutations in genes associated with myeloid leukemia such as *RAS*, *FLT3*, or *cKIT*. We believe, based on our studies that the *CALM-AF10* transgene is a Class II event and probably blocks differentiation in hematopoietic precursor cells. A candidate gene approach that interrogates these specific Class I events would be useful in our mouse model system to potentially identify secondary events that could collaborate with the *CALM-AF10* transgene.

The *CALM-AF10* transgenic mouse model has applications for preclinical research. There is evidence of impaired humoral and cell-mediated immunity. First, clinically healthy *CALM-AF10* mice have impaired thymocyte differentiation. A follow-up

experiment would be to challenge these mice with infectious agents and monitor their cellular immune response to infection. Secondly, because there was evidence of *Igh* gene rearrangements, and a decrease in IgH-6 gene expression by microarray analysis, this model could also be useful for humoral immunity studies. It is feasible to speculate that these mice have decreased serum IgM and IgG given the findings in both clinically healthy and tumor-bearing mice.

Of note, a recurring lesion in both non-retroviral, as well as retroviral-infected mice, was the perivascular infiltration in peripheral tissue including liver, kidney, and lung. Little work has been done to address the molecular features of these unique lesions. Interrogation of this lesion could shed new insight into mechanisms that influence neoplastic cell trafficking into peripheral tissues, as well as the interactions between neoplastic cells and blood vessels.

In this study evidence is offered to support our hypothesis that the *CALM-AF10* transgene leads to acute leukemia in mice. This model has many useful features including hematopoietic progenitor and stem cells biology, impaired differention. This model can also be used to study the complex gene interactions associated with *CALM-AF10* leukemias. Finally, this mouse model can has potential for identifying targets of therapeutic interest that can be used in patients with *CALM-AF10* leuekmia.

Appendix I

```
   1 ggcccgtacg gccttctgac acaactgtgt tcactagcaa cctcaaacag acaccatgat
  61 catgtccggc cagagcctga cggaccgaat cactgccgcc cagcacagtg tcaccggctc
 121 tgccgtatcc aagacagtat gcaaggccac gacccacgag atcatggggc ccaagaaaaa
 181 gcacctggac tacttaattc agtgcacaaa tgagatgaat gtgaacatcc cacagttggc
 241 agacagttta tttgaaagaa ctactaatag tagttgggtg gtggtcttca aatctctcat
 301 tacaactcat catttgatgg tgtatggaaa tgagcgtttt attcagtatt tggcttcaag
 361 aaacacgttg tttaacttaa gcaatttttt ggataaaagt ggattgcaag gatatgacat
 421 gtctacattt attaggcggt atagtagata tttaaatgag aaagcagttt catacagaca
 481 agttgcattt gatttcacaa aagtgaagag aggggctgat ggagttatga gaacaatgaa
 541 cacagaaaaa ctcctaaaaa ctgtaccaat tattcagaat cagatggatg cacttcttga
 601 ttttaatgtt aatagcaatg aacttacaaa tggggtaata aatgctgcct tcatgctcct
 661 gttcaaagat gccattagac tgtttgcagc atacaatgaa ggaattatta atttgttgga
 721 aaaatatttt gatatgaaaa agaaccaatg caaagaaggt cttgacatct ataagaagtt
 781 cctaactagg atgacaagaa tctcagagtt cctcaaagtt gcagagcaag ttggaattga
 841 cagaggtgat ataccagacc tttcacaggc ccctagcagt cttcttgatg ctttggaaca
 901 acatttagct tccttggaag gaaagaaaat caaagattct acagctgcaa gcagggcaac
 961 tacactttcc aatgcagtgt cttccctggc aagcactggt ctatctctga ccaaagtgga
1021 tgaaagggaa aagcaggcag cattagagga agaacaggca cgtttgaaag ctttaaagga
1081 acagcgccta aaagaacttg caaagaaacc tcatacctct ttaacaactg cagcctctcc
1141 tgtatccacc tcagcaggag ggataatgac tgcaccagcc attgacatat tttctacccc
1201 tagttcttct aacagcacat caaagctgcc caatgatctg cttgatttgc agcagccaac
1261 ttttcaccca tctgtacatc ctatgtcaac tgcttctcag gtagcaagta catggggaga
1321 tccttttctct gctactgtag atgctgttga tgatgccatt ccaagcttaa atcctttcct
1381 cacaaaaagt agtggtgatg ttcacctttc catttcttca gatgtatcta cttttactac
1441 taggacacct actcatgaaa tgtttgttgg attcactcct tctccagttg cacagccaca
1501 cccttcagct ggccttaatg ttgactttga atctgtgttt ggaaataaat ctacaaatgt
1561 tattgtagat tctgggggct ttgatgaact aggtggactt ctcaaaccaa cagtggcctc
1621 tcagaaccag aaccttcctg ttgccaaact cccacctagc aagttagtat ctgatgactt
1681 ggattcatct ttagccaacc ttgtgggcaa tcttggcatc ggaaatggaa ccactaagaa
1741 tgatgtaaat tggagtcaac caggtgaaaa gaagttaact ggggggatcta actggcaacc
1801 aaaggttgca ccaacaaccg cttggaatgc tgcaacaatg gcacccccctg taatggccta
1861 tcctgctact acaccaacag gcatgatagg atatggaatt cctccacaaa tgggaagtgt
1921 tcctgtaatg acgcaaccaa ccttaatata cagccagcct gtcatgagac ctccaaaccc
1981 ctttggccct gtatcaggag cacagagatg tgaactttgt ccccataagg atggagcttt
2041 aaaaagaaca gataatgggg gttgggccca tgtggtttgt gccctgtata ttccagaggt
2101 acaatttgcc aatgtttcca caatggaacc aattgtttta cagtctgttc cgcatgatcg
2161 ttataataag acttgctaca tttgtgatga acaaggaaga gaaagcaaag cagccactgg
2221 tgcttgcatg acatgtaata aacatggatg tcgacaggct ttccatgtaa catgcgctca
2281 gtttgccgga ctgctttgtg aagaagaagg taatggtgcc gataatgtcc aatactgtgg
2341 ctactgtaaa taccatttta gtaagctgaa aaagagcaaa cggggatcta ataggtcata
2401 tgatcaaagt ttaagtgatt cttcctctca ctctcaggat aaacatcatg agaaagagaa
2461 aaaaaaatat aaagagaagg acaaacacaa acagaaacac aagaagcagc cagaaccatc
2521 acctgcattg gttccatcct tgactgttac tacagaaaaa acttatacaa gcactagcaa
2581 caactctata tctggatcat tgaagcgctt ggaagatact actgcacgat ttacaaatgc
2641 aaatttccag gaagtctctg cacacacctc tagtggaaaa gatgtttcag agactagagg
2701 gtcagagggc aaagggaaga aatcttcagc tcacagctca ggtcaaaggg gaagaaagcc
2761 tggtggtgga agaaatccag gaacaactgt gtcagcagct agccctttc ctcaaggcag
2821 tttttcagga actccaggca gtgtaaagtc atcttctgga agttcagtgc agtctcccca
2881 ggatttcctg agctttacag actcagatct gcgtaatgac agttactctc actcccaaca
2941 gtcatcagca accaaagatg tacataaagg agagtctgga agccaggaag ggggggtaaa
3001 tagttttagt accttaattg gcctcccttc aacctcagct gttacttcac agcctaaaag
3061 ctttgaaaat tcacctggag atttgggtaa ttccagcctt cctacagcag gatataagcg
3121 ggctcaaact tctggcatag aagaagaaac tgtaaaggaa aagaaaagga aaggaaataa
3181 acaaagtaag catgggcctg gcagacccaa aggaaacaaa aatcaagaga atgtttctca
3241 tctctcagtt tcttctgctt caccaacatc atctgtagca tcagctgcag gaagcataac
3301 aagctctagt ctgcagaaat ctcctacatt gctcaggaat ggaagtttac agagcctcag
```

```
3361 tgttggctca tctccagttg gttcagaaat ttccatgcag tatcggcatg atggagcttg
3421 cccaacaact agtatttata acagcaatga tgtagcagta tcgtttccaa atgtagtatc
3481 tggctcggga tctagtactc ctgtctccag ctctcactta cctcagcagt cttctgggca
3541 tttgcaacaa gtaggagcgc tctctccctc agctgtgtca tctgcagccc ctgctgttgc
3601 tacaactcag gcaaatactc tatctggatc ttctctcagt caggcaccat ctcatatgta
3661 tggcaataga tcaaattcat caatggcagc tcttatagct cagtctgaaa acaatcaaac
3721 agatcaagat cttggagaca atagccgcaa cctagttggc agaggaagct caccccgagg
3781 aagtctctcg ccacgatccc ctgtaagcag cttacagatt cgctatgatc aaccaggcaa
3841 cagcagtttg gaaaatctgc ctccagtagc agccagcata gaacagcttt tggagaggca
3901 gtggagtgaa ggacagcaat ttttactaga acagggtact cctagtgaca ttttaggaat
3961 gctgaagtca ttacaccaac ttcaagttga aaaccgaaga ttagaggaac aaattaaaaa
4021 cttgactgcc aaaaaggaac ggcttcagtt attgaatgca cagctttcag tgccttttcc
4081 aacaataaca gcaaatccta gtccgtctca tcaaatacac acattttcag cacagactgc
4141 tcctactact gattccttga acagcagtaa gagccctcat ataggaaaca gctttttacc
4201 tgataattct cttcctgtat taaatcagga cttaacctcc agtggacaaa gtaccagcag
4261 ctcatcagct ctttctaccc cacctcctgc tgggcagagt ccggctcaac aaggctcagg
4321 agtgagtgga gttcagcagg tcaatggcgt gacagtgggg gcactagcta gtggaatgca
4381 gcctgtaact tccaccattc ctgccgtgtc tgcagtgggt ggaataattg gagctttgcc
4441 aggtaaccaa ctggcaatta atggcattgt aggagcttta aatggggtta tgcagactcc
4501 tgtcacaatg tcccagaacc ctacccctct cacccacaca accgtaccac ctaatgcaac
4561 acatccaatg ccagctacac tgactaacag tgcctcagga ctaggattac tttctgacca
4621 gcaacgacaa atacttattc atcaacagca gtttcagcag ttgttaaatt ctcaacagct
4681 cacaccagaa caacatcaag ccttttttgta tcagttaatg caacatcacc accagcagca
4741 ccaccaacct gaacttcagc agctgcagat ccctggacca acacaaatac ccataaacaa
4801 ccttcttgca ggtacacagg caccccccact tcacacagct accaccaacc catttctcac
4861 catccatgga gataatgcaa gtcagaaagt agcaagactt agtgataaaa ctgggcctgt
4921 agctcaagag aaaagttgac acctgagaaa catctagaaa ttgcctatcc tgctgttcta
4981 gcacttcatc tggctgcctt tgcagtcctt ttactacagc tatgaagaaa cgcaacaaga
5041 aactcaatgc acaacaaagg attaattgct gcaaggacat tcttgtaagg ctttgattag
5101 ttttcttgtt gctttgttgc actgaaatgg aattcccatg cccctacccc ttaccccagt
5161 tttttgaaca tggaaagaaa atttaataac tttttaaagt gacataattt acatgcaata
5221 tgtttatcaa ctcaagaatt taatatagtt ggtacacaac tagttttgtt tataaattgg
5281 agatgcaaat agcaaaacta aatacttgct ccatttacaa actacttgat tttattgtac
5341 aagttgaaat atgctctttt gtttgggtta cagtatgctt gctctaagtc aaattccaag
5401 gaactaattt cttctcctgg agttgcattg attcagtatt acaaatatat agcacatcac
5461 ctgggacttg gcaatctttg ttaaaaaaaa atttcctttc taatgggatt tggccaattt
5521 tggtaatgaa gttaggatgg taatgtctgc atctgctaaa ggtaattttc ttttgagaat
5581 tgctttcttt agtgttaaga cctactcata ttttgaagaa atcttgagtt aagtgagttc
5641 tgaggctgct gggggaacca gatcaattca aagctaaata cttctttcag aaaggggcca
5701 ctgtggaaag tgctggtggg gtttgccctt gatcaagtgc ctccattgtg ctgcaagggc
5761 tgtagacagc agggtgggac agtcagtcct ccgagcagca ggaatcatcc cgtcacctgc
5821 agccttccca tgcttccgcc tttattcaga actttctgtg ccactgtaga tagctcaggc
5881 aaaactatta cctgggtatt tatccactaa tgagtcacaa gaaaaggagt ggatttggta
5941 agaatagaga tttgttttat ttaaaccact tcccattact gaccattaaa agctcaccac
6001 tagagttcct gaaacaggtg aaacctgtat gacagccctt ccactttggg gagccacgct
6061 tttgatgtga cagtaccgca gagtgattcc cccactgagg atgtcatcat caaactcttc
6121 tttggtgtgt gaattattag tggaaaagac ccagctgtaa ttagacctcc actgtgtact
6181 tagctggaag aacatgttaa ttctgcaata tgtttcttgg ttaaacattg cacagttctt
6241 acctcatttc tgtaaataaa gttttgtgaa tctgttttgt attgtgacaa attcataaga
6301 taacattgat attttgattt gtaatatttc taattggtag atttaattga aaagtaaaat
6361 taatttattt ttatatgttc aggggaattt taaagtcaaa tcttttgtag ataatttaaa
6421 aaatcagtgt ggtttatttt acttatttaa cccactggtt gttattctgt aacagtttgt
6481 ataaatggta aattttgaat gtgttgttat tttacctaga tgtaaaattc cacatgtatt
6541 aaaatgtaca aaatgttttg ttaataaaat ttaataatgt ttataaaaaa aaaaaaaaaa
6601 aaaaaaaaaa aagggcggcc gctctagagt atccctcgag gggcccaagc ttacgcgat
```

Legend: Nucleotides 1-12 are plasmid backbone, 13-58 are human beta-globin, 59-2006 are CALM, and 2007-6584 are AF10.

Appendix II

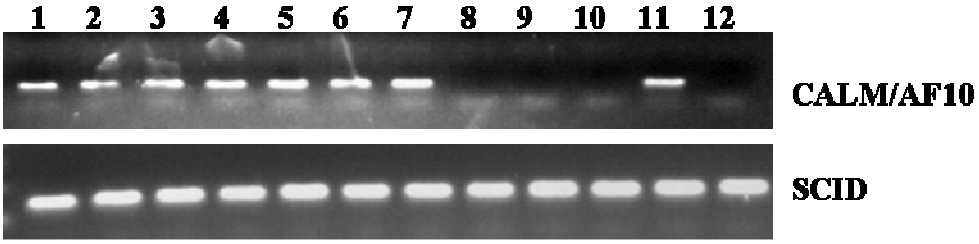

Genotyping of *CALM-AF10* mice. This is a representative PCR result from genotyping of *CALM-AF10* offspring. Note, lanes 1-7 and 11 represent *CALM-AF10* positive mice; lanes 8, 9, and 10 represent mice negative for the transgene; lane 12 is water control. The lower panel represents the *SCID* DNA quality control.

Appendix III

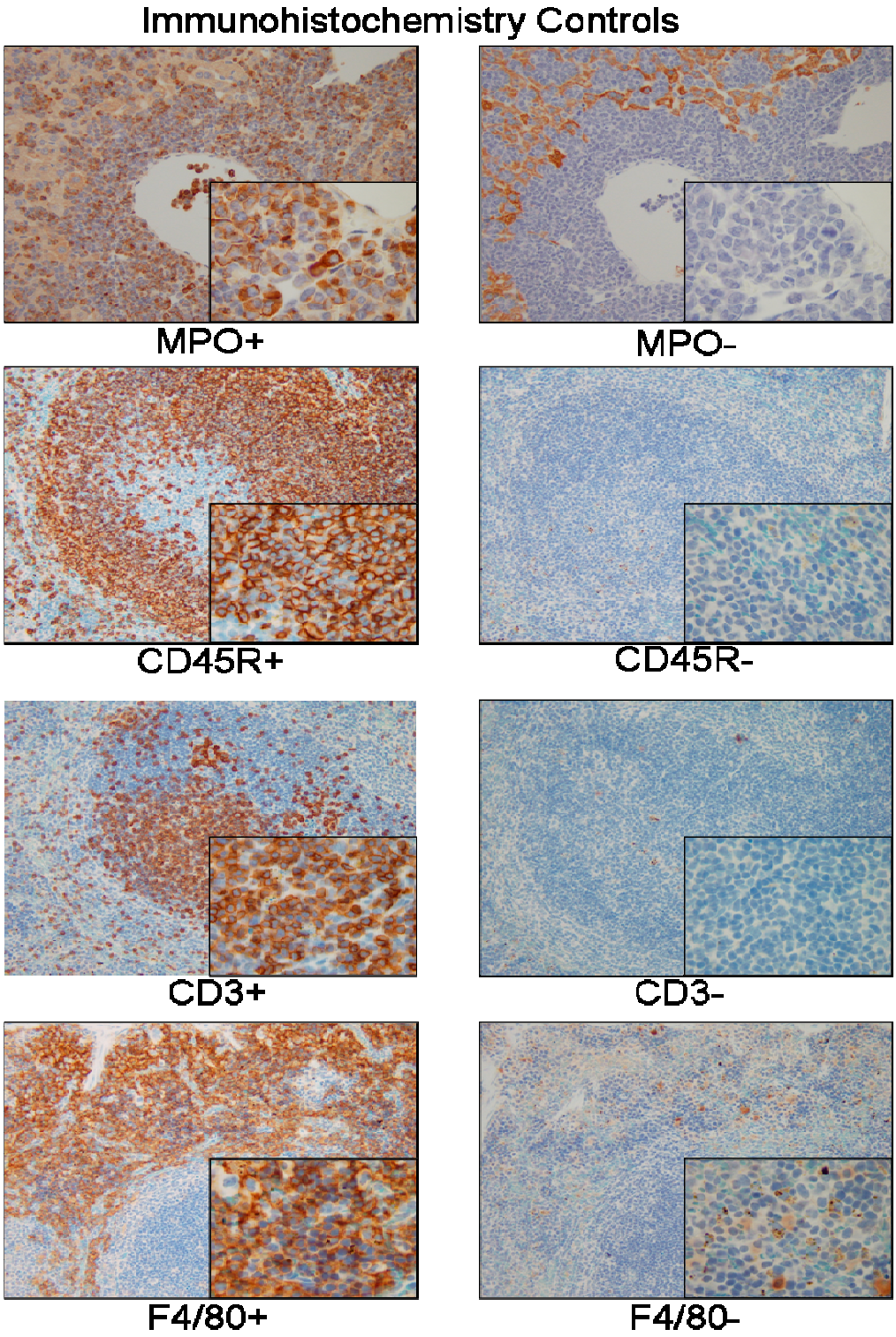

Appendix IV

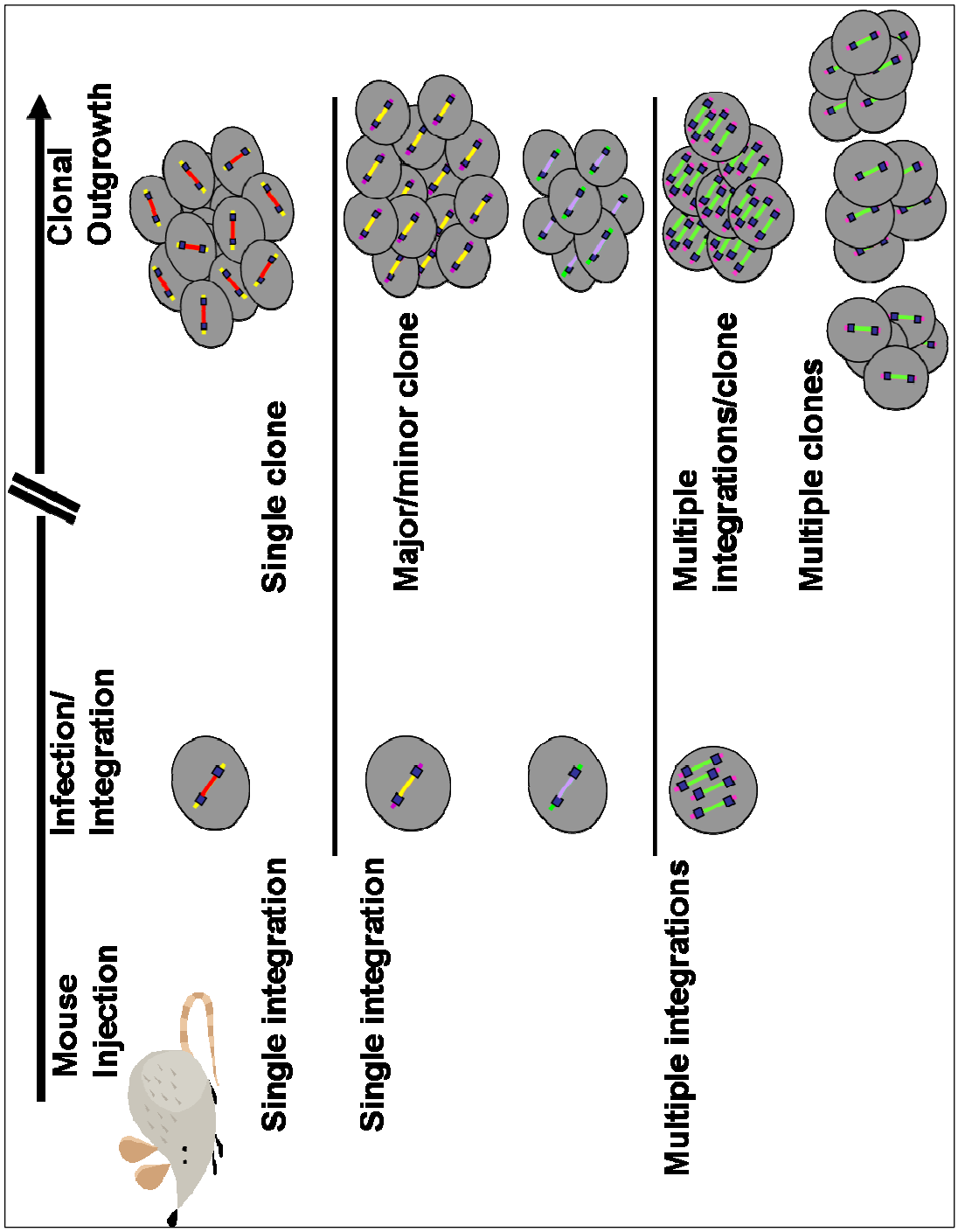
Mouse Injection
Infection/ Integration
Clonal Outgrowth
Single integration
Single clone
Single integration
Major/minor clone
Multiple integrations
Multiple integrations/clone
Multiple clones

Appendix V

Retroviral Integration Sites

Chromosome	Location	Mouse ID	Gene	Phenotype
1	12,378,313	39	no gene determined	B-ALL
1	39,150,002	9	*Npas2*	Biphen
1	39,552,852	21	*Creg2*	B-ALL
1	54,722,952	17	*Ankrd44*	B-ALL
1	64,542,390	30	*2310038H17Rik*	ANLL
1	71,906,799	9	*AK016843*	Biphen
1	88,534,415	15	*4930429A22Rik*	ANLL
1	107,808,316	47	*AA959805*	ANLL
1	108,478,223	6	*BC12*	ANLL
1	166,654,770	31	*Dpt*	ANLL
1	175,717,510	13	*Ifi204*	ANLL
1	194,900,850	6	*Traf3ip3*	ANLL
2	4,431,225	10	*Frmd4a*	Biphen
2	6,625,143	76	*Cugbp2*	ANLL
2	21,149,073	72	*Thnsl1*	Biphen
2	22,623,996	29	*AK079736*	Biphen
2	25,288,474	29	*Ptgds*	Biphen
2	28,349,450	9	*Ralgds*	Biphen
2	28,428,791	88	*Gfilb*	ANLL
2	30,356,804	66	*Cstad*	T-ALL
2	31,936,904	14	*Ppapdc3*	B-ALL
2	33,692,356	98	*2610528K11Rik*	B-ALL
2	45,041,528	36	*Zfhx1b*	ANLL
2	45,093,140	21	*Zfhx1b*	B-ALL
2	45,099,048	27	*Zfhx1b*	B-ALL
2	45,101,941	5	*Zfhx1b*	B-ALL
2	45,103,868	17	*Zfhx1b*	B-ALL
2	45,104,975	98	*Zfhx1b*	B-ALL
2	49,669,349	30	*2310010M24Rik*	ANLL
2	69,661,682	42	*M55334*	Biphen
2	73,287,719	18	*Waspip*	Biphen
2	74,873,167	70	*Mtx2*	Biphen
2	91,298,699	21	*Lrp4*	B-ALL
2	102,799,503	80	*Pdhx*	ANLL
2	116,801,284	67	*Spred1*	ANLL
2	117,095,572	66	*Rasgrp1*	T-ALL
2	118,347,894	25	*Pak6*	B-ALL
2	143,937,495	102	*Snx5*	ANLL
2	163,460,902	9	*Ada*	Biphen
3	28,762,768	28	*BC050866*	ANLL
3	30,260,030	6	*Evi1*	ANLL
3	30,287,734	14	*Evi1*	B-ALL
3	30,296,436	29	*Evi1*	Biphen

Retroviral Integration Sites Continued

Chromosome	Location	Mouse ID	Gene	Phenotype
3	30,297,768	31	*Evi1*	ANLL
3	30,334,581	36	*Evi1*	ANLL
3	53,129,110	14	*Lhfp*	B-ALL
3	96,283,440	23	*Bola1*	B-ALL
3	101,150,307	18	*Igsf2*	Biphen
3	103,187,870	35	*NRas*	ANLL
3	107,979,920	21	*Eps813*	B-ALL
3	116,974,438	98	*AK144215*	B-ALL
3	127,783,021	30	*T2bp*	ANLL
3	135,362,484	13	*1500009M05Rik*	ANLL
3	137,374,333	88	*Txn12*	ANLL
4	3,880,574	21	*Chchd7*	B-ALL
4	3,881,017	42	*Chchd7*	Biphen
4	19,825,466	27	*Atp6v062*	B-ALL
4	37,365,340	23	*AK029761*	B-ALL
4	56,136,319	9	no gene determined	Biphen
4	57,956,743	13	*Akap2*	ANLL
4	58,403,609	67	*Musk*	ANLL
4	59,857,534	67	*3110003ARik*	ANLL
4	87,505,624	69	*Mllt3*	ANLL
4	87,506,224	47	*Mllt3*	ANLL
4	87,507,253	14	*Mllt3*	B-ALL
4	94,795,845	38	*AK156722*	B-ALL
4	106,407,720	6	*Ssbp3*	ANLL
4	117,956,058	80	*Mpl*	ANLL
4	117,956,360	10	*Mpl*	Biphen
4	133,088,597	39	*Rps6ka1*	B-ALL
4	135,149,622	10	*AK134078*	Biphen
4	141,065,267	47	*Casp9*	ANLL
4	148,545,307	14	*Pik3cd*	B-ALL
4	154,149,872	17	*Prkcz*	B-ALL
4	154,196,007	31	*Prkcz*	ANLL
5	20,767,008	35	*A530088I07Rik*	ANLL
5	59,110,298	46	no gene determined	ANLL
5	62,106,040	38	*AK090048*	B-ALL
5	64,437,560	35	*BC059824*	ANLL
5	97,157,449	38	*DV045711*	B-ALL
5	107,995,097	44	*Evi5*	ANLL
5	111,661,045	67	*Mn1*	ANLL
5	111,672,110	38	*Mn1*	B-ALL
5	111,673,890	46	*Mn1*	ANLL
5	111,675,787	39	*Mn1*	B-ALL
5	111,751,056	80	*Mn1*	ANLL

Retroviral Integration Sites Continued

Chromosome	Location	Mouse ID	Gene	Phenotype
5	111,778,020	25	*Mn1*	B-ALL
5	117,424,372	102	*Taok3*	ANLL
5	118,757,401	42	*CX763467*	Biphen
5	118,776,213	25	*CX763467*	B-ALL
5	123,642,855	20	*BC17a*	ANLL
5	150,869,891	5	*AK034023*	B-ALL
6	30,628,910	5	*Tsga14*	B-ALL
6	52,606,503	14	*Hibadh*	B-ALL
6	99,240,070	35	*Foxp1*	ANLL
6	99,351,171	88	*Foxp1*	ANLL
6	101,600,686	10	*AK050931*	Biphen
6	122,865,978	42	*Necap1*	Biphen
6	136,463,497	27	*Atf7ip*	B-ALL
6	136,894,758	46	*Arhgdib*	ANLL
6	139,354,636	20	*AK015023*	ANLL
6	145,203,054	20	*Kras*	ANLL
6	145,246,479	27	*Kras*	B-ALL
7	3,685,107	23	*Lair1*	B-ALL
7	18,826,062	69	*ApoC2*	ANLL
7	23,135,748	46	*Nalp5*	ANLL
7	25,388,035	5	*AK141500*	B-ALL
7	28,090,560	70	*Supt5h*	Biphen
7	30,100,048	28	*BF158903*	ANLL
7	45,550,595	15	*Sec1*	ANLL
7	45,732,883	14	*Grin2d*	B-ALL
7	48,872,735	39	*AK084063*	B-ALL
7	58,601,420	72	*Atp10a*	Biphen
7	63,696,673	36	*Otud7*	ANLL
7	79,776,366	30	*Ap3s2*	ANLL
7	80,135,456	30	*Ngrn*	ANLL
7	80,939,544	21	*Alpk3*	B-ALL
7	87,006,481	14	*AK169304*	B-ALL
7	100,103,567	28	*Pgm2l1*	ANLL
7	113,962,540	39	*Copb1*	B-ALL
7	113,986,816	98	*Copb1*	B-ALL
7	127,834,231	69	*Itgam*	ANLL
7	131,998,390	23	*AK212323*	B-ALL
7	132,193,327	25	*AK212323*	B-ALL
7	142,270,422	25	*Lsp1*	B-ALL
7	144,857,798	20	*AK007224*	ANLL
8	10,924,764	5	*AK014460*	B-ALL
8	10,992,091	15	*Irs2*	ANLL
8	11,576,209	21	*Ankrd10*	B-ALL

Retroviral Integration Sites Continued

Chromosome	Location	Mouse ID	Gene	Phenotype
8	13,095,649	76	*AK020930*	ANLL
8	37,625,616	6	*AK082764*	ANLL
8	83,347,838	44	*Gypa*	ANLL
8	87,074,472	42	*CJ191375*	Biphen
8	113,823,939	72	*St3ga12*	Biphen
8	114,707,232	27	*Cfdp1*	B-ALL
8	129,742,437	42	*AK050164*	Biphen
9	32,292,302	14	*Fli1*	B-ALL
9	44,161,347	10	*AK014147*	Biphen
9	57,201,584	80	*AK038628*	ANLL
9	57,351,271	96	*Mpi*	ANLL
9	61,049,727	69	*Tle3*	ANLL
9	63,412,090	74	*2310007F21Rik*	ANLL
9	86,368,231	88	*Pgm3*	ANLL
9	86,420,670	39	*Mod1*	B-ALL
9	90,040,590	30	*Tbc1d2b*	ANLL
9	107,967,452	5	*Bsn*	B-ALL
9	111,114,687	23	*Mlh1*	B-ALL
9	113,900,595	31	*BC011245*	ANLL
9	115,015,692	15	*Osbpl10*	ANLL
9	118,245,732	21	*BF016740*	B-ALL
9	120,872,653	96	*Ctnnb1*	ANLL
10	6,082,314	28	*AV503505*	ANLL
10	13,429,502	30	*Aig1*	ANLL
10	13,776,534	47	*Hivep2*	ANLL
10	19,049,748	25	*Olig3*	B-ALL
10	19,519,107	10	*Slc35d3*	Biphen
10	61,902,461	36	*Prg1*	ANLL
10	66,466,991	29	*D10Ucla1*	Biphen
11	8,585,738	9	*Tns3*	Biphen
11	18,934,224	46	*Meis1*	ANLL
11	22,870,377	47	*Commd1*	ANLL
11	24,127,662	28	*AK139779*	ANLL
11	27,953,124	88	*Def6*	ANLL
11	49,952,680	102	*Rnf130/Tbc1d9b*	ANLL
11	51,847,171	25	*Cdk13*	B-ALL
11	58,030,359	38	*Iigp2*	B-ALL
11	69,405,390	6	*Trp53*	ANLL
11	70,000,905	9	*Mgl1*	Biphen
11	76,553,046	66	*Gosr1*	T-ALL
11	77,335,993	98	*1300007F04Rik*	B-ALL
11	79,336,856	36	*Nf1*	ANLL
11	79,343,850	17	*Nf1*	B-ALL

Retroviral Integration Sites Continued

Chromosome	Location	Mouse ID	Gene	Phenotype
11	79,344,840	98	*Nf1*	B-ALL
11	79,345,029	23	*Nf1*	B-ALL
11	94,816,159	98	*Ppplr9b*	B-ALL
11	95,483,829	96	*Phb*	ANLL
11	95,549,894	69	*Phb*	ANLL
11	97,132,332	35	*Mrpl45*	ANLL
11	113,198,658	38	*Slc39a11*	B-ALL
11	114,301,628	20	*C0809189*	ANLL
11	121,621,466	15	*AK079017*	ANLL
12	7,188,662	6	*Psma3*	ANLL
12	21,454,732	30	*Ddef2*	ANLL
12	78,054,162	39	*DV 659889*	B-ALL
12	83,921,882	17	*Rgs6*	B-ALL
12	83,921,882	31	*Rgs6*	ANLL
12	111,887,124	20	*Tnfaip2*	ANLL
12	114,992,643	46	*BC096667*	ANLL
12	115,915,686	67	*BC028249*	ANLL
12	118,746,963	20	*Sp4*	ANLL
13	28,562,017	66	*Sox4*	T-ALL
13	28,612,959	21	*BC025054*	B-ALL
13	102,637,523	74	*Pik3r1*	ANLL
14	18,718,332	46	*Gng2*	ANLL
14	29,470,236	23	*Rft1*	B-ALL
14	60,395,119	15	*Kpna3*	ANLL
14	66,796,360	21	*Dock5*	B-ALL
14	68,011,066	23	*Stc1*	B-ALL
14	74,572,199	98	*Tpt1*	B-ALL
14	75,519,298	36	*CK128313*	ANLL
14	75,675,612	47	*CK128313*	ANLL
15	27,803,018	10	*Trio*	Biphen
15	62,003,093	66	*AAk090048*	T-ALL
15	72,798,579	96	*1810044A24Rik*	ANLL
15	79,487,459	18	*Pgea1*	Biphen
15	79,828,786	69	*Pdgfb*	ANLL
15	90,685,460	67	*Kif21a*	ANLL
15	100,502,653	20	*Ela1*	ANLL
15	101,149,578	98	*6030408B16Rik*	B-ALL
15	101,804,832	30	*Krt85*	ANLL
15	102,061,235	18	*Itgb7*	Biphen
15	103,087,078	28	*BY227355*	ANLL
16	21,849,020	35	*Tmem41a*	ANLL
16	22,034,071	28	*C330012H03Rik*	ANLL
16	30,834,719	13	*AK139695*	ANLL

Retroviral Integration Sites Continued

Chromosome	Location	Mouse ID	Gene	Phenotype
16	45,467,470	13	*Slc9a10*	ANLL
16	45,467,557	21	*s1c9a10*	B-ALL
16	48,637,202	14	*Ift57*	B-ALL
16	49,708,746	69	*Ift57*	ANLL
16	49,719,563	36	*Ift57*	ANLL
16	95,547,315	6	*Erg*	ANLL
16	95,604,074	69	*Erg*	ANLL
17	5,194,932	46	*Arid1b*	ANLL
17	8,228,372	66	*T2*	T-ALL
17	26,740,523	30	*BC054732*	ANLL
17	29,586,014	13	*Mdga1*	ANLL
17	35,476,754	67	*BC025573*	ANLL
17	35,481,038	76	*BC025573*	ANLL
17	35,629,534	96	*H2-T24*	ANLL
17	48,550,193	69	*Nfya*	ANLL
17	56,974,517	15	*Vav1*	ANLL
17	56,976,462	74	*Vav1*	ANLL
17	75,048,418	67	*Ltbp1*	ANLL
17	83,065,753	72	*AW548124*	Biphen
17	83,825,134	10	*AK007978*	Biphen
17	84,028,403	42	*AK040143*	Biphen
17	87,089,800	39	*Mcfd2*	B-ALL
17	87,253,687	21	*Ttc7*	B-ALL
17	354,814,421	67	*BC025573*	ANLL
18	61,224,277	80	*Csfir*	ANLL
18	67,424,965	39	*Impa2*	B-ALL
18	78,060,362	31	*Pstpip2*	ANLL
19	6,349,813	102	*Map4k2*	ANLL
19	10,090,248	35	*Rab3il1*	ANLL
19	10,650,554	15	*Cybasc3*	ANLL
19	37,113,459	47	*Cpeb3*	ANLL
19	53,518,776	69	*AK146072*	ANLL
19	55,754,176	25	*Tcf7l2*	B-ALL
19	57,396,578	98	*AK043887*	B-ALL
X	7,121,530	14	*Gata1*	B-ALL
X	7,127,514	47	*Gata1*	ANLL
X	18,319,512	66	*AK170409*	T-ALL
X	47,400,164	46	*Mbnl3*	ANLL
X	160,324,926	21	*Fancb*	B-ALL

Appendix VI

Table of oligonucleotides

Oligo name	Oligonucleotide sequence
ZEBF1	TGAGCATCATTAAGCAGTGAGCAG
ZEBR2	AGTTGACTGTAGGTGGACTTGGTG
ZEBEX1F1	AGGGAGGTGGAATTTCATTTCTTCC
ZEBEX1F2	AAGCGTTTGCGGAGACTTCAAGG
ZEBEX1R1	AGGCGAAGAAACAGCTCCCGGAGC
ZEBEX1R2	AAAGAAAGCCTGCCACCAAAGAGC
SCID A	GGAAGAGTTTTGAGCAGACAATG
SCID B	CATCACAAGTTATAACAGCTGGG
CALM1640	TGTTCCTGTAATGACGCAACCAACC3
AF10510	CTCTGGAATATACAGGGCACAAACA3
β-ACTINMF	TGTTCCTGTAATGACGCAACCAACC
β-ACTINMR	CTCTGGAATATACAGGGCACAAACA
β-ACTINHF	AGGCCGGCTTCGCGGGCGAC
β-ACTINHR	CTCGGGAGCCACACGCAGCTC
EVI2_F	GAGGTGTCATCTTACCCAGTGCTC
EVI2_R	ATCAGAAATCAGAGGGCCTGTGTC
NF1.F.3	TTCAAGGCCTTGAAAACGTTAAGC
NF1.R.3	CTATATGTTCAGCCAGCTTCCCAGG
ZEB2_F1	GCAGCCGGCGCTCACCTTCC
ZEB2_F2	CTCACCTTCCCTTAAATCC
ZEB2_R1	AATGTTGTAAGAAATGTGCC
ZEB2_R2	AATCGTTGTGGACAAATTAAGC

Appendix IV

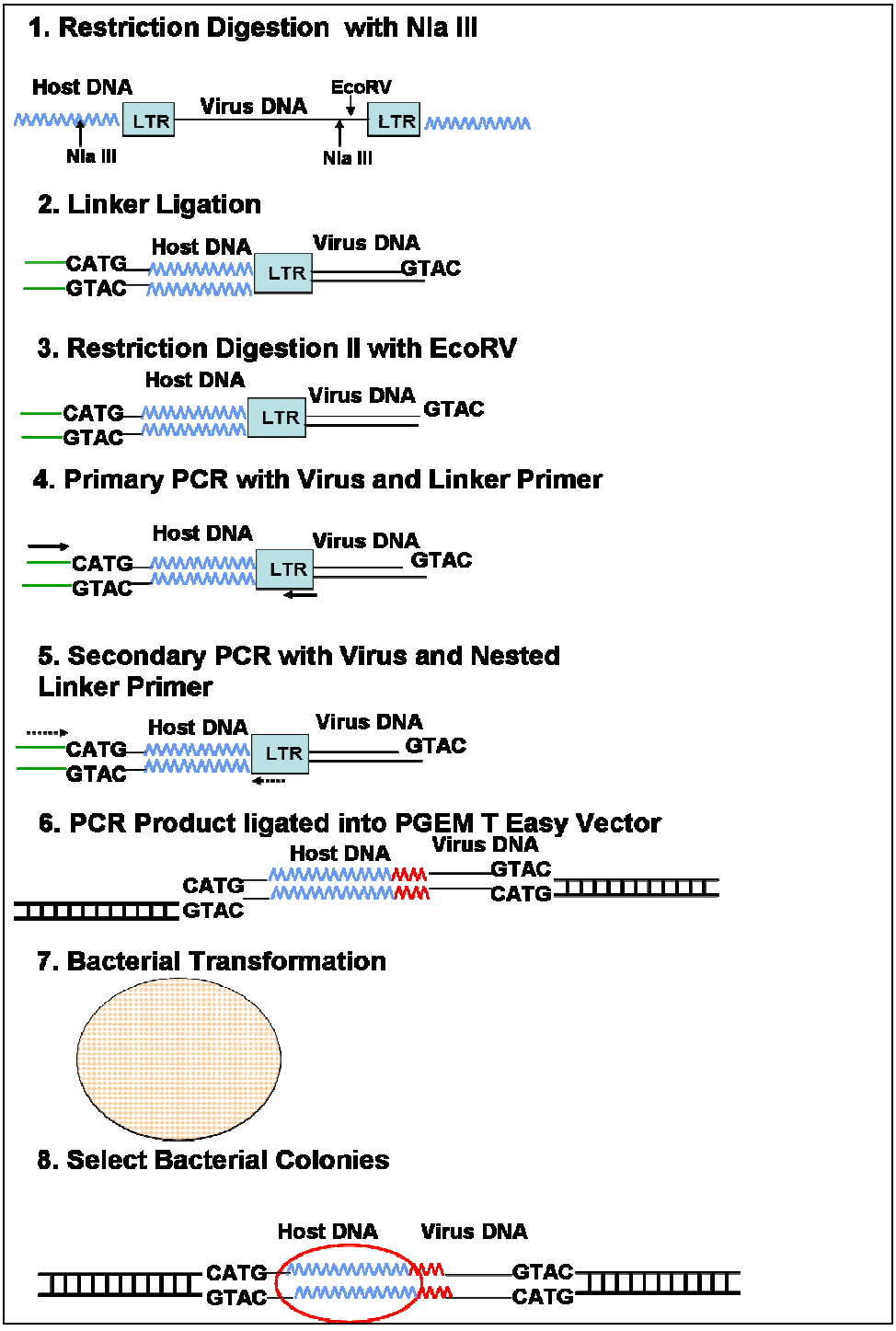
1. Restriction Digestion with Nla III
Host DNA
LTR
Virus DNA
EcoRV
LTR
Nla III
Nla III
2. Linker Ligation
Host DNA
Virus DNA
CATG
GTAC
LTR
GTAC
3. Restriction Digestion II with EcoRV
Host DNA
Virus DNA
CATG
GTAC
LTR
GTAC
4. Primary PCR with Virus and Linker Primer
Host DNA
Virus DNA
CATG
GTAC
LTR
GTAC
5. Secondary PCR with Virus and Nested Linker Primer
Host DNA
Virus DNA
CATG
GTAC
LTR
GTAC
6. PCR Product ligated into PGEM T Easy Vector
Host DNA
Virus DNA
CATG
GTAC
GTAC
CATG
7. Bacterial Transformation
8. Select Bacterial Colonies
Host DNA
Virus DNA
CATG
GTAC
GTAC
CATG

Bibliography

Aasland, R., T. J. Gibson, et al. (1995). "The PHD finger: implications for chromatin-mediated transcriptional regulation." Trends Biochem Sci **20**(2): 56-9.

Abdelhaleem, M., K. Beimnet, et al. (2007). "High incidence of CALM-AF10 fusion and the identification of a novel fusion transcript in acute megakaryoblastic leukemia in children without Down's syndrome." Leukemia **21**(2): 352-3.

Abdou, S. M., D. M. Jadayel, et al. (2002). "Incidence of MLL rearrangement in acute myeloid leukemia, and a CALM-AF10 fusion in M4 type acute myeloblastic leukemia." Leuk Lymphoma **43**(1): 89-95.

Abramovich, C. and R. K. Humphries (2005). "Hox regulation of normal and leukemic hematopoietic stem cells." Curr Opin Hematol **12**(3): 210-6.

Adams, J. M., A. W. Harris, et al. (1999). "Transgenic models of lymphoid neoplasia and development of a pan-hematopoietic vector." Oncogene **18**(38): 5268-77.

Adjei, A. A. (2001). "Blocking oncogenic Ras signaling for cancer therapy." J Natl Cancer Inst **93**(14): 1062-74.

Ahle, S. and E. Ungewickell (1986). "Purification and properties of a new clathrin assembly protein." Embo J **5**(12): 3143-9.

Aoi Jo, I. T., Eiichi Ishii, Norio Asou, Takashi Igarashi, Yasuhide Hayashi, and Hitoshi Ichikawa (2007). Age-Associated Difference in Gene Expression of Pediatric Myelo-Monocytic and MLL-Rearranged AML. 49th ASH Annual Meeting, Atlanta, GA, American Society of Hematology.

Aplan, P. D. (2006). "Causes of oncogenic chromosomal translocation." Trends Genet **22**(1): 46-55.

Aravind, L. and D. Landsman (1998). "AT-hook motifs identified in a wide variety of DNA-binding proteins." Nucleic Acids Res **26**(19): 4413-21.

Archangelo, L. F., J. Glasner, et al. (2006). "The novel CALM interactor CATS influences the subcellular localization of the leukemogenic fusion protein CALM/AF10." Oncogene **25**(29): 4099-109.

Armstrong, S. A., T. R. Golub, et al. (2003). "MLL-rearranged leukemias: insights from gene expression profiling." Semin Hematol **40**(4): 268-73.

Asnafi, V., I. Radford-Weiss, et al. (2003). "CALM-AF10 is a common fusion transcript in T-ALL and is specific to the TCRgammadelta lineage." Blood **102**(3): 1000-6.

Bacher, U., W. Kern, et al. (2005). "Population-based age-specific incidences of cytogenetic subgroups of acute myeloid leukemia." Haematologica **90**(11): 1502-10.

Balciunaite, G., R. Ceredig, et al. (2005). "A B220+ CD117+ CD19- hematopoietic progenitor with potent lymphoid and myeloid developmental potential." Eur J Immunol **35**(7): 2019-30.

Bedigian, H. G., D. A. Johnson, et al. (1984). "Spontaneous and induced leukemias of myeloid origin in recombinant inbred BXH mice." J Virol **51**(3): 586-94.

Begley CG, Aplan PD, et al. (1989). "Chromosomal translocation in a human leukemic stem-cell line disrupts the T-cell antigen receptor delta-chain diversity region and results in a previously unreported fusion transcript." Proceedings of the National Academy of Sciences of the United States of America **86**(6): 2031-5.

Beltran, M., I. Puig, et al. (2008). "A natural antisense transcript regulates Zeb2/Sip1 gene expression during Snail1-induced epithelial-mesenchymal transition." Genes Dev **22**(6): 756-69.

Bergeron, J., E. Clappier, et al. (2006). "HOXA cluster deregulation in T-ALL associated with both a TCRD-HOXA and a CALM-AF10 chromosomal translocation." Leukemia **20**(6): 1184-7.

Bernardi, R., S. Grisendi, et al. (2002). "Modelling haematopoietic malignancies in the mouse and therapeutical implications." Oncogene **21**(21): 3445-58.

Bijl, J., M. Sauvageau, et al. (2005). "High incidence of proviral integrations in the Hoxa locus in a new model of E2a-PBX1-induced B-cell leukemia." Genes Dev **19**(2): 224-33.

Bohlander, S. K., V. Muschinsky, et al. (2000). "Molecular analysis of the CALM/AF10 fusion: identical rearrangements in acute myeloid leukemia, acute lymphoblastic leukemia and malignant lymphoma patients." Leukemia **14**(1): 93-9.

Bollag, G., D. W. Clapp, et al. (1996). "Loss of NF1 results in activation of the Ras signaling pathway and leads to aberrant growth in haematopoietic cells." Nat Genet **12**(2): 144-8.

Borkhardt, A., O. A. Haas, et al. (1995). "A novel type of MLL/AF10 fusion transcript in a child with acute megakaryocytic leukemia (AML-M7)." Leukemia **9**(10): 1796-7.

Braun, B. S. and K. Shannon (2008). "Targeting Ras in myeloid leukemias." Clin Cancer Res **14**(8): 2249-52.

Buchberg, A. M., H. G. Bedigian, et al. (1990). "Evi-2, a common integration site involved in murine myeloid leukemogenesis." Mol Cell Biol **10**(9): 4658-66.

Buijs, A., S. Sherr, et al. (1995). "Translocation (12;22) (p13;q11) in myeloproliferative disorders results in fusion of the ETS-like TEL gene on 12p13 to the MN1 gene on 22q11." Oncogene **10**(8): 1511-9.

Buske, C., M. Feuring-Buske, et al. (2001). "Overexpression of HOXA10 perturbs human lymphomyelopoiesis in vitro and in vivo." Blood **97**(8): 2286-92.

Calvo, K. R., D. B. Sykes, et al. (2000). "Hoxa9 immortalizes a granulocyte-macrophage colony-stimulating factor-dependent promyelocyte capable of biphenotypic differentiation to neutrophils or macrophages, independent of enforced meis expression." Mol Cell Biol **20**(9): 3274-85.

Calvo, K. R., D. B. Sykes, et al. (2002). "Nup98-HoxA9 immortalizes myeloid progenitors, enforces expression of Hoxa9, Hoxa7 and Meis1, and alters cytokine-specific responses in a manner similar to that induced by retroviral co-expression of Hoxa9 and Meis1." Oncogene **21**(27): 4247-56.

Cao, Y., H. Chang, et al. (2007). "Alteration of adhesion molecule expression and cellular polarity in hepatocellular carcinoma." Histopathology **51**(4): 528-38.

Carlson, K. M., C. Vignon, et al. (2000). "Identification and molecular characterization of CALM/AF10fusion products in T cell acute lymphoblastic leukemia and acute myeloid leukemia." Leukemia **14**(1): 100-4.

Castilla, L. H., P. Perrat, et al. (2004). "Identification of genes that synergize with Cbfb-MYH11 in the pathogenesis of acute myeloid leukemia." Proc Natl Acad Sci U S A **101**(14): 4924-9.

Caudell, D. and P. D. Aplan (2008). "The role of CALM-AF10 gene fusion in acute leukemia." Leukemia **22**(4): 678-85.

Caudell, D., Z. Zhang, et al. (2007). "Expression of a CALM-AF10 fusion gene leads to Hoxa cluster overexpression and acute leukemia in transgenic mice." Cancer Res **67**(17): 8022-31.

Chaplin, T., P. Ayton, et al. (1995). "A novel class of zinc finger/leucine zipper genes identified from the molecular cloning of the t(10;11) translocation in acute leukemia." Blood **85**(6): 1435-41.

Chaplin, T., O. Bernard, et al. (1995). "The t(10;11) translocation in acute myeloid leukemia (M5) consistently fuses the leucine zipper motif of AF10 onto the HRX gene." Blood **86**(6): 2073-6.

Cho, B. C., J. D. Shaughnessy, Jr., et al. (1995). "Frequent disruption of the Nf1 gene by a novel murine AIDS virus-related provirus in BXH-2 murine myeloid lymphomas." J Virol **69**(11): 7138-46.

Cline, M. J. (1994). "The molecular basis of leukemia." N Engl J Med **330**(5): 328-36.

Dastot-Le Moal, F., M. Wilson, et al. (2007). "ZFHX1B mutations in patients with Mowat-Wilson syndrome." Hum Mutat **28**(4): 313-21.

Debernardi, S., A. Bassini, et al. (2002). "The MLL fusion partner AF10 binds GAS41, a protein that interacts with the human SWI/SNF complex." Blood **99**(1): 275-81.

Dell'Angelica, E. C., J. Klumperman, et al. (1998). "Association of the AP-3 adaptor complex with clathrin." Science **280**(5362): 431-4.

Deshpande, A. J., M. Cusan, et al. (2006). "Acute myeloid leukemia is propagated by a leukemic stem cell with lymphoid characteristics in a mouse model of CALM/AF10-positive leukemia." Cancer Cell **10**(5): 363-74.

Dik, W. A., W. Brahim, et al. (2005). "CALM-AF10+ T-ALL expression profiles are characterized by overexpression of HOXA and BMI1 oncogenes." Leukemia **19**(11): 1948-57.

DiMartino, J. F., P. M. Ayton, et al. (2002). "The AF10 leucine zipper is required for leukemic transformation of myeloid progenitors by MLL-AF10." Blood **99**(10): 3780-5.

Dreyling, M. H., J. A. Martinez-Climent, et al. (1996). "The t(10;11)(p13;q14) in the U937 cell line results in the fusion of the AF10 gene and CALM, encoding a new member of the AP-3 clathrin assembly protein family." Proc Natl Acad Sci U S A **93**(10): 4804-9.

Dreyling, M. H., K. Schrader, et al. (1998). "MLL and CALM are fused to AF10 in morphologically distinct subsets of acute leukemia with translocation t(10;11): both rearrangements are associated with a poor prognosis." Blood **91**(12): 4662-7.

Dudley, J. P. (2003). "Tag, you're hit: retroviral insertions identify genes involved in cancer." Trends Mol Med **9**(2): 43-5.

Ellis, C. A. and G. Clark (2000). "The importance of being K-Ras." Cell Signal **12**(7): 425-34.

Ferrando, A. A. and A. T. Look (2003). "Gene expression profiling in T-cell acute lymphoblastic leukemia." Semin Hematol **40**(4): 274-80.

Forster, A., R. Pannell, et al. (2005). "Chromosomal translocation engineering to recapitulate primary events of human cancer." Cold Spring Harb Symp Quant Biol **70**: 275-82.

Frohling, S., C. Scholl, et al. (2005). "Genetics of myeloid malignancies: pathogenetic and clinical implications." J Clin Oncol **23**(26): 6285-95.

Garcia-Fernandez, J. (2005). "The genesis and evolution of homeobox gene clusters." Nat Rev Genet **6**(12): 881-92.

GFCH, G. F. d. C. H. (1991). "t(10;11)(p13-14;q14-21): a new recurrent translocation in T-cell acute lymphoblastic leukemias. ." Genes Chromosomes Cancer **3**(6): 411-5.

Gilbert, D. J., P. E. Neumann, et al. (1993). "Susceptibility of AKXD recombinant inbred mouse strains to lymphomas." J Virol **67**(4): 2083-90.

Gilliland, D. G. and M. S. Tallman (2002). "Focus on acute leukemias." Cancer Cell **1**(5): 417-20.

Golub, T. R., D. K. Slonim, et al. (1999). "Molecular classification of cancer: class discovery and class prediction by gene expression monitoring." Science **286**(5439): 531-7.

Greene, M. E., G. Mundschau, et al. (2003). "Mutations in GATA1 in both transient myeloproliferative disorder and acute megakaryoblastic leukemia of Down syndrome." Blood Cells Mol Dis **31**(3): 351-6.

Gregory, P. A., A. G. Bert, et al. (2008). "The miR-200 family and miR-205 regulate epithelial to mesenchymal transition by targeting ZEB1 and SIP1." Nat Cell Biol **10**(5): 593-601.

Grier, D. G., A. Thompson, et al. (2005). "The pathophysiology of HOX genes and their role in cancer." J Pathol **205**(2): 154-71.

Grubach, L., C. Juhl-Christensen, et al. (2008). "Gene expression profiling of Polycomb, Hox and Meis genes in patients with acute myeloid leukaemia." Eur J Haematol.

Hanahan, D. and R. A. Weinberg (2000). "The hallmarks of cancer." Cell **100**(1): 57-70.

Harris, N. L., E. S. Jaffe, et al. (2001). WHO classification of tumours of haematopoietic and lymphoid tissues: Introduction. Pathology & Genetics of Tumours of Haematopoietic and Lymphoid Tissues. E. S. Jaffe, Harris, Nancy Lee, Stein, Harald, Vardiman, James W. Lyon, IARC Press**:** 12-13.

Harris, P. and P. Ralph (1985). "Human leukemic models of myelomonocytic development: a review of the HL-60 and U937 cell lines." J Leukoc Biol **37**(4): 407-22.

Hess, J. L. (2004). "MLL: a histone methyltransferase disrupted in leukemia." Trends Mol Med **10**(10): 500-7.

Heuser, M., G. Beutel, et al. (2006). "High meningioma 1 (MN1) expression as a predictor for poor outcome in acute myeloid leukemia with normal cytogenetics." Blood **108**(12): 3898-905.

Hwang, H. C., C. P. Martins, et al. (2002). "Identification of oncogenes collaborating with p27Kip1 loss by insertional mutagenesis and high-throughput insertion site analysis." Proc Natl Acad Sci U S A **99**(17): 11293-8.

Iwasaki, M., T. Kuwata, et al. (2005). "Identification of cooperative genes for NUP98-HOXA9 in myeloid leukemogenesis using a mouse model." Blood **105**(2): 784-93.

Jacks, T., T. S. Shih, et al. (1994). "Tumour predisposition in mice heterozygous for a targeted mutation in Nf1." Nat Genet **7**(3): 353-61.

Jones, L. K., T. Chaplin, et al. (2001). "Identification and molecular characterisation of a CALM-AF10 fusion in acute megakaryoblastic leukaemia." Leukemia **15**(6): 910-4.

Kelly, L. M. and D. G. Gilliland (2002). "Genetics of myeloid leukemias." Annu Rev Genomics Hum Genet **3**: 179-98.

Klebig, M. L., M. D. Wall, et al. (2003). "Mutations in the clathrin-assembly gene Picalm are responsible for the hematopoietic and iron metabolism abnormalities in fit1 mice." Proc Natl Acad Sci U S A **100**(14): 8360-5.

Kobayashi, H., F. Hosoda, et al. (1997). "Hematologic malignancies with the t(10;11)(p13;q21) have the same molecular event and a variety of morphologic or immunologic phenotypes." Genes Chromosomes Cancer **20**(3): 253-9.

Kobayashi, H., M. J. Thirman, et al. (1995). "U937 cell line has a t(10;11)(p13-14;q14-21) rather than a deletion of 11q." Genes Chromosomes Cancer **13**(3): 217-8.

Kogan, S. C., J. M. Ward, et al. (2002). "Bethesda proposals for classification of nonlymphoid hematopoietic neoplasms in mice." Blood **100**(1): 238-45.

Korf, B. R. (2000). "Malignancy in neurofibromatosis type 1." Oncologist **5**(6): 477-85.

Korpal, M., E. S. Lee, et al. (2008). "The miR-200 Family Inhibits Epithelial-Mesenchymal Transition and Cancer Cell Migration by Direct Targeting of E-cadherin Transcriptional Repressors ZEB1 and ZEB2." J Biol Chem **283**(22): 14910-4.

Krishnamachary, B., D. Zagzag, et al. (2006). "Hypoxia-inducible factor-1-dependent repression of E-cadherin in von Hippel-Lindau tumor suppressor-null renal cell carcinoma mediated by TCF3, ZFHX1A, and ZFHX1B." Cancer Res **66**(5): 2725-31.

Kroon, E., J. Krosl, et al. (1998). "Hoxa9 transforms primary bone marrow cells through specific collaboration with Meis1a but not Pbx1b." Embo J **17**(13): 3714-25.

Kroon, E., U. Thorsteinsdottir, et al. (2001). "NUP98-HOXA9 expression in hemopoietic stem cells induces chronic and acute myeloid leukemias in mice." Embo J **20**(3): 350-61.

Kumon, K., H. Kobayashi, et al. (1999). "Mixed-lineage leukemia with t(10;11)(p13;q21): an analysis of AF10-CALM and CALM-AF10 fusion mRNAs and clinical features." Genes Chromosomes Cancer **25**(1): 33-9.

La Starza, R., B. Crescenzi, et al. (2006). "Dual-color split signal fluorescence in situ hybridization assays for the detection of CALM/AF10 in t(10;11)(p13;q14-q21)-positive acute leukemia." Haematologica **91**(9): 1248-51.

Lai Cheong, J. E., V. Wessagowit, et al. (2005). "Molecular abnormalities of the desmosomal protein desmoplakin in human disease." Clin Exp Dermatol **30**(3): 261-6.

Lam, D. H. and P. D. Aplan (2001). "NUP98 gene fusions in hematologic malignancies." Leukemia **15**(11): 1689-95.

Lang, R. B., L. W. Stanton, et al. (1982). "On immunoglobulin heavy chain gene switching: two gamma 2b genes are rearranged via switch sequences in MPC-11 cells but only one is expressed." Nucleic Acids Res **10**(2): 611-30.

Largaespada, D. A. (2000). "Genetic heterogeneity in acute myeloid leukemia: maximizing information flow from MuLV mutagenesis studies." Leukemia **14**(7): 1174-84.

Largaespada, D. A., C. I. Brannan, et al. (1996). "Nf1 deficiency causes Ras-mediated granulocyte/macrophage colony stimulating factor hypersensitivity and chronic myeloid leukaemia." Nat Genet **12**(2): 137-43.

Largaespada, D. A., J. D. Shaughnessy, Jr., et al. (1995). "Retroviral integration at the Evi-2 locus in BXH-2 myeloid leukemia cell lines disrupts Nf1 expression without changes in steady-state Ras-GTP levels." J Virol **69**(8): 5095-102.

Lekanne Deprez, R. H., P. H. Riegman, et al. (1995). "Cloning and characterization of MN1, a gene from chromosome 22q11, which is disrupted by a balanced translocation in a meningioma." Oncogene **10**(8): 1521-8.

Li, J., H. Shen, et al. (1999). "Leukaemia disease genes: large-scale cloning and pathway predictions." Nat Genet **23**(3): 348-53.

Lin, Y. W. and P. D. Aplan (2004). "Leukemic transformation." Cancer Biol Ther **3**(1): 13-20.

Lin, Y. W., C. Slape, et al. (2005). "NUP98-HOXD13 transgenic mice develop a highly penetrant, severe myelodysplastic syndrome that progresses to acute leukemia." Blood **106**(1): 287-95.

Linder, B., L. K. Jones, et al. (1998). "Expression pattern and cellular distribution of the murine homologue of AF10." Biochim Biophys Acta **1443**(3): 285-96.

Linder, B., R. Newman, et al. (2000). "Biochemical analyses of the AF10 protein: the extended LAP/PHD-finger mediates oligomerisation." J Mol Biol **299**(2): 369-78.

Lombaerts, M., T. van Wezel, et al. (2006). "E-cadherin transcriptional downregulation by promoter methylation but not mutation is related to epithelial-to-mesenchymal transition in breast cancer cell lines." Br J Cancer **94**(5): 661-71.

Lowenberg, B., J. R. Downing, et al. (1999). "Acute myeloid leukemia." N Engl J Med **341**(14): 1051-62.

Matutes, E., R. Morilla, et al. (1997). "Definition of acute biphenotypic leukemia." Haematologica **82**(1): 64-6.

Meyerholz, A., L. Hinrichsen, et al. (2005). "Effect of clathrin assembly lymphoid myeloid leukemia protein depletion on clathrin coat formation." Traffic **6**(12): 1225-34.

Miething, C., R. Grundler, et al. (2007). "Retroviral insertional mutagenesis identifies RUNX genes involved in chronic myeloid leukemia disease persistence under imatinib treatment." Proc Natl Acad Sci U S A **104**(11): 4594-9.

Mikkers, H., J. Allen, et al. (2002). "High-throughput retroviral tagging to identify components of specific signaling pathways in cancer." Nat Genet **32**(1): 153-9.

Morerio, C., A. Rapella, et al. (2005). "MLL-MLLT10 fusion gene in pediatric acute megakaryoblastic leukemia." Leuk Res **29**(10): 1223-6.

Morse, H. C., 3rd, M. R. Anver, et al. (2002). "Bethesda proposals for classification of lymphoid neoplasms in mice." Blood **100**(1): 246-58.

Moskow, J. J., F. Bullrich, et al. (1995). "Meis1, a PBX1-related homeobox gene involved in myeloid leukemia in BXH-2 mice." Mol Cell Biol **15**(10): 5434-43.

Mowat, D. R., M. J. Wilson, et al. (2003). "Mowat-Wilson syndrome." J Med Genet **40**(5): 305-10.

Mucenski, M. L., B. A. Taylor, et al. (1988). "Identification of a common ecotropic viral integration site, Evi-1, in the DNA of AKXD murine myeloid tumors." Mol Cell Biol **8**(1): 301-8.

Mukherjee, S., R. N. Ghosh, et al. (1997). "Endocytosis." Physiol Rev **77**(3): 759-803.

Mullighan, C. G., A. Kennedy, et al. (2007). "Pediatric acute myeloid leukemia with NPM1 mutations is characterized by a gene expression profile with dysregulated HOX gene expression distinct from MLL-rearranged leukemias." Leukemia **21**(9): 2000-9.

Nakamura, F., K. Maki, et al. (2003). "Monocytic leukemia with CALM/AF10 rearrangement showing mediastinal emphysema." Am J Hematol **72**(2): 138-42.

Nakamura T, Largaespada DA, et al. (1996). "Fusion of the nucleoporin gene Nup98 to Hoxa9 by the chromosome translocation t(7;11)(p15;p15) in human myeloid leukaemia." Nature Genetics **12**(2): 154-158.

Nakamura, T., D. A. Largaespada, et al. (1996). "Cooperative activation of Hoxa and Pbx1-related genes in murine myeloid leukaemias." Nat Genet **12**(2): 149-53.

Narita, M., K. Shimizu, et al. (1999). "Consistent detection of CALM-AF10 chimaeric transcripts in haematological malignancies with t(10;11)(p13;q14) and identification of novel transcripts." Br J Haematol **105**(4): 928-37.

Niemeyer, C. M. and S. E. Sallen (1998). Acute Lymphoblastic Leukemia. Nathan and Oski's Hematology of Infancy & Childhood. D. G. Nathan and S. H. Orkin. Philadelphia, W. B. Saunders. **2:** 1245-46.

O'Marcaigh, A. S. and K. M. Shannon (1997). "Role of the NF1 gene in leukemogenesis and myeloid growth control." J Pediatr Hematol Oncol **19**(6): 551-4.

Ogilvy, S., D. Metcalf, et al. (1999). "Promoter elements of vav drive transgene expression in vivo throughout the hematopoietic compartment." Blood **94**(6): 1855-63.

Okada, Y., Q. Feng, et al. (2005). "hDOT1L links histone methylation to leukemogenesis." Cell **121**(2): 167-78.

Okada, Y., Q. Jiang, et al. (2006). "Leukaemic transformation by CALM-AF10 involves upregulation of Hoxa5 by hDOT1L." Nat Cell Biol **8**(9): 1017-24.

Passegue, E., C. H. Jamieson, et al. (2003). "Normal and leukemic hematopoiesis: are leukemias a stem cell disorder or a reacquisition of stem cell characteristics?" Proc Natl Acad Sci U S A **100 Suppl 1**: 11842-9.

Pearson, J. C., D. Lemons, et al. (2005). "Modulating Hox gene functions during animal body patterning." Nat Rev Genet **6**(12): 893-904.

Pineault, N., C. Abramovich, et al. (2004). "Differential and common leukemogenic potentials of multiple NUP98-Hox fusion proteins alone or with Meis1." Mol Cell Biol **24**(5): 1907-17.

Pineault, N., C. Buske, et al. (2003). "Induction of acute myeloid leukemia in mice by the human leukemia-specific fusion gene NUP98-HOXD13 in concert with Meis1." Blood **101**(11): 4529-38.

Rabbitts, T. H. (1991). "Translocations, master genes, and differences between the origins of acute and chronic leukemias." Cell **67**(4): 641-4.

Rabbitts, T. H. (1994). "Chromosomal translocations in human cancer." Nature **372**(6502): 143-9.

Rabbitts, T. H. (2001). "Chromosomal translocation master genes, mouse models and experimental therapeutics." Oncogene **20**(40): 5763-77.

Rabbitts, T. H. and M. R. Stocks (2003). "Chromosomal translocation products engender new intracellular therapeutic technologies." Nat Med **9**(4): 383-6.

Raimondi, S. C. (1993). "Current status of cytogenetic research in childhood acute lymphoblastic leukemia." Blood **81**(9): 2237-51.

Renneville, A., C. Roumier, et al. (2008). "Cooperating gene mutations in acute myeloid leukemia: a review of the literature." Leukemia **22**(5): 915-31.

Reuter, C. W., M. A. Morgan, et al. (2000). "Targeting the Ras signaling pathway: a rational, mechanism-based treatment for hematologic malignancies?" Blood **96**(5): 1655-69.

Rhoades, K. L., C. J. Hetherington, et al. (1996). "Synergistic up-regulation of the myeloid-specific promoter for the macrophage colony-stimulating factor receptor by AML1 and the t(8;21) fusion protein may contribute to leukemogenesis." Proc Natl Acad Sci U S A **93**(21): 11895-900.

Ries, L. A. G., Melbert D, et al. (2008). SEER Cancer Statistics Review,1975-2005, National Cancer Institute.

Robinson, M. S. and J. S. Bonifacino (2001). "Adaptor-related proteins." Curr Opin Cell Biol **13**(4): 444-53.

Rolink, A., E. ten Boekel, et al. (1996). "A subpopulation of B220+ cells in murine bone marrow does not express CD19 and contains natural killer cell progenitors." J Exp Med **183**(1): 187-94.

Rowe, W. P., W. E. Pugh, et al. (1970). "Plaque assay techniques for murine leukemia viruses." Virology **42**(4): 1136-9.

Rowley, J. D. (1999). "The role of chromosome translocations in leukemogenesis." Semin Hematol **36**(4 Suppl 7): 59-72.

Rowley, J. D. (2001). "Chromosome translocations: dangerous liaisons revisited." Nat Rev Cancer **1**(3): 245-50.

Rubnitz, J. E., F. G. Behm, et al. (1996). "11q23 rearrangements in acute leukemia." Leukemia **10**(1): 74-82.

Salmon-Nguyen, F., M. Busson, et al. (2000). "CALM-AF10 fusion gene in leukemias: simple and inversion-associated translocation (10;11)." Cancer Genet Cytogenet **122**(2): 137-40.

Schmid, S. L. (1997). "Clathrin-coated vesicle formation and protein sorting: an integrated process." Annu Rev Biochem **66**: 511-48.

Shimizu, R., J. D. Engel, et al. (2008). "GATA1-related leukaemias." Nat Rev Cancer **8**(4): 279-87.

Shipley, J., S. Williams, et al. (1995). "Characterization of a t(10;11)(p13-14;q14-21) in the monoblastic cell line U937." Genes Chromosomes Cancer **13**(2): 138-42.

Slape, C. and P. D. Aplan (2004). "The role of NUP98 gene fusions in hematologic malignancy." Leuk Lymphoma **45**(7): 1341-50.

Slape, C., H. Hartung, et al. (2007). "Retroviral insertional mutagenesis identifies genes that collaborate with NUP98-HOXD13 during leukemic transformation." Cancer Res **67**(11): 5148-55.

Slape, C. a. A. P. (2008). Retroviral Insertional Mutagenesis. Encyclopedia of Cancer. M. e. Schwab, Elsevier.

Solomon, E., J. Borrow, et al. (1991). "Chromosome aberrations and cancer." Science **254**(5035): 1153-60.

Sonnenberg, A. and R. K. Liem (2007). "Plakins in development and disease." Exp Cell Res **313**(10): 2189-203.

Soulier, J., E. Clappier, et al. (2005). "HOXA genes are included in genetic and biologic networks defining human acute T-cell leukemia (T-ALL)." Blood **106**(1): 274-86.

Speleman, F., B. Cauwelier, et al. (2005). "A new recurrent inversion, inv(7)(p15q34), leads to transcriptional activation of HOXA10 and HOXA11 in a subset of T-cell acute lymphoblastic leukemias." Leukemia **19**(3): 358-66.

Sundstrom, C. and K. Nilsson (1976). "Establishment and characterization of a human histiocytic lymphoma cell line (U-937)." Int J Cancer **17**(5): 565-77.

Suzuki, T., H. Shen, et al. (2002). "New genes involved in cancer identified by retroviral tagging." Nat Genet **32**(1): 166-74.

Takei, K., O. Mundigl, et al. (1996). "The synaptic vesicle cycle: a single vesicle budding step involving clathrin and dynamin." J Cell Biol **133**(6): 1237-50.

Tebar, F., S. K. Bohlander, et al. (1999). "Clathrin assembly lymphoid myeloid leukemia (CALM) protein: localization in endocytic-coated pits, interactions with clathrin, and the impact of overexpression on clathrin-mediated traffic." Mol Biol Cell **10**(8): 2687-702.

Tefferi, A. and D. G. Gilliland (2007). "Oncogenes in myeloproliferative disorders." Cell Cycle **6**(5): 550-66.

Thandla, S. and P. D. Aplan (1997). "Molecular biology of acute lymphocytic leukemia." Seminars in Oncology **24**(1): 45-56.

Thorsteinsdottir, U., E. Kroon, et al. (2001). "Defining roles for HOX and MEIS1 genes in induction of acute myeloid leukemia." Mol Cell Biol **21**(1): 224-34.

Thorsteinsdottir, U., A. Mamo, et al. (2002). "Overexpression of the myeloid leukemia-associated Hoxa9 gene in bone marrow cells induces stem cell expansion." Blood **99**(1): 121-9.

Thorsteinsdottir, U., G. Sauvageau, et al. (1997). "Overexpression of HOXA10 in murine hematopoietic cells perturbs both myeloid and lymphoid differentiation and leads to acute myeloid leukemia." Mol Cell Biol **17**(1): 495-505.

Touw, I. P. and S. J. Erkeland (2007). "Retroviral insertion mutagenesis in mice as a comparative oncogenomics tool to identify disease genes in human leukemia." Mol Ther **15**(1): 13-9.

van Oostveen, J., J. Bijl, et al. (1999). "The role of homeobox genes in normal hematopoiesis and hematological malignancies." Leukemia **13**(11): 1675-90.

van Wely, K. H., A. C. Molijn, et al. (2003). "The MN1 oncoprotein synergizes with coactivators RAC3 and p300 in RAR-RXR-mediated transcription." Oncogene **22**(5): 699-709.

Wechsler, D. S., L. D. Engstrom, et al. (2003). "A novel chromosomal inversion at 11q23 in infant acute myeloid leukemia fuses MLL to CALM, a gene that encodes a clathrin assembly protein." Genes Chromosomes Cancer **36**(1): 26-36.

Wechsler, J., M. Greene, et al. (2002). "Acquired mutations in GATA1 in the megakaryoblastic leukemia of Down syndrome." Nat Genet **32**(1): 148-52.

Wendland, B. and S. D. Emr (1998). "Pan1p, yeast eps15, functions as a multivalent adaptor that coordinates protein-protein interactions essential for endocytosis." J Cell Biol **141**(1): 71-84.

Wolff, L. (2006). Retroviral insertional mutagensis and its application to genetically engineered mice. Progress in virus research. S. Thebault. Hauppauge, NY, Nova Science Publishers**:** 267-99.

Wolff, L., R. Koller, et al. (2003). "A Moloney murine leukemia virus-based retrovirus with 4070A long terminal repeat sequences induces a high incidence of myeloid as well as lymphoid neoplasms." J Virol **77**(8): 4965-71.

Zhang, B., Y. H. Koh, et al. (1998). "Synaptic vesicle size and number are regulated by a clathrin adaptor protein required for endocytosis." Neuron **21**(6): 1465-75.